Fluorinated surfactants in droplet-based microfluidics: Influence of their composition on the properties of emulsion drops

Thèse N° 9304

Gianluca Nicolas ETIENNE

2019

ÉCOLE POLYTECHNIQUE
FÉDÉRALE DE LAUSANNE

"If it disagrees with experiment, it's wrong. And that simple statement is the key to science. It doesn't make a difference how beautiful your guess is, it doesn't matter how smart you are, who made the guess, or what his name is. If it disagrees with experiment, it's wrong. That's all there is to it."

Richard Feynman

ACKNOWLEDGEMENTS

First, I would like to thank my advisor Esther Amstad, for supervising me during my master's thesis at Harvard University and giving me the opportunity to join her in building up the Soft Materials Laboratory at EPFL. It was a great experience being the first PhD student and seeing the team grow. I am very grateful for her door always being open and her unlimited ideas when I felt stuck in my research. I am also grateful for the other members of my committee: Francesco Stellacci, who helped push my science forward; Andrew DeMello, who initially introduced me to the world of microfluidics during my master's studies; and Jean-Christoph Baret for many great discussions.

I want to thank all past and current members of the Soft Materials Laboratory. A large reason why this experience has been so positive is due to you. I could not have wished for a better team. Antoine Vian was there from the beginning and helped build up the whole lab. I am thankful for our friendship and great discussions on things in and outside science. Huachuan Du, Mathias Steinacher, Michael Kessler, Alvaro Charlet, Johan Longo, Armend Håti, Bjoern Schulte, Jui-Chia Chang, Aysu Okur, Amin Hodaei, Irvine Ong and Matteo Hirsch were likewise great lab mates and friends. Mercedes, our secretary, always had a positive attitude, which made this a pleasant journey. I also want to thank all the students I could supervise during my PhD.

Outside our lab, I would like to thank Guiseppe Sforazzini, who has taught me all the skills to perform synthesis in a chemistry lab and how to write a proper lab book. Evi Zdrali, Marjan Bioçanin, Enzo Bomal, Halil Okur for your helpful discussions throughout my thesis.

Most of my time outside of my work I spent with people from Swingtime Lausanne. Building up a swing dance scene and teaching weekly classes in Lausanne gave me a lot of joy. I am grateful for all the new friends I met. I especially want to mention Ann Sychterz, Mathieu and Florence Huruguen, Cedric Tsui, Elif Oruc, Flavia Ciaranfi, Keyne Damiens, Suzanne Badoux, Maxime Felder, Camille Sigg, Fabienne Furger.

Mainly, I would like to thank Sarah Cotterill, for her love, humor, and support during my PhD. For believing in this relationship even if it meant doing five years of Lausanne-Boston long distance. I also want to thank the whole Cotterill family, Ron, Peggy, and Abby who welcomed me in their home.

Lastly, I would like to thank my parents Marina and Beni and my brother Elio who always supported me in whatever I did and gave me endless encouragement. Without them, I would not be here. I also want to thank my four grandparents, Anna and Pino, Dorli and Beni, who supported me throughout my career.

ABSTRACT

Miniaturization has been a driving force in many areas of science and technology, most notably in the electronics industry. Droplet-based microfluidics, a methode to produce emulsion drops in a controlled way and at high-throughputs, enables the miniaturization and automation of biological and chemical experiments. Each emulsion drop is used as a closed reaction vessel, enabling the performance of thousands of experiments per second, at throughputs traditional technologies cannot meet. Droplet-based microfluidics is a driving technology in the advances of genomics, proteomics, single-cell analysis, high-throughput screening, and diagnostics. Crucial for using emulsion drops as reaction vessels is that they do not break and that they are tight, not allowing material to be exchanged between drops. To prevent emulsion drops from coalescing, they can be stabilized with surfactants. They adsorb at the liquid-liquid interface, lower the interfacial tension, and add steric stability. For most drop-based biological assays, aqueous drops are dispersed in fluorinated oils. These drops are stabilized with fluorinated surfactants, composed of two perfluoropolyether blocks linked to a polyethylene glycol (PEG) block. These surfactants impart good stability to emulsion drops but can contribute to an exchange of reagents between them.

In this thesis, we studied how the composition of fluorinated surfactants influences the properties of emulsion drops. Therefore we synthesized different fluorinated surfactants and varied the length of the hydrophilic block and the number of hydrophobic blocks a surfactant contains. We show that the mechanical and thermal stability of single emulsion drops strongly depends on the composition of the surfactants. The stability of drops stabilized with triblock copolymers inversely scales with the interfacial tension, where as the stability of drops coated with diblock copolymers scales with the surfactant packing density. To investigate the transport of reagents across oil phases, we employ water-oil-water double emulsions as templates. We show that the leakage, resulting in cross-contamination, is mainly caused by emulsion drops with sizes around 100 nm that spontaneously form at the water-oil interface. These drops result in leakage of larger objects such as plasmids with 11'000 base pairs or 100 nm polystyrene beads. We show that the leakage can be reduced by an order of magnitude if surfactants that only moderately lower the interfacial tension are used to stabilize double emulsions or if the shell thickness of double emulsions is reduced to values similar to the diameter of the spontaneously forming drops. Lastly, we developed novel types of surfactants containing a catechol group in the hydrophilic block, that can be ionically cross-linked at the interface of a drop, creating a viscoelastic shell. We demonstrate that by cross-linking the surfactant at the drop interface, we create capsules that show high mechanical stability, and are impermeable to encapsulants. Leveraging their stickiness, we demonstrate that these capsules, if densely packed, can be printed into 3D structures.

Keywords: *fluorinated surfactants, emulsion drops, double emulsions, cross-contamination, capsules*

Zusammenfassung

Für viele Jahre war die Miniaturisierung eine treibende Kraft für die Wissenschaft und Technologie, vor allem in der Elektronikindustrie. Tropfenbasierte Mikrofluidik, eine Methode mit der man Emulsionstropfen in kontrollierter Art und mit hohem Durchsatz herzustellen kann, ermöglicht die Miniaturisierung und Automatisierung von biologischen und chemischen Experimenten. Jeder Emulsionstropfen wird dabei als ein geschlossenes Gefäss betrachtet, wobei man tausende Experimente pro Sekunde durchführen kann. Die tropfenbasierte Mikrofluidik ist eine treibende Technologie für Fortschritte in der Genomikforschung, in der Proteomik, der Einzelzellanalyse, beim hoch-durchlauf Aussieben oder in der Diagnostik. Damit Emulsionstropfen als Reaktionsgefässe benutzt werden können, ist es entscheidend, dass sie dicht sind und nicht kaputtgehen. Um diese Tropfen zu stabilisieren werden Tenside benutzt, welche an der Grenzfläche adsorbieren und die Grenzflächenspannung heruntersetzten. Zusätzlich stabilisieren sie den Tropfen sterische. Für die meisten tropfenbasierten biologischen Assays, werden wässerige Tropfen in fluoriniertem Öl benutzt. Diese Tropfen werden mit einem fluorinierten Tensid stabilisiert, welches aus zwei perfluorinierten Polyäther blöcken welche mit einem Polyethyleneglykol verbunden sind besteht.

In dieser Doktorarbeit haben wir untersucht wie die Zusammensetzung der fluorinierten Tenside die Eigenschaften von Emulsionstropfen beeinflusst. Dafür haben wir die Länge des hydrophilen Blockes sowie die Anzahl des hydrophoben Blockes vom Tensid variiert. Wir zeigen, dass die mechanischen und thermischen Eigenschaften von einer Einfachemulsion stark von der Zusammensetzung des Tensides abhängt. Die Stabilität von Einfachemulsionen die mit Triblockcopolymeren stabilisiert sind, korreliert reziprok mit der Grenzflächenspannung. Die Stabilität von Einfachemulsionstropfen die mit Diblockcopolymeren beschichtet sind, skaliert mit der Packungsdichte der Tenside. Um den Transport von wasserlöslichem Material durch die Ölschicht zu untersuchen, haben wir Wasser in Öl in Wasser Doppelemulsionen hergestellt. Wir zeigen, dass die Undichtheit welche zu Kreuzkontamination zwischen den Tropfen führen kann, ein Resultat von kleinen Emulsionstropfen um die 100 Nanometer ist, welche sich spontan an der Wasser-Öl Grenzfläche formen. Diese kleinen Emulsionstropfen können sogar grössere Materie wie Plasmide mit 11'000 Basenpaaren oder 100 nm grosse Polystyrol Partikel transportieren. Wir zeigen wie dieser Transport um eine Grössenordnung reduziert werden kann, wenn Tenside die nur mässig die Grenzflächenspannung heruntersetzen, oder wenn die Ölschalendicke die gleiche Grössenordnung wie die kleinen Emulsionstropfen hat. Im letzten Teil, haben wir eine neue Art von Tensiden entwickelt, welche eine Brenzcatechingruppe im hydrophilen Block enthält. Dieser Teil kann an der Grenzfläche vernetzt werden kann und führt zu einer Schale mit viskoelastischen eigenschaften. Wir zeigen, dass wir durch das Vernetzen der Tenside an der Grenzfläche, Kapseln mit einer hohen mechanischen Stabilität und undurchlässig für kleine Moleküle herstellen können. Die Kapseloberfläche ist klebrig und bei hoher Packungsdichte können die Kapseln in 3D

Strukturen gedruckt werden.

Schlagwörter: *Fluoriniertes Tensid, Emulsionstropfen, Doppelemulsionen, Kreuzkontamination, Kapseln*

FOREWORD

This project summarizes the work on how the composition of fluorinated surfactants influences the properties of emulsion drops. This manuscript presents the work that was done in the scope of this thesis and is divided into 5 chapters:

- **Chapter 1** gives a general introduction to emulsion science and how surfactants are used to stabilize emulsions. Additionally, we introduce the fundamentals of droplet-based microfluidics which was the main technique used to study the performance of surfactants.

- The experimental techniques and methods used throughout the work can be found in **Chapter 2**.

- A first study of the influence of the surfactant composition on the mechanical and thermal stability of single emulsion drops can be found in **Chapter 3**. We stabilize single emulsion drops with different fluorinated surfactants and study how the composition influences the stability. This chapter is an adaptation of the previously published paper titled: "Influence of Fluorinated Surfactant Composition on the Stability of Emulsion Drops". [1]

- Surfactants are necessary to stabilize emulsion drops but also contribute to the transport of material from one drop to another. We study the mechanism that can lead to this cross-contamination in **Chapter 4**, using double emulsions as templates. This chapter is an adaptation of the previously published paper titled: "Cross-talk between emulsion drops: How are hydrophilic reagents transported across oil phases?". [2]

- In **Chapter 5**, we introduce a novel type of surfactant that can be reversibly cross-linked at an interface by forming a metal-coordinate complex. We show that by cross-linking the surfactant at the interface, we can transform an emulsion drop into a capsule with high mechanical stability. Additionally, we can prevent the leakage from emulsion drops and print densely packed capsules into 3D structures. This chapter is under submission as "Bio-inspired self-healing capsules: Delivery vehicles and beyond".

- In **Chapter 6** we summarize our work.

Contents

Chapter 1

Introduction

In this chapter, I give an introduction to emulsions and show different stabilization methods of emulsions. Further on, I will introduce the basics of microfluidics, a technology to produce emulsions of controlled sizes.

Contents

1.1 Basic Concepts of Emulsion Science

1.1.1 Definitions

An emulsion is a mixture of two (or more) immiscible liquids where one phase is dispersed in another phase. We encounter emulsions often in daily life — for example, in food products such as butter (water drops dispersed in oil), milk and ice cream (oil drops dispersed in water) or mayonnaise (oil dispersed in water). Emulsions are also common in cosmetics such as body lotions or creams, in paints, or as pesticides in the agriculture industry. [3–5]

We define the liquid that forms the drops as the *dispersed phase* and the surrounding liquid as the *continuous phase*. An emulsion consisting of two phases is called a *single emulsion*. There are two types of single emulsion drops, namely water in oil emulsion (W/O) and oil in water (O/W) emulsions, as schematically shown in Figures 1.1a and b. Emulsions can also be made of multiple drops contained inside other drops, which are called *multiple emulsions*. An emulsion containing two phases inside a drop is called a *double emulsion*. If the *core* consists of a water phase, the *shell* of an oil phase, and the *outer phase* of another water phase it is called a water in oil in water (W/O/W) double emulsion, as shown schematically in Figure 1.1c.
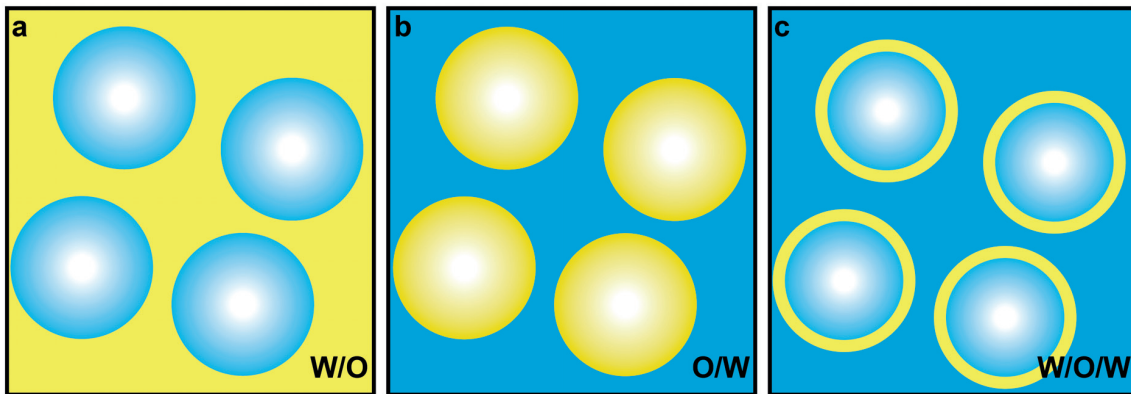
Figure 1.1: Schematic illustration of an (**a**) water in oil emulsion (W/O), (**b**) oil in water emulsion (O/W), and (**c**) water in oil in water (W/O/W) double emulsion.

1.1.2   Stability of Emulsions

Water and oil do not mix, but if you shake the mixture hard enough, you can form drops of one phase dispersed in another — after a short time, the two phases will usually separate again.

Energy is required to create new interfacial area, and the energy per surface area is called *surface energy*, γ. For liquids, it is more common to use tension per unit length which is often given in mN/m. [6] This force per unit length is called *surface tension*, if used between a liquid and a gas, or called *interfacial tensions* if used between two liquids.

This interfacial tension arises from different intermolecular forces between water and oil, therefore it can strongly change depending on the chemical nature of the two phases used. To successfully form an emulsion we must introduce enough energy to the system to overcome the energy penalty imposed by the need to create new interfaces. The total interfacial energy, E_γ, is given as

$$\Delta E_\gamma = \gamma \Delta A \tag{1.1}$$

where A is the total interfacial area. By dispersing one phase in another, new water-oil interfaces are produced, which costs energy. For a fixed amount of energy, the smaller the interfacial tension gets, the bigger ΔA becomes, which will result in smaller drops. No matter how low

the energy becomes, there is always an energetic penalty in forming new interfaces and therefore emulsions are generally not in thermodynamic equilibrium.

After emulsion drops are formed, they want to minimize their interfacial energy, ΔE_γ, over time by reducing the interfacial area, A, which ultimately results in a phase separation. Different mechanisms lead to this process known as *aging* of an emulsion. In the case of *drop coalescence*, the thin film of stabilizers (see section 1.2) between two individual drops breaks, leading them to fuse into a single larger drop but with a smaller interfacial area, as shown in Figure 1.2a. [4,5,7,8] If emulsion drops in a solution have different sizes, *Ostwald ripening* can occur. In this process, smaller drops will shrink, and larger ones will grow at the expense of the smaller ones, as schematically illustrated in Figure 1.2b. [5,7,8] Ostwald ripening is due to a difference in Laplace pressure. The Laplace pressure p is due to pressure differences on both sides of the interface resulting in curved interfaces. This pressure is inversely proportional to the drop radius r with

$$\Delta p = \frac{2\gamma}{r} \tag{1.2}$$

. [4] Since this pressure is higher in drops with a smaller radius, solvent molecules from small drops will diffuse to the bigger ones. Another mechanism is *flocculation*, where single emulsion drops stick together forming flocs, as shown in Figure 1.2c. [4,5] This process can be reversible and must not lead to complete breakage of the emulsion. Lastly, *creaming* or *sedimentation* occurs in almost all emulsions over time if there is a density difference between the two phases, as shown in Figure 1.2d. [4] All of these processes can lead to the full breakage of the emulsions resulting in a complete phase separation, as shown in Figure 1.2e.
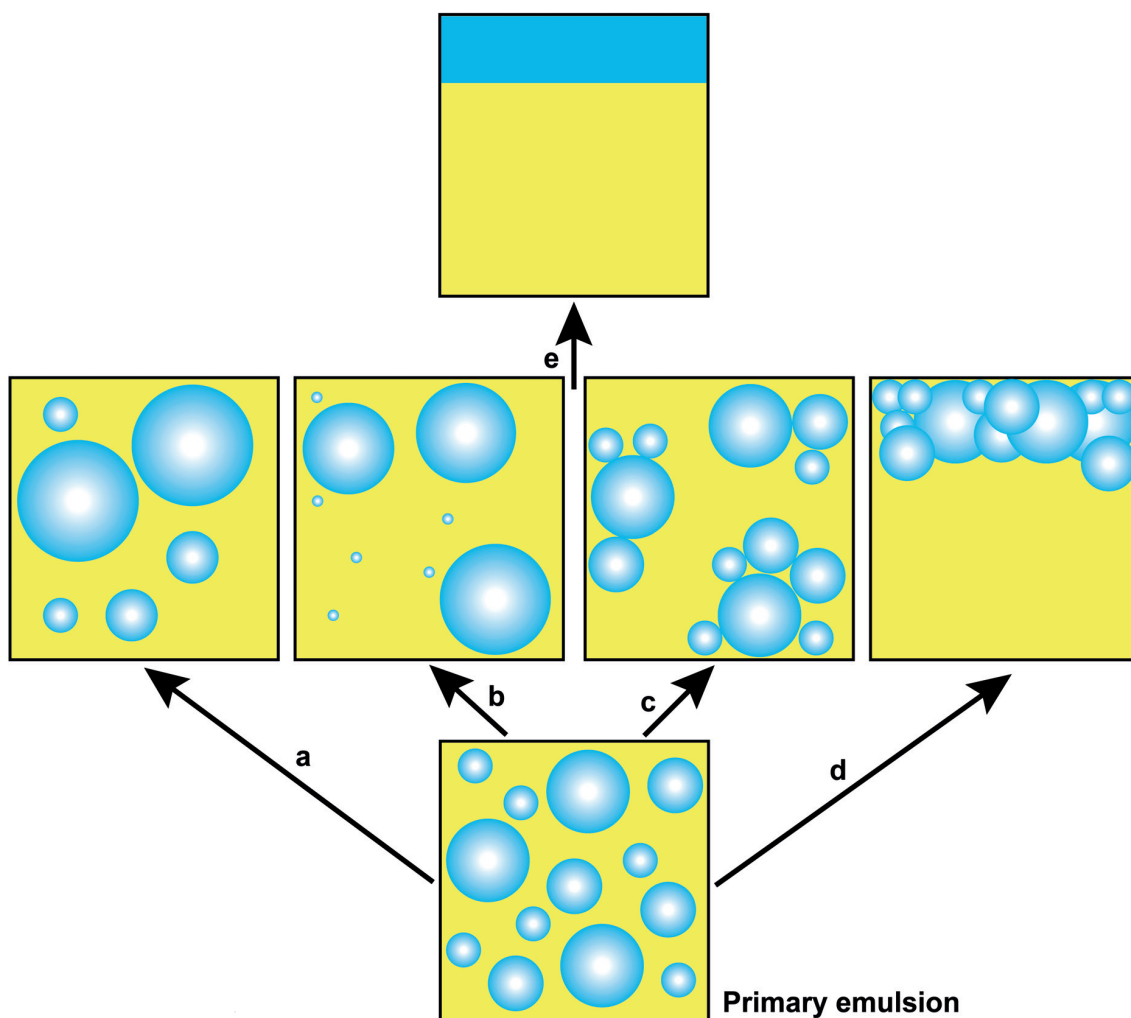
Figure 1.2: Schematic illustration of mechanisms leading to the aging of emulsions. (**a**) Coalescence, (**b**) Ostwald ripening, (**c**) flocculation, and (**d**) creaming can lead to the disappearance of emulsions such that two separate phases result. (**e**) all of these processes can finally lead to breakage of the emulsion resulting in a phase separation.

To kinetically prevent emulsions from coalescing they can be stabilized using surfactants (as described in more detail in section 1.2). Surfactants are amphiphilic molecules that adsorb at a liquid-liquid interface, as shown in Figures 1.3a and b. The composition of the surfactant influences the stability of emulsion drops. Since surfactants are generally small molecules, they can diffuse quickly towards a new interface and are therefore convenient to use when emulsions are produced at a high rate.

Alternatively, emulsions can be stabilized using solid nanoparticles that adsorb at the interface, as shown in Figure 1.3c. [9–11] Emulsions stabilized by nanoparticles are called *Pickering emulsions*. Colloidal particles that have affinities to both phases adsorb at the liquid-liquid interface, thereby decreasing the interfacial area between the two liquids ΔA such that ΔE_γ decreases. Once Pickering emulsions are formed, they show a very high stability. However, due to the bigger size of the nanoparticles compared to the surfactants, colloidal particles adsorb slower

at the interface making them more difficult to use for droplet-based microfluidics applications (explained more in detail in section 1.4) where fast adsorption is required.
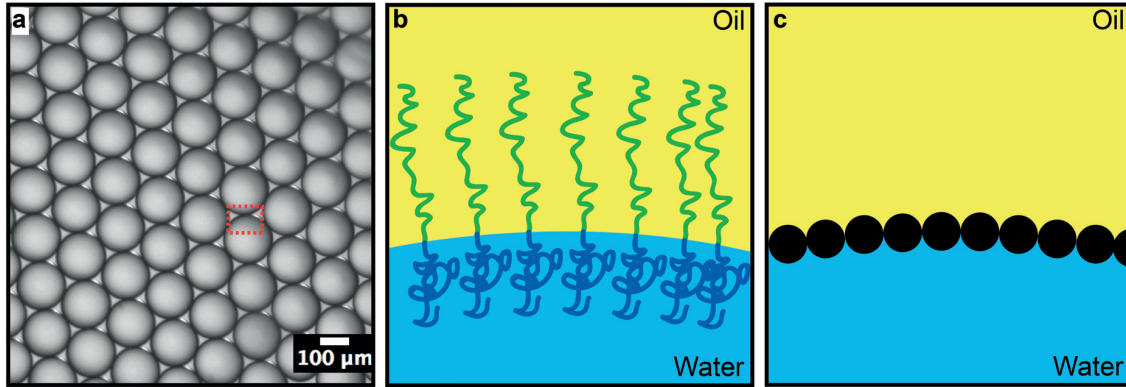
Figure 1.3: (**a**) Microscope image of water in oil emulsions. (**b**) Schematic illustration of polymeric surfactants adsorbed at an oil-water interface, (**c**) schematic illustration of particles adsorbed at an oil-water interface forming a Pickering emulsion.

1.2 Surfactants

1.2.1 Definitions and Applications

Surfactants, or surface active agents, are amphiphilic molecules containing at least one hydrophilic and at least one hydrophobic group. The chemical structure of a typical surfactant, sodium dodecyl sulfate (SDS) or synonymously sodium lauryl sulfate (SLS), is shown in Figure 1.4.
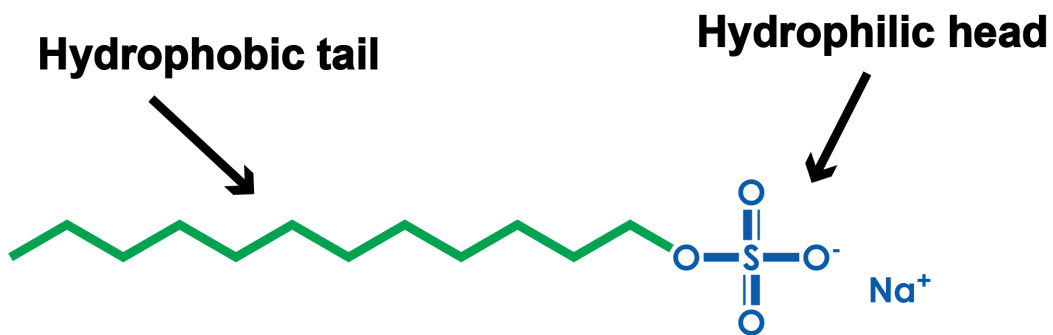
Figure 1.4: Chemical structure of sodium dodecyl sulfate (SDS), a typical surfactant. The hydrophobic tail (green) and the hydrophilic head group (blue) are shown in the sketch.

Due to this amphiphilic character, surfactants can adsorb at an interface, arranging in a way where the hydrophilic part points to the aqueous phase and the hydrophobic part to the oil phase.

6

Surfactants have a strong influence on the stability of emulsions and can add stability to drops in three different ways: [4]

- Surfactants reduce the interfacial tension, γ and therefore the interfacial energy, E_γ.

- The adsorbed surfactant molecules at the interface of emulsion drops can form a thin film. When drops come into contact due to thermal convection, mechanical agitation, or Brownian motion this surfactant film can act as a steric hindrance and prevent or delay the coalescence of drops.

- If the surfactants are charged, they can induce a charge to the surface of the drop such that they electrostatically repel each other.

Surfactants are widely used in different fields in industry. The most ancient use of surfactants is for *detergents and cleaners*. Soaps have been produced for more than 2000 years. Surfactants in detergents can bind to dirt and be washed away by water resulting in cleaner material. In *cosmetics and personal care products*, surfactants are used to produce creams and emulsions but also lipstick, mascara, and hair dyes. In the *textile and fiber* industry surfactants are used in the dying of textiles, lowering the surface tension and allowing the spreading of the dye into the fiber matrix. Surfactants are also used in the *tanning of leather*, to create a protective layer on the skin, keeping it flexible and preventing it from sticking together. In *paints, lacquers and other coating products* surfactants are used to create a uniform dispersion of pigments in the solvent, or to allow better wetting. In the paper-making industry, surfactants are used to produce *paper and cellulose* products. In *mining and ore flotation*, surfactants are used to separate the desired mineral from the bulk. In *plant protection and pest control*, they are used as emulsifiers for spray preparations or as wetting agents. In preparation of *foods*, such as foams, bread, mayonnaise, salad dressing and ice cream, surfactants are crucial. In the *chemical industry*, they are used, for example, for the production of polymers using emulsion polymerization. In *oilfield chemicals and petroleum production*, surfactants are used to alter the wetting characteristics of the oil-rock and steam interface to improve the rate of recovery. In *pharmaceuticals*, surfactants are used as formulation aides for the delivery of ingredients in solutions, emulsions, dispersions, gel capsules or tablets. [4]

Surfactants can be categorized in anionic, cationic, zwitterionic, and nonionic surfactants, depending on the charge present at the hydrophilic group. The different types of surfactants are used for various applications since their composition influences their performance. Anionic surfactants possess a negative charge on the head group and are the most often used surfactant in, for example, soaps. [3] Cationic surfactants have a positively charged head group and adsorb strongly on most solid surfaces. They are therefore often used as fabric softeners, conditioners or as anticaking agents. [3] Zwitterionic surfactants have both a positive and a negative charge, they are less irritating to skin and can adsorb on negatively and positively charged surfaces but

they are often insoluble in many organic solvents. [3] Non-ionic surfactants can be either solubilized in water or in oil and are often used for biological applications since there is no charge that can interact with biological matter.

Commonly, surfactants are classified according to their hydrophilicity or hydrophobicity using the hydrophilic-lipophilic balance or HLB value:

$$HLB = 20 \times \frac{M_h}{M_{tot}} \tag{1.3}$$

where M_h is the molecular weight of the hydrophilic group and M_{tot} the molecular weight of the total surfactant. The value ranges from 1 (very hydrophobic) to 20 (very hydrophilic). This measure has become a common tool in characterizing surfactants in industry although it is not ideal. It assigns a fixed value to a surfactant independent of the parameters of the system they are used in. It might work well to compare different ethoxylates at room temperature, but it makes a comparison between different types of surfactants difficult. HLB values do not take into account the surfactant structure, concentration, temperature or salinity of the liquids. A more sophisticated way of characterizing surfactants for formulations is the HLD Hydrophilic-Lipophilic deviation (HLD) value. [12] It takes into account the temperature, the salinity, the type of oil, and the type of the surfactant head group. [13]

$$HLD = F(S) - k \times EACN - \beta \Delta T + Cc \tag{1.4}$$

Here $F(S)$, is a function of the salinity of the aqueous solution, k is a factor to the $EACN$ (the Effective Alkane Carbon Number), which needs to be found in the literature or experimentally determined and is the value for the oiliness of the oil, β depends on the type of surfactant and can be found in the literature, Cc is a characteristic value which needs to be determined experimentally but depends on how hydrophilic or hydrophobic a surfactant is. [14] If the HLD = 0, there is a perfect balance between hydrophilicity and hydrophobicity of the surfactants, if O/W emulsion is desired a HLD < 0 and for W/O emulsion a HLD > 0 is desired.

1.2.2 Adsorption of Surfactants

When surfactants are in solution and an interface is present, surfactants molecules can adsorb at that interface. When surfactants adsorb at an interface the hydrophobic group orients towards the oil/air and the hydrophilic group towards the water, thereby reducing the free energy of the system. The adsorption of the surfactant molecules at a surface does not only decrease the surface tension but also structures the liquid molecules near the interface. [3]

To relate the final equilibrium surface tension to the amount of surfactant adsorbed at an interface the *Gibbs adsorption theorem* or *Gibbs equation* can be used. The Gibbs adsorption theorem can be derived from the Gibbs free energy, ΔG, and the surface excess, the excess of

surfactant molecules at the surface. The surface excess concentration is given as $\Gamma = n^\sigma/A$, where n^σ is the number of surfactants at the interface and A the area. [4, 15, 16]. The basic equation under consideration of constant temperature are pressure is given as:

$$d\gamma = -\sum_i \Gamma_i d\mu_i \tag{1.5}$$

γ is the interfacial tension, Γ_i the interfacial excess concentration and μ_i the chemical potential of every component i. The differential of the chemical potential depends on the activity $a_i = x_i * f_i$ where x_i is the mole fraction and f_i the activity coefficient. [4, 15]

$$d\mu_i = RTdln(a_i) \tag{1.6}$$

where R is the ideal gas constant and T the temperature. By taking equation 1.5, and filling in the two components, the solvent and surfactant, one has to consider that by definition the solvent has an interfacial excess concentration Γ_s of zero leading to

$$-\frac{d\gamma_{eq}}{RT} = \Gamma_{eq}dlna_{a_i} \tag{1.7}$$

[15] For non-ionic surfactants the Gibbs equation results in

$$\Gamma_{eq} = -\frac{1}{RT} \times \frac{d\gamma_{eq}}{dlnC} \tag{1.8}$$

where C is the concentration of surfactant in solution. [15] This equation is valid for low surfactant concentrations, where the interfacial tension depends strongly on the surfactant concentration. For systems where the interfacial tension is known, and non-ionic surfactants are used, equation 1.8 can be used to calculate the surface excess concentration. [4]

1.2.3   Critical Micelle Concentration

If the interaction between single surfactant molecules is stronger than between a surfactant molecule and a solvent molecule, aggregates, assemblies of surfactant molecules can form. The concentration of surfactant molecules in solution where these aggregates of a few surfactant molecules start to form is called *critical aggregation concentration (cac)*. To minimize the interaction of the hydrophobic group with the water phase, surfactants can assemble into new, well-defined larger structures, such as micelles, as shown in Figure 1.5a. The concentration when surfactants self-assemble into these larger well-defined aggregates is called the *critical micelle concentration (cmc)*. These larger aggregates always coexist with free surfactant molecules in solution. [6, 15] The critical aggregation concentration is lower than the critical micelle concentration.

There are different techniques to determine the cmc. When measuring the interfacial tension as a function of the concentration of the surfactant in solution, one can observe a decrease in the interfacial tension due to the adsorption of surfactants at the interface. At a certain concentration, γ does not significantly change anymore with increasing surfactant concentration. The cmc is the point where the slope of the interfacial tension as a function of the surfactant concentration suddenly becomes negligible, as shown in Figure 1.5b. [15] Other methods include the measurement of a change in the electrical conductivity, or an increase in light scattering. [3]
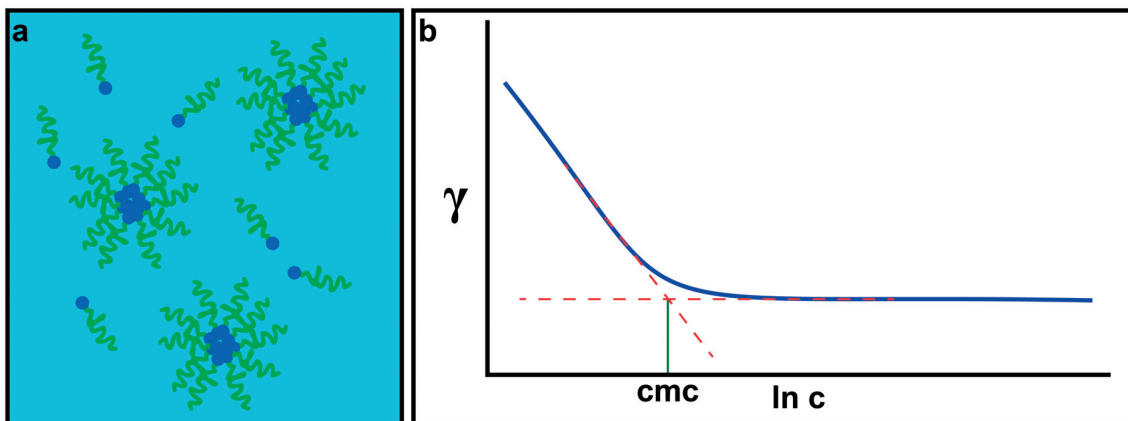
Figure 1.5: (**a**) Schematic illustration of surfactant molecules with a hydrophilic head group and a hydrophobic tail in a water solution. Their concentration is above the cmc, where micelles form. (**b**) Surface tension, γ, as a function of the logarithm of surfactant concentration. The concentration where the two extrapolated lines meet is called the cmc.

The type of aggregates surfactant molecules can self-assemble into depends on the structure of the surfactant molecules: They can form micelles or bigger aggregates such as vesicles as summarized in Table 1.6. The size of the hydrophilic part and the length of the hydrophobic part affects the strengths of the interactions between the surfactant molecules and the solvent and will influence the types of aggregates they will form. To link the size of the hydrophobic and the hydrophilic block to the kind of aggregates that can form, we introduce the *packing parameter*. The packing parameter is defined as:

$$\alpha = \frac{v}{a_0 \times l_c} \tag{1.9}$$

where v is the volume of the hydrophobic chain, l_c the maximum effective length the hydrophobic chain can assume and a_0 the optimal area of the hydrophilic group. [6] α is the cross-section area of the hydrophobic part divided by the cross-section area of the hydrophilic part. When $\alpha \leq \frac{1}{3}$ spherical micelles will form, when $\frac{1}{3} < \alpha < \frac{1}{2}$ non-spherical (ellipsoidal) micelles form, $\alpha \approx \frac{1}{2}$ cylindrical or rod-like micelles form and when $\frac{1}{2} < \alpha < 1$ various interconnected structures will form, as shown in Figure 1.6. If $\alpha \approx 1$ vesicles and extended bilayers will from and if $\alpha > 1$ "inverted" structures will form.
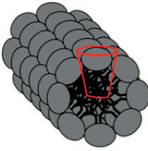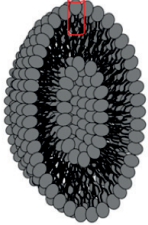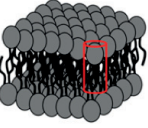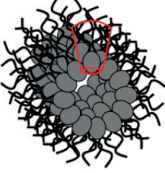
Aspect Ratio	$\alpha < 1/3$	$1/3 < \alpha < 1/2$	$1/2 < \alpha < 1$	$\alpha \sim 1/2$	$\alpha > 1$
Amphiphile Topology	Cone	Truncated Cone (TC)		Rod	Inverted TC
Aggregate Topology	Spherical Micelles	Cylindrical Micelles	Lamellar Phases Vesicles	Planar	Inverted Micelles

Figure 1.6: Illustration of different aggregates that can be formed depending on the packing parameter. [17]

These larger self-assembled aggregates are often fluid like and soft, with the surfactant molecules in constant motion: they will adsorb and desorb from the interface but also diffuse, twist and turn. [6]

1.2.4   Spontaneous Emulsification

To form an emulsion drop, new interfacial area must be created, which costs energy, as explained in section 1.1.2. This energy cost is partially or fully compensated by a gain in entropy caused by the increasing number of drops formed. More than hundred years ago, people observed that upon bringing certain immiscible phases containing a surfactant into contact, emulsion drops would spontaneously form. Although *spontaneous emulsification* has long been observed, the mechanism of spontaneous drop formation is still not fully understood. [18] It is possible that it can occur through different mechanisms depending on the system. [19]. More recently spontaneous emulsification has been studied in a controlled way. By forming a drop of water in hexadecane containing Span 80 as a surfactant, the formation of tiny emulsion drops at the interface without agitation were observed under a microscope. [20]. When adding salts at high concentrations to the aqueous phase the formation of drops could be suppressed. Spontaneous emulsification has also been observed upon bringing water in contact with dodecane containing Span 80, where small drops form at the interface and grow over time to several micrometers in diameter. [19] It has been shown that for higher surfactant concentrations the process was faster, and below 0.025% of surfactant, no formation of drops could be observed. This is in agreement with a more recent study where spontaneous emulsification of water in kerosene containing Span80 was only observed above the cmc. Higher surfactant concentrations lead to more drops and higher

salt concentrations to fewer drops. [21] The same phenomena has been observed at water and toluene containing asphaltenes, high molecular polar components in crude oil, interfaces. The spontaneous formation of emulsion drops was observed using bright-field microscopy and could be verified by using different dyes in the oil and water phase and analyzing them with a fluorescence confocal microscope. [22]

Spontaneous emulsification has been observed even in water-triglyceride-water double emulsion containing polyglycerolricinoleate as a surfactant in the oil phase. They show that the number of drops increases with time and the rate of the drop formation increases exponentially with the concentration of surfactant. It has been shown that if there is no surfactant in the oil phase the spontaneous formation of emulsion drops does not happen. [23]

Even though there are many different theories on the mechanism of spontaneous emulsification, [18, 24–30] recent studies have in common that (i) there needs to be a surfactant present in the phase where the emulsions form and (ii) the concentration of the surfactant needs to be above a certain concentration for spontaneous emulsification to occur. A possible mechanism for spontaneous emulsification could be that the surfactant molecules at the interface induce a spontaneous curvature, since their packing density at the interface depends on their shape and size in addition to the amphiphilicity. Therefore interfaces can spontaneously curve to accommodate more surfactant molecules while keeping the free energy minimal. [22] Others propose that aggregates such as inverse micelles form in solution that at contact with the interface can get filled with water. [23] Another option could be that small convective flows shear off tiny emulsion drops from the interface.

1.3   Characterization of Surfactants

1.3.1   Pendant Drop

The *pendant drop* method is a commonly used technique to determine the interfacial tension of two liquids. In this technique, a drop of one liquid is hanging or raising from a flat needle either in air or in a second immiscible liquid. The drop is illuminated from the backside and a camera in front of the drop records the size and shape of the drop, as shown schematically in Figure 1.7.
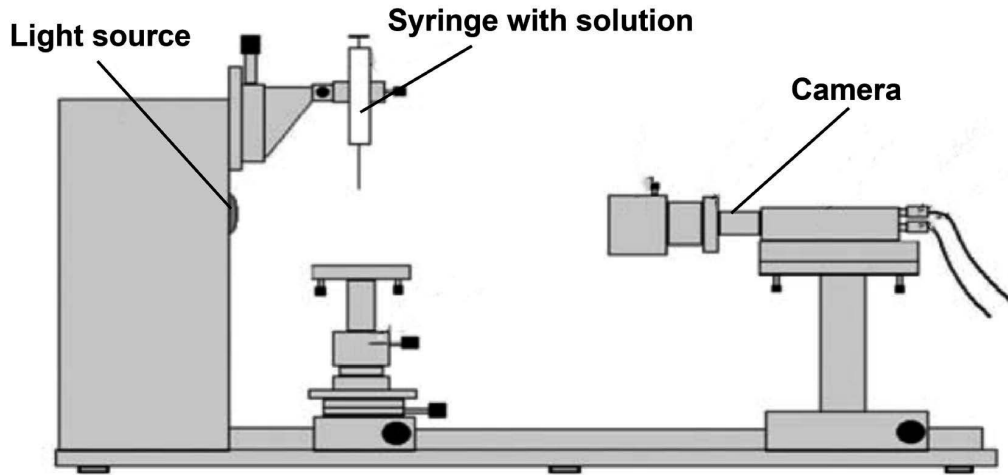
Figure 1.7: Schematic illustration of a typical pendant drop setup. The drop is formed at the tip of a flat needle that is connected to a syringe. Light illuminates the drop and a camera records the drop shape. Figure adapted from [24].

The drop shape in the recorded image is analyzed using the the Young-Laplace equation, that relates the pressure difference between inside and outside of the drop with the curved liquid surface/interface by

$$\Delta P = P_i - P_0 = \gamma \times (\frac{1}{R_1} + \frac{1}{R_2}) \tag{1.10}$$

Here ΔP is the pressure difference across the drop interface, γ the interfacial tension and R_1 and R_2 the radii of the drop curvature. Because the drop hanging from a needle is non-spherical, two radii are needed. R_1 and R_2 at a selected point are obtained by taking the normal to that surface, drawing two planes where one is at a right angle to the other, and finding the curves formed in the two planes. The force balance of the hanging drop results from gravity that acts on the drop pulling it down, whereas the surface or interfacial tension is keeping the drop attached to the needle. Since gravitation causes a pressure difference across the z-axes, the Laplace pressure in function of the z-axes can be defined as follows:

$$\Delta P = \Delta P_0 + (\Delta \rho_i)gz \tag{1.11}$$

Here ΔP_0 is the reference pressure at z=0, $\Delta \rho_i$ the difference in densities of the two phases, g the gravity and z the vertical distance between the plane and a given point. By combining equation 1.10 and 1.11 and introducing geometrical considerations, the interfacial tension can be derived from the shape of the drop. [15, 24] If we characterize the liquid drop towards air we measure the *surface tension*; if we measure it in another liquid, we obtain the *interfacial tension*.

1.3.2   Wilhelmy Plate

An alternative method to measure the surface tension is by using the *Wilhelmy plate*. This is a flat metal plate that is placed at a liquid-air interface and the force acting on the plate is measured. [24] To receive precise results, the plate needs to be completely wetted by the solvent resulting in a contact angle of the solvent on the Wilhelmy plate of 0° [15]. The force measured is

$$F = \gamma \times 2(x + y) \tag{1.12}$$

where x is the horizontal length of the plate and y the thickness of the plate. Since F, x, and y can easily be measured, the surface tension γ can be determined. [15] As an alternative to the Wilhelmy plate, paper plates made from filter paper can be used. [31]

1.3.3   Langmuir Trough

To measure the surface tension as a function of the surfactant molecule packing at the interface, a *Langmuir trough* can be used. In this technique, the trough is filled with a liquid and a Wilhelmy plate is inserted. A defined amount of surfactant molecules are dissolved in a volatile solvent that is immiscible in water and deposited on the water surface of the trough. The solvent will evaporate and the surfactant molecules will be dispersed at the water surface. When the amount of surfactants at the surface is low, the distance between the different surfactant molecules will be large and their interaction will be weak. Under these conditions, the surfactants will have little impact on the surface tension of the water which is measured using the Wilhelmy plate. Now, one can apply a force with the two barriers and push the surfactant molecules together. At one point surfactants start to pack more densely and interact with their neighbors. This two-dimensional pressure is called the *surface pressure* Π. The surface pressure is linked to the interfacial tension by

$$\Pi = \gamma_0 - \gamma \tag{1.13}$$

where γ_0 is the surface tension of pure water and γ the surface tension when the surfactant is present. The interfacial tension is measured by the Wilhelmy plate as described in section 1.3.2. By knowing the amount of surfactant molecules added and the volume of the trough, one can determine the mean molecular area, the area of water surface available to each molecule, as follows:

$$A_m = \frac{A_L}{N_S} \tag{1.14}$$

, where A_m is the mean molecular area, A_L is the geometrical area of the surface occupied by the monolayer and N_S is the amount of surfactants at the surface.

Usually one measures these relations at a constant temperature and these curves are known as

surface pressure - area isotherms or simply *isotherms*. Depending on the surface pressure surfactant molecules arrange in different configurations at the interface resulting in defined phases ranging from gaseous to liquid-expanded, to liquid-condensed to solid, as schematically illustrated in Figure 1.8. [15]
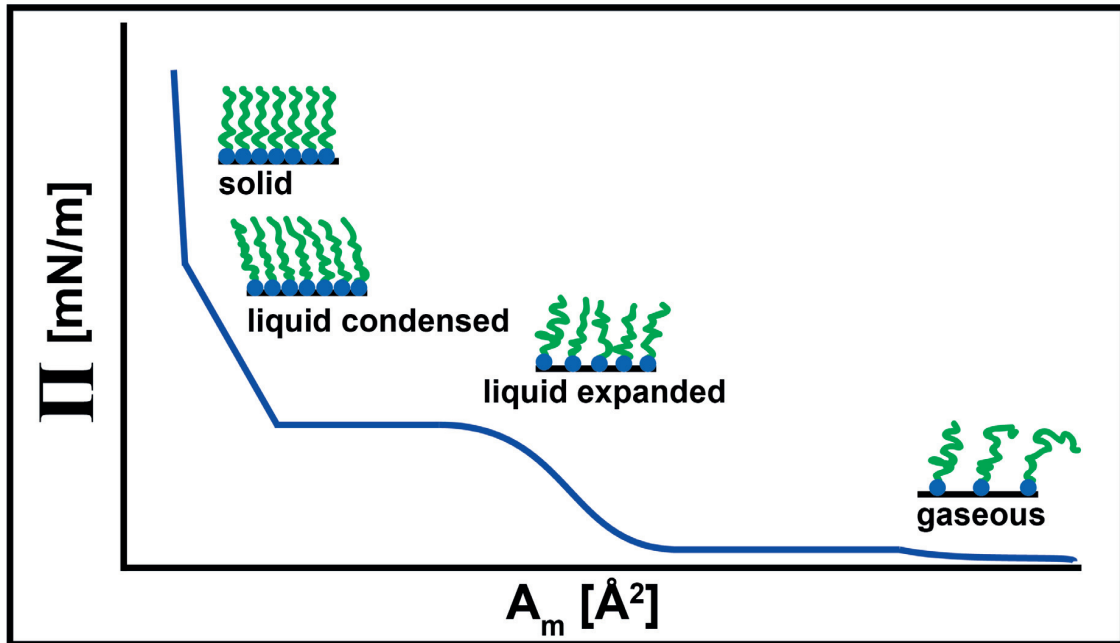
Figure 1.8: Schematic illustration of typical surface pressure, Π, against mean molecular area (A_m) isotherm showing the different regimes of surfactant packings during compression.

The behavior and existence of the different phases depends on the physical and chemical properties of the surfactant molecules, the temperature, and the sub-phase composition. [15]

1.4   Droplet-Based Microfluidics

1.4.1   Techniques to Produce Emulsion Drops

Emulsions can be produced using a variety of techniques such as mechanical agitation for example with a rotor-stator system [32] or a homogenizer [33]. With these techniques, the size distribution of drops can be relatively large. To get more control over the size distribution of emulsion drops, membrane emulsification can be used. [34] In this technique, the disperse phase is pressed through a membrane with well-defined pores into the continuous phase. The pore size determines the size of the resulting emulsion drops, [34] but very narrow size distributions cannot be achieved. [35] The best control over drops size distribution can be achieved by using droplet-based microfluidics. [36]

1.4.2   Microfluidics

Microfluidics is the science and technology of systems that manipulate liquids flowing in channels with dimensions of tens to hundreds of micrometers. [37] The flow rates in the channels are regulated by automated syringe pumps or pressure driven pumps to allow a steady flow of liquids in the channels. Due to the small channel dimensions laminar flow often dominates. [38] This gives good temporal and spatial control over the fluid flow inside a microfluidic device. [37] By performing experiments on a much smaller scale "on chip" has several advantages: They allow the use of small sample and reagent volumes, resulting in reduced costs, but also allow high throughput and fast and accurate detection of reagents.

Advances in microfabrication, have allowed the production of microfluidic devices using soft lithography techniques [39] using polydimethylsiloxane (PDMS), a transparent elastomer. This technology made microfluidics accessible to many researchers around the world. Even large-scale integration of multiple channels with valves allowed handling of hundreds of individual micro-chambers on a single chip. [40] However, if very large numbers of samples must be analyzed, or if very small sample volumes must be used, single phase microfluidics might fail due to the limited numbers of channels and chambers that can be implemented on one chip. Additionally, interactions of the liquid with the wall of the chip can lead to contaminations. Some of these limitations can be overcome by droplet-based microfluidics.

1.4.3   Droplet-based Microfluidics

Droplet-based microfluidics is a subgroup of microfluidics where immiscible fluids are flown through tiny channels to produce emulsion drops with a well-defined size in the range of a few to hundreds of micrometer at rates of several thousand per second. Various emulsion drops produced with a microfluidic device are shown in Figure 1.9.
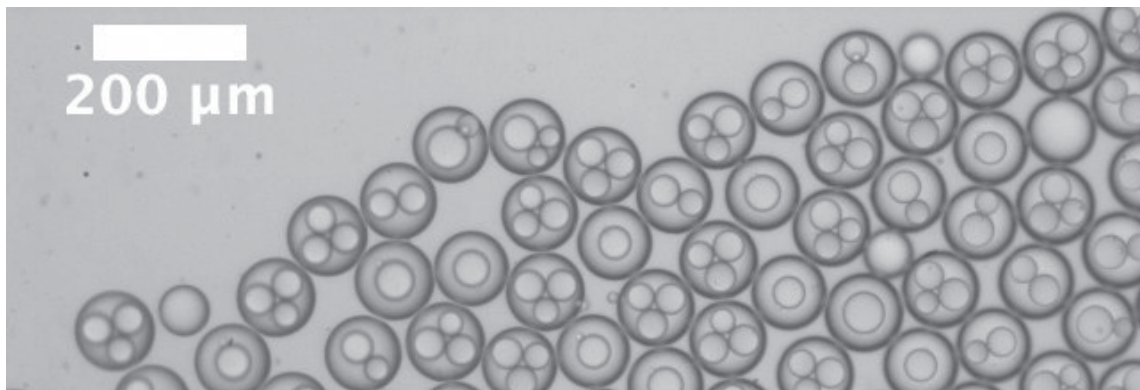
Figure 1.9:   Single-, double, and multiple emulsions produced using a microfluidic device.

Different junction designs are commonly used to produce emulsion drops in a controlled manner. The most simple geometry is the *T-junction*, where one fluid is flown perpendicular to

another, thereby shearing off a plug of the dispersed phase, as shown in Figure 1.10a. [41] In *flow focusing* devices, the dispersed phase gets sheared off by the continuous phase that is injected into the main channel from two sides, as schematically illustrated in Figure 1.10b. [42] This geometry is commonly used and results in drops with a very narrow size distribution. Depending on the angles of the incoming oil flow, monodisperse drops can be produced over a wide range of flow rates. [43] In step emulsification the drop formation does not require a secondary flow to trigger a droplet breakup. [44–46] The drop forms at a step, as shown in Figure 1.10c.
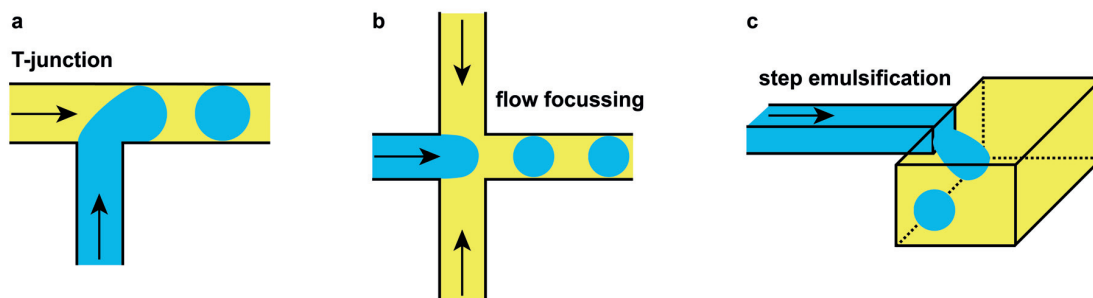
Figure 1.10: Schematic illustration of different commonly used channel geometries for drop formation. (**a**) T-junction, (**b**) flow focusing, and (**c**) step emulsification.

The drop formation is not only determined by the geometry of the channels but also depends on the drag of the outer fluid pulling the drop downstream and the interfacial tension, γ, that resists that flow. The capillary number, Ca, puts these two forces in relation:

$$Ca = \frac{\eta U}{\gamma} \tag{1.15}$$

η is the viscosity of the continuous phase, U the flow velocity of the continuous phase, and γ the interfacial tension between the two phases. [38] At capillary numbers of around 0.5 or lower, the drop breakup can be controlled by the interfacial tension, at high capillary numbers above 0.5 it is determined by the viscous forces resulting in more elongated drops that pinch off due to Rayleigh instabilities. [36, 38]

1.4.4   Applications of Droplet-Based Microfluidics

The ability to encapsulate microorganisms such as cells, DNA, RNA, bacteria, and molecules in a controlled manner in drops using small sample volumes allows for new possibilities in diagnostics and research in microbiology. [47]. Performing biological and chemical reactions inside drops has several advantages compared to traditional techniques that use Petri dishes, multiwell plates and flasks as containers: [47]

- *Confinement*: By confining a microorganism to one drop, enables to study them in an isolated environment. It allows observation of one single organism instead of a population.

For example, the metabolism and molecules secreted from a cell can be studied without being affected by neighboring cells. Since the volume of the drop is small, the secreted molecules are accumulated faster and can be detected easier. Since the volume of one drop is small, only small amounts of reagents are consumed. Additionally, droplet-based microfluidics allows sorting of drops of interest in a controlled manner — to isolate, for example, interesting individuals in a big population.

- *High-throughput*: By producing drops whose diameter varies by only 2% [48] at a rate of 10'000 per second, allows the screening of a large number of parameters in a short amount of time. Even screening of millions of individual drops becomes feasible, which with current technologies is not possible at reasonable costs and time. This opens up possibilities to study small variations for example in the phenotype and genotype of a large population of bacteria using high-throughput screening.

- *Multi-step operations*: The variety of manipulations of drops on a chip enables execution of iterative multi-step operations on a single drop. This allows performing long-term reactions and screening of several parameters.

The possibilities to manipulate drops on a chip in a controlled way makes this technology very powerful for applications in biology and chemistry. Driven by the idea of performing the same operations as one would on a macroscopic scale, but on a microscopic scale, has led to the development of various designs to manipulate drops in a controlled way on a microfluidic chip. Splitting [49, 50] is often used to extract a sample of a drop that one wants to analyze or it can be used to increase the number of drops, as shown in Figure 1.11a. On the contrary by merging two drops and thereby initiating a reaction can be achieved using a merging module, as shown in Figure 1.11b. [51–53] To add a small amount from a continuous flow into a drop, a pico-injection module has been developed, as shown in Figure 1.11c. [54]. To dilute the content of a drop in a controlled way, a droplet dilution module has been developed, as shown in Figure 1.11d. [55] Storage or incubation [56] is used as a method to store drops for a certain time while a reaction inside occurs, as shown in Figure 1.11e. By merging two channels, two populations of drops can by synchronized, as shown in Figure 1.11f. Mixing [57] the content inside drops at a controlled speed, and sorting of drops, [58] can be crucial for many biochemical assays when it comes to separating empty drops from cell-containing ones. An example of a sorting module is shown in Figure 1.11g.
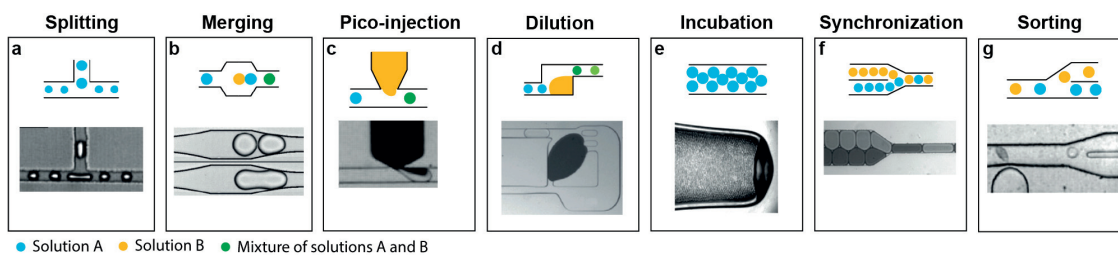
Figure 1.11: Schematic illustration and microscope images of some common drop manipulation techniques. Figure modified from [59].

Droplet-based microfluidics is currently used in a large variety of applications, such as antibody [60, 61] and drug screening, [62] and drug dose-response studies, [63] combinatorial screening, [64, 65] directed evolution of enzymes, [66, 67], single-cell DNA and genomic studies, [68] single cell RNA and transcriptomics studies, [69, 70] and chemical synthesis. [71, 72]

Compared to all the advantages of droplet-based microfluidics, compartmentalization of fluids into drops also has a few disadvantages. First, it is difficult to exchange the media inside the drop in a controlled manner and therefore adding any washing step is challenging. This can lead to lower survival rates of organisms inside drops. [73] Second, surfactants are very good in keeping drops separated but they can contribute to cross-contamination between emulsion drops which reduces the accuracy of screening assays. Cross-contamination can occur if (i) drops come into direct contact and coalesce or (ii) if the content of drops can be transported through the oil shell by the support of surfactant molecules. [74] Challenges still exist in keeping drops stable during handling especially at high salt concentrations or high temperatures used, for example, during thermocycling in polymerase chain reaction (PCR) reactions. Many of these challenges are related to the performance of the surfactant used to stabilize these emulsion drops, where a better understanding and the design of new surfactants could overcome some of the limitations of droplet-based microfluidics.

1.4.5   Fluorinated Continuous Phase

Droplet-based microfluidics has gained the most attention in microbiology and biotechnology. Working with biological material has high requirements on the types of solvents and types of surfactants one can use. For example, if cells are encapsulated in drops, a high oxygen permeability of the oil phase is desired. Biologically inert fluorocarbons fulfill these requirements. [75] In these compounds, some or all of the hydrogen atoms are replaced by fluorine atoms. These fluorinated oils are biocompatible [76–78], which is important to keep encapsulated organisms such as cells alive. Due to weak inter-molecular interactions, fluorinated carbon chains have very weak interactions with other molecules, and are therefore not miscible with water or most organic solvents. [79] Also due to the low cohesive energy, gases such as oxygen, carbon dioxide and others are highly soluble in fluorinated solvents. [7, 79–81] Additionally fluorinated oils are

compatible with PDMS, which is commonly used to fabricate microfluidic devices. [82] Water in fluorinated oil drops can be stabilized with fluorinated surfactants. [83] This system has become the standard system used for droplet-based applications in biology or biotechnology. [66, 84–89]

1.4.6   Fluorinated Surfactants

To stabilize water in fluorinated oil emulsion drops, fluorinated surfactants must be used. In these surfactants the hydrogen atoms in the hydrophobic part are replaced by fluorine atoms, making the surfactant adsorb at a fluorinated oil water interface. People have been using fluorinated surfactants comprised of a short fluorinated group linked to short hydrophilic groups such as perfluorinated ocantanol [90–95] or perfluorinated decanol. [96] Other developments linked slightly longer perfluorinated groups to acids [77] or a polyethylene glycol (PEG) group. [77, 97]

Over the past 20 years microfluidic devices and designs, used to manipulate drops in a controlled way, have been developed very rapidly. Stabilizing water in fluorinated oil in a robust way while manipulating them on chip has been challenging in the field. A big leap towards the application of droplet-based microfluidics came along with the development of a new type of fluorinated surfactant made of two perfluoro polyether blocks linked to a PEG block, as shown in Figure 1.12. [83]
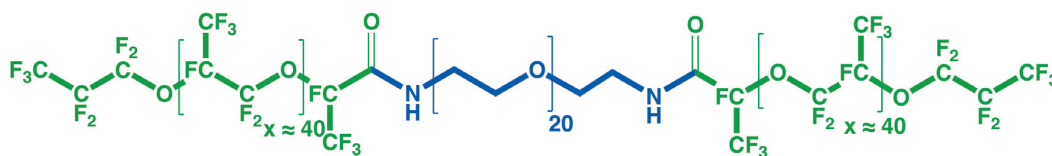
Figure 1.12: Chemical structure of a commonly used fluorinated surfactant made of two perfluorinated polyether blocks (FSH) linked to a polyethylene glycol block.

Surfactants with this structure have become the standard system to use for droplet-based microfluidics that employs fluorinated oils as a continuous phase. [66, 73, 83–89, 98–100]. To simplify the synthesis, the same fluorinated block, FSH, has been used with -COOH, [101–103] -COONH$_4$, [75, 104–106] -dimorpholinophosphate, [75, 107–109] and -tris-(hydroxymethyl)methyl groups. [110]

Since the discovery of these fluorinated block copolymer surfactant, a few modifications have been done at the synthesis replacing PEG with polyglycerol groups, [111] or using click chemistries to make novel fluorinated block copolymer surfactants. [112] At the same time, fluorinated surfactants with different structures have been introduced. [113–117]

Efficient fluorinated surfactants were discovered about 10 years ago, but for much of that time were commercially unavailable. Today, several companies provide fluorinated surfactants in pure form or as ready to use solutions such as Emulseo, RAN Biotechnolgies, 10X Genomics, BioRad, Sphere Fluidics, Dolomite, RainDance Technologies.

Although recently developed fluorinated surfactants are more efficient at stabilizing emulsion drops during droplet manipulations, stabilizing them at high temperatures or at high salt concentrations is still challenging. In addition, molecular transport between drops, as a result of differences in chemical potentials, can lead to cross-contamination between emulsion drops. Drops containing a fluorophore and empty drops were trapped in alternating order, and it could be observed how the fluorophore concentration decreases in the full drops and increases in the empty drops until they reach equilibrium, as shown in Figure 1.13. In this case, the advantage of studying one drop as a closed vessel might break down if the experimental time scale is longer than the time scale to equilibrate the chemical potential. Therefore ideal fluorinated surfactants should succeed in stabilizing emulsion drops under harsh conditions and prevent any possibility of cross-talk between emulsion drops. [74]
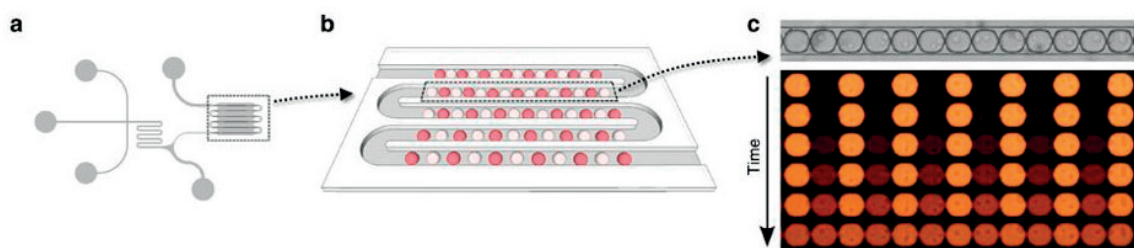
Figure 1.13: Microfluidic device to trapp water in fluorinated oil single emulsion drops that alternatively contain a fluorophore dye and are empty imaged after 0, 1.5, 3, 6, 12 and 24h. Over time the dye is transported from the fluorophore loaded drop into an empty drop. Figure adapted from [118].

1.4.7   Double Emulsions

Although double emulsions are not commonly used in industry, they have many advantages over single emulsion drops. Regarding stability, single emulsion drops containing high salt concentrations are prone to coalesce where double emulsions under the same conditions are more stable. [119] Water in fluorinated oil single emulsions usually cream at the surface, due to their density difference. By contrast, double emulsions with fluorinated shells sink in aqueous media, making them easier to handle and analyze them. Because double emulsions are dispersed in an aqueous solution, they can be characterized and sorted with automated cell sorting such as FACS. [120,121] Moreover, nutrients for cells can be introduced into double emulsions by dissolving them in the outer phase and transporting them to the core. Additionally, double emulsions can be great templates to produce microcapsules by solidifying the shell. [122]

1.4.8   Production of Double Emulsions

Double emulsions in the size range of around 100 μm can be produced in a controlled way using microfluidic glass capillary devices [123] or PDMS based devices [105, 124]. Glass microcapillary devices are produced by heating glass microcapillaries and pulling them to the desired thickness of the tips. [36] A circular capillary (injection capillary) is introduced into a bigger square capillary. From the other side, a tapered collection capillary is introduced. The orifice of this capillary has to be aligned manually with the injection capillary.

The inner phase flows through the injection capillary, where the middle phase is flown between the injection capillary and the outer capillary. From the opposite side, the outer phase is introduced, between the collection capillary and the outer square capillary. At the junction, where the injection capillary meets the collection capillary, double emulsion can be formed, as shown in Figure 1.14. The size of the orifice will determine the size of the formed drops. In addition, the dimensions of the double emulsions can to some extent be controlled with the fluid flow rate. Since glass is chemically inert to a lot of organic solvents, it is a very convenient material to perform microfluidic experiments. However, capillaries must be aligned manually, making it difficult for scale up as each device is slightly different.
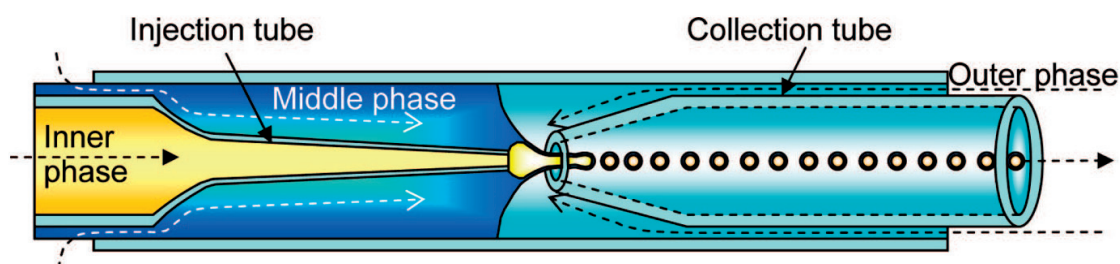
Figure 1.14:   Schematic illustration of double emulsion production using a microfluidic glass capillary device. [125]

Another technique to produce double emulsions is to use microfluidic PDMS devices that are made by using soft lithography [126] and are therefore easy to fabricate, cheap, versatile in terms of channel geometry and reproducible. [126] By contrast, many organic solvents swell PDMS, making it impossible to use the devices with these solvents, unless the channels are made solvent resistant. [82] This can be achieved for example by coating them with parylene. [127] Recently a glass microfluidic device made by selective etching has been introduced through chemical vapor deposition, combining the "copy-paste" approach of the PDMS devices with the solvent compatibility of glass. [128] An optical micrograph of a PDMS-based microfluidic device in operation is shown in Figure 1.15.
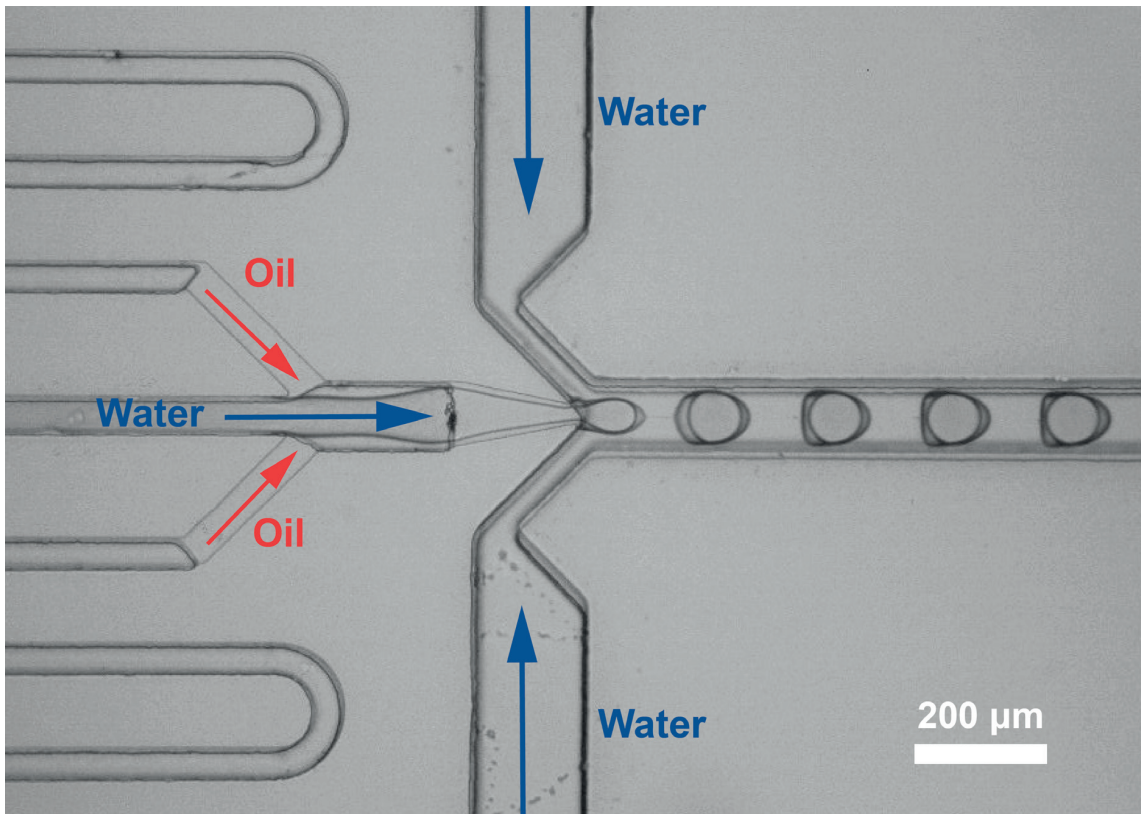
Figure 1.15: Optical microscopy image of a microfluidic PDMS double emulsion device in operation. Arrows indicate the flow direction of the water and oil phases.

To make water/oil/water double emulsions, it is necessary to selectively surface treat the different channels. To ensure the middle oil phase wets the channel walls in the first part of the device, the surfaces of the channels must be rendered hydrophobic. To let the water wet the collection channel the main channel downstream the last junction must be hydrophilic. Surface treatment can be achieved by selectively injecting appropriate solutions into the different channels, as detailed in section 2.4.1

Chapter 2

Materials and Methods

In this chapter, we detail the experimental methods and techniques used throughout this work. Parts of this chapter are taken from G. Etienne, M. Kessler, E. Amstad: "Influence of fluorinated surfactant composition on the stability of emulsion drops" [1] and G. Etienne, A. Vian, M. Biočanin, B. Deplancke, E. Amstad: "Cross-talk between emulsion drops: how are hydrophilic reagents transported across oil phases?". [2]

Contents

2.1 Surfactant Synthesis

The synthesis of the fluorinated surfactants is based on a coupling reaction of the activated fluorinated block containing an acid chloride end group and an amine group attached to the PEG. The surfactant synthesis is based on the method described previously that was slightly adapted. [83] The schematic of the synthesis for the triblock and diblock copolymer surfactant is shown in Figure 2.1.
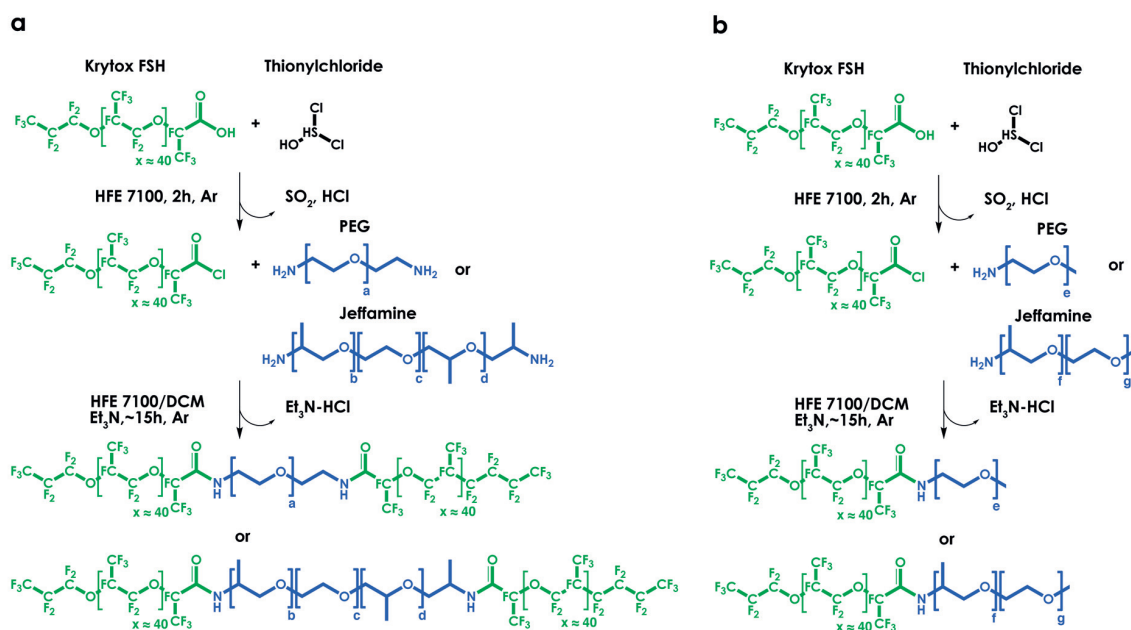
Figure 2.1: Reaction scheme of the synthesis of the (**a**) triblock copolymer and (**b**) diblock copolymer surfactant. The letters indicate the approximate lengths of the different blocks in the hydrophilic groups. A summary is given in Table 2.1.

In brief, 1 mol equivalent of Krytox FSH 157 (∼7000 g/mol, Chemours, USA) is dissolved at 0.1 g/mL in dry Novec HFE-7100 (3M, USA). HFE-7100 is dried using molecular sieves and bubbled with argon. The reaction is performed under argon using dry glassware. The carboxylic end group of the Krytox FSH 157 is activated by adding 10 mol equivalent of thionyl chloride (Merck, Germany) and refluxed at 65°C for 2h under argon atmosphere. Unreacted thionyl chloride is removed by heating the reaction to 90°C under reduced pressure for 1 hour. After cooling the activated Krytox FSH to room temperature, it is re-dissolved in dry HFE-7100 under argon. To dry the hydrophilic block, 1.1 mol equivalent of the hydrophilic block for diblock copolymers or 0.57 mol equivalent of the hydrophilic block for triblock copolymers are dissolved in trifluorotoluene (Sigma-Aldrich, USA) at 0.1 g/mL and heated to 120°C. By slowly reducing the pressure the solvent is evaporated using a bridge connected to a Schlenk flask. To synthesize the diblock copolymer we use monofunctional amine-terminated PEG (Jenkem Mw 295 g/mol, 5000 g/mol) and Jeffamine (Huntsman M-600, M-1000, M-2005) and for the synthesis of the triblock copolymer we use homobifunctional amine terminated PEG (Jenkem Mw 368 g/mol, 600 g/mol, 5000 g/mol) and Jeffamine (Huntsman, Jeffamine ED-600, ED-900, ED-2003). After the majority of the solvent is evaporated and the reaction mixture is cooled to room temperature, anhydrous dichloromethane (Sigma-Aldrich, USA) is added until all the PEG is re-dissolved. To drive the reaction to completion, 1.5 mol equivalent of triethylamine (Sigma-Aldrich, USA) is added to the PEG solution. The PEG solution is added to the activated Krytox and refluxed overnight at 65°C under argon atmosphere. The surfactant is subsequently purified from excess unreacted PEG by dissolving the product in a mixture of methanol (Sigma-Aldrich, USA) and

Name	Molecular Weight Hydrophilic Block [g/mol]	Molecular Weight PEG [g/mol]	Repeat Units	Ratio of R_g [-]	α' [-]	cmc [mM]	$\gamma_{(1\,wt.\%)}$ [mN/m]	$\gamma_{(5\,mM)}$ [mN/m]	ρ [1 nm^{-2}]
FSH$_2$-PEG310	~370	~310	a=7	0.408	0.23	~0.5	~15.8	~7.9	0.77
FSH$_2$-PEG600	~600	~594	a=13.5	0.570	0.36	~1	~10.9	~3.6	0.73
FSH$_2$-Jeffamine600	~640	~400	b+d=3.6, c=9	0.463	0.27	~1	~8.5	~2.7	0.62
FSH$_2$-Jeffamine900	~930	~550	b+d=6, c=12.5	0.546	0.34	~2	~4.3	~2.6	0.68
FSH$_2$-Jeffamine2000	~2090	~1720	b+d=6, c=39	0.964	0.73	~0.3	~26.1	~23.1	0.64
FSH-PEG220	~280	~220	e=5	0.345	0.37	~0.5	~10.9	~7.6	1.17
FSH-Jeffamine600	~580	~40	f=9, g=1	0.154	0.13	~2	~9.7	~4.3	1.03
FSH-Jeffamine1000	~1030	~840	f=3, g=19	0.672	0.90	~4	~18.3	~12.8	2.10
FSH-Jeffamine2000	~1960	~260	f=29, g=6	0.377	0.42	~0.3	~21.8	~16.9	1.38

Table 2.1: Overview of the different fluorinated surfactants synthesized and their properties. R_g is the radius of gyration, α' is the inverse packing parameter and ρ the packing density at the water-air interface.

HFE-7100. To separate the surfactant from unreacted PEG, we centrifuge the product at 3000 g and 3°C for 15 min (Mega Star, 1.6R, VWR) and removed the top layer. This washing step is repeated three times before the surfactant is dried using a rotary evaporator (Hei-VAP, Heidolph, Germany) and a freeze dryer (FreeZone 2.5, Labconco, USA).

2.2 Characterization of Surfactants

2.2.1 Structure of Krytox

To characterize the surfactant we measure Matrix-Assisted Laser Desorption Ionization (MALDI-TOF) (MALDI-TOF AutoFlex speed (Bruker)) of Krytox 157 FSH, as shown in Figure 2.2. Since the Krytox could not be ionized easily, only parts of the polymer could be detected, and it was not possible to determine the exact molecular weight of the Krytox. The pattern of the detected signal corresponded to the repeat unit of the perfluoro polyether. The MALDI experiments were performed by Dr. Bjoern Schulte.
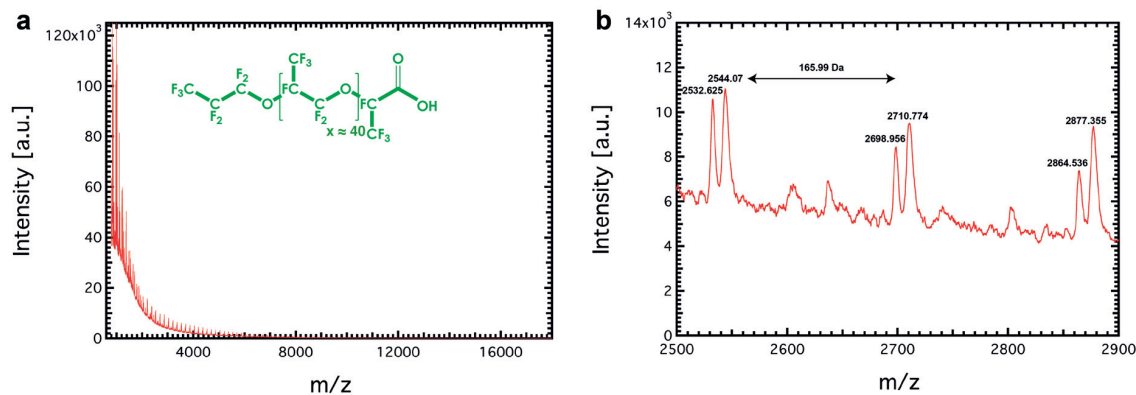
Figure 2.2: (**a**) Overview and (**b**) zoom in MALDI spectra of Krytox 157 FSH. The repeating pattern corresponds to the repeat unit of Krytox molecule with a molecular weight of 166 g/mol.

2.2.2   Infrared Spectroscopy

The surfactants are analyzed using Fourier transform infrared spectroscopy (Nicolet 6700, ThermoFisher Scientific, USA), as shown in Figure 2.3. The peak at 1775 cm^{-1} results from the -COOH of the Krytox. [118,129,130] Upon coupling of FSH to Jeffamine600 a peak at 1700 cm^{-1} appears, as shown in Figure 2.3. We assign this peak to the (C=O) bond of the amide, which is formed during the coupling reaction of the acid chloride end group of the Krytox FSH 157 and the amine end group of the hydrophilic block. [129,131] We observe the same changes upon coupling FSH to the other hydrophilic blocks, as shown in Figures A.1-A.8 in the appendices on page 94. Others observe the newly formed peak at around 1720 cm^{-1}. [112,118,132]
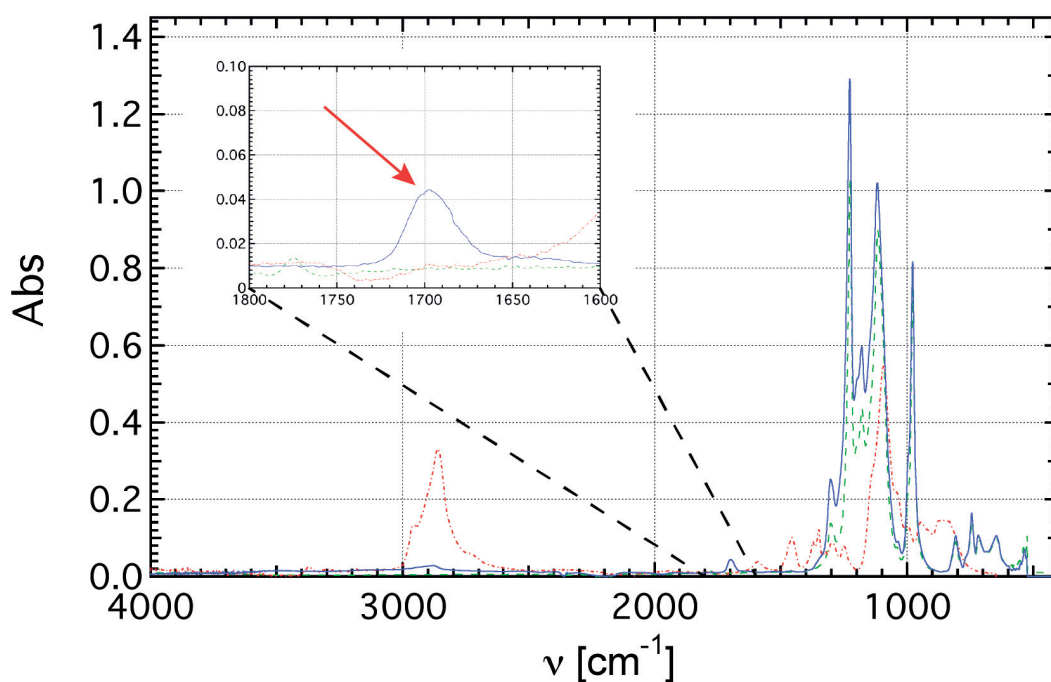
Figure 2.3: The absorption (Abs) is shown as a function of the wavenumber (ν) for the fluorinated block FSH ($\_$ $\_$), Jeffamine 600 ($\_$.) and the FSH$_2$-Jeffamine600 ($\_$). The small peak appearing at 1700 cm^{-1}, indicated with a red arrow in the inset, is assigned to the amide bond that indicates successful coupling of the Jeffamine and FSH blocks.

2.2.3   Pendant Drop

Additionally, the surfactants are analyzed by measuring the interfacial tension with the pendant drop method using a drop shape analyzer (Krüss, DSA30, Germany). A drop of oil containing fluorinated surfactant is formed in a water bath, as shown in Figure 2.4.
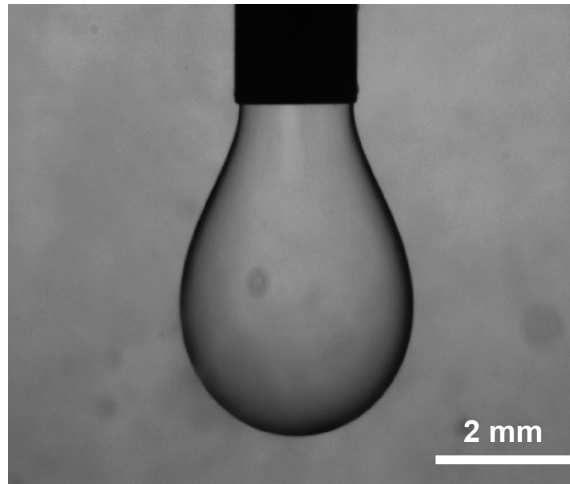
Figure 2.4: Image of a fluorinated oil drop in water used to deduce the interfacial tension with the pendant drop setup.

First, the diameter of the drop is enlarged to a maximum such that the drop does not fall from the needle. Once the injection volume is known, the interfacial tension is measured at 1 s intervals. It initially decreased until it reached the plateau value which we report. Each measurement is repeated at least three times to determine the average value and its standard deviation. For the interfacial tension of pure HFE-7500 in water, we measure $\sim$ 50 mN/m. At a concentration of 5 mM of the different surfactants, a concentration that exceeds the cmc of surfactants in HFE-7500, the interfacial tension values are between 2.6 - 23.1 mN/m, as summarized in table 2.1 on page 28.

2.3   PDMS Microfluidic Device Fabrication

We fabricate our microfluidic devices from poly(dimethyl siloxane) (PDMS) (Dow Corning, USA) using soft lithography. [39] A schematic of the fabrication of the microfluidic device is shown in Figure 2.5.

Master production

Print photomask   **Spincoat photoresist onto silicon wafer**   **UV light exposure through photomask**   **Develop**

Microfluidic device production

Pour PDMS and let it cure   **Cut PDMS from mould**   **Bond to glass slide or PDMS**
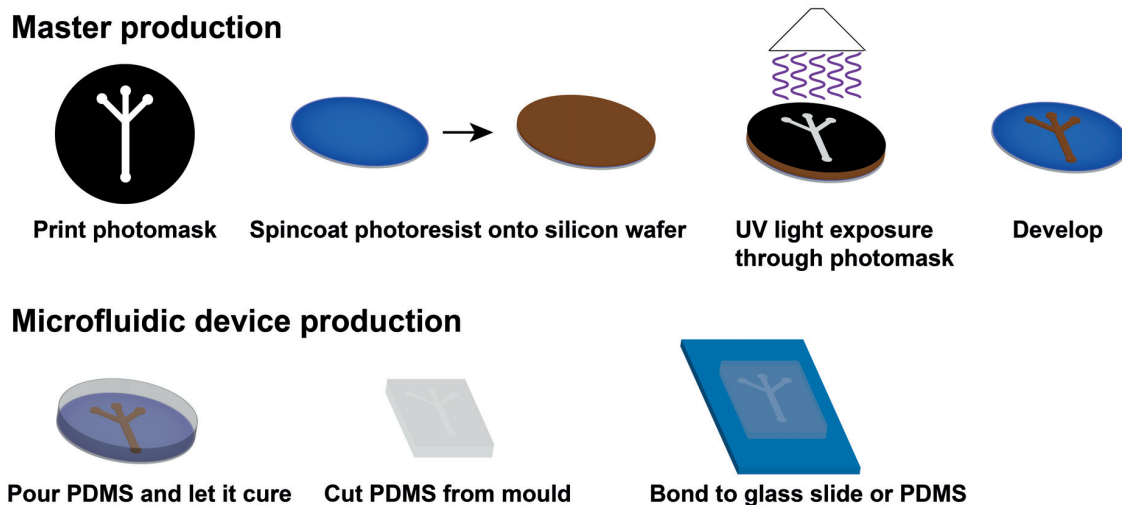
Figure 2.5: Schematic illustration of the fabrication of a microfluidic device.

The desired channel layout is drawn in AutoCAD (AutoCAD 2017) and printed with a high resolution onto a photomask (25400 dots per inch, dpi) (OutputCity, USA). In a first step, the negative photoresist SU-8 (Series 3000,Microchem, USA) is spin coated onto a silicon wafer with a well-defined thickness. The wafer containing the photoresist is pre-baked on a hotplate at 95°C. The photomask is placed onto the wafer and exposed to UV-light. The exposed areas are cross-linked because UV light can pass through the photomask and locally initiate a polymerization reaction. After exposure to UV light, the wafer is post-baked on a hotplate at 95°C. For double emulsion device, additional layers are spin coated onto the wafer. In this step, it is crucial to align the photomask correctly before the second layer is exposed to UV light. Next, the photoresist which was not cross-linked can be removed by dissolving it in propylene glycol methyl ether acetate (PGMEA, Sigma-Aldrich). The wafer containing the desired pattern is called the *master*. To facilitate the removal of PDMS, we render the surface of the wafer fluorophilic. Therefore, we treat it with a solution of 2 wt% of trichloro(1H,1H,2H,2H-perfluorooctyl)silane (Sigma-Aldrich, USA) dissolved in HFE-7500 for 2 minutes. Uncured PDMS and a cross-linker (Sylgard 184 silicone elastomer kit, Dow Corning) are mixed in a 10:1 ratio, and poured onto the wafer. The wafer containing the PDMS and cross-linker was degassed for several minutes and placed in an oven at 70°C overnight. Under heat, the PDMS cross-links and can be peeled off the wafer, now containing the structure of the surface of the PDMS. Holes to connect the tubing from the syringe pumps are punched into the PDMS using a 1 mm hole puncher. In the last step, the PDMS can be activated in an oxygen plasma and bonded to a glass slide or another PDMS piece, resulting in a microfluidic device.

To produce double emulsions, the device consists of two PDMS pieces bonded together. The double emulsion device contains two junctions, where first the inner and the middle phases co-flow and the second where the double emulsions are formed. To facilitate drop formation at the

second junction, it is 3D. At this junction, the outer phase shears off the double emulsion from all four sides. A profilometer image of the two PDMS pieces that form the double emulsion device is shown in Figure 2.6.
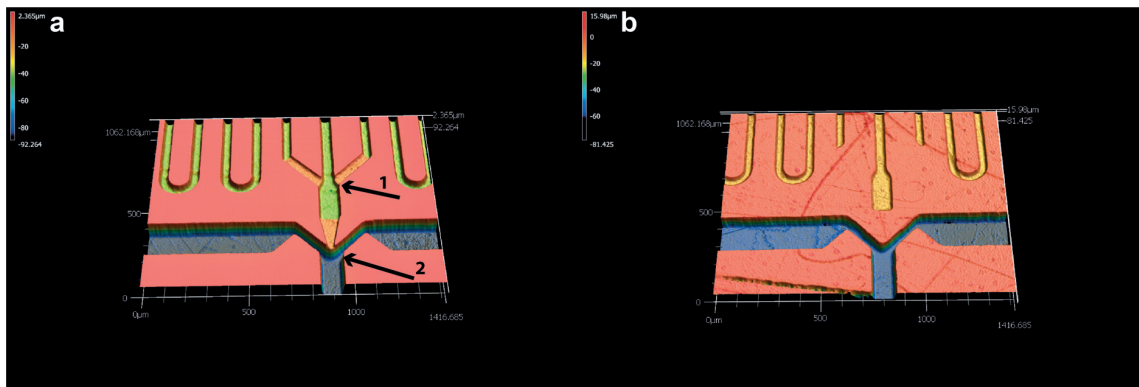
Figure 2.6:   Profilometer image of the two PDMS pieces that will be bonded together to form the double emulsion device. The arrow in the image indicates the first 2D and second 3D junction.

2.4   Production of Emulsion Drops

2.4.1   Surface Treatment of Devices

To form drops in microfluidic devices, channels must be non-wetting to the inner phase. To form aqueous drops in a fluorinated oil, the channel walls are made fluorophilic by injecting an HFE-7500-based solution containing 2 wt% of trichloro(1H,1H,2H,2H-perfluorooctyl)silane (Sigma-Aldrich, USA) for 10 min.

To produce double emulsions, the different parts of the main channel of the microfluidic device must be surface treated differently. First, the PDMS device is activated with 1M NaOH solution that is kept in the channels for 10 min before it is removed with compressed air. To render the main channel downstream the 3D junction hydrophilic, we treat it with an aqueous solution containing 2 wt% polydiallyldimethylammonium chloride (Sigma-Aldrich, USA). To render the injection channels fluorophilic, we treat them with an HFE-based solution containing 2 vol.% of trichloro(1H,1H,2H,2H-perfluorooctyl)silane (Sigma-Aldrich, USA). The solutions are kept in the channels for 30 min before the channels were dried with compressed air.

2.4.2   Production of Single Emulsion Drops

For the production of single emulsion drops, liquids are injected with syringe pumps (Cronus Sigma 1000, Labhut, UK). Aqueous drops are produced using a flow focusing PDMS-based microfluidic devices, as described in section 2.3.

2.4.3 Production of Double Emulsion Drops

For the production of double emulsion drops, liquids are injected with syringe pumps (Cronus Sigma 1000, Labhut, UK). Typically the outer phase is injected at $\sim$6000 μL/h, the middle phase at $\sim$1300 μL/h, and the inner phase at $\sim$1200 μL/h. The inner phase often contains 15% PEG 6000 (Carl Roth, Germany), to increase the viscosity and facilitate the formation of the double emulsion. To study the leakage of a dye, it is added to the inner phase. The middle phase is composed of HFE-7500 containing different concentrations of a surfactant. The outer aqueous phase is composed of water containing 10 wt% polyvinyl alcohol (PVA) 13000-18000 g/mol (Sigma-Aldrich, USA), which helps stabilize the double emulsions. The osmolarity of the two aqueous phases is measured using an osmometer (Advanced Instruments, Fiske 210) and matched by adding D(+)-Saccharose.

Chapter 3

Influence of Fluorinated Surfactant Composition on the Stability of Emulsion Drops

Gianluca Etienne, Michael Kessler and Esther Amstad

In this chapter, we explain how the composition of fluorinated surfactants affects the stability of single emulsion drops. We compare diblock to triblock copolymer surfactants and in addition we study how a change in the molecular weight of the hydrophilic block affects mechanical and temperature stability. Finally, we provide guidelines for the selection of optimized surfactants as a function of the composition of the inner and outer phase.

This chapter is adapted from the paper entitled **"Influence of Fluorinated Surfactant Composition on the Stability of Emulsion Drops"**, authored by Gianluca Etienne, Michael Kessler and Esther Amstad, published in *Macromolecular Chemistry and Physics*, in 2017, volume 218 [1].

Gianluca Etienne performed all the experiments and Michael Kessler helped with repeats of the experiments to get statistics.

Contents

3.1 Abstract

Aqueous drops of a well-defined size are often used as small containers for conducting chemical and biochemical reactions, cell assays and as templates to produce microparticles. To prevent their coalescence, they must be stabilized, for example, using surfactants. The ability of different nonionic diblock and triblock copolymer surfactants to stabilize water drops that are dispersed in fluorinated oils is compared. In particular, the influence of the length of their hydrophilic poly(ethyleneglycol) block on the drop stability is studied. The stability of drops coated with triblock copolymers inversely scales with the interfacial tension, whereas that of drops coated with diblock copolymers scales with their packing density. Surfactants whose ratio of the radii of gyration of PEG to the hydrophobic block (FSH) is between 0.54 and 0.67 impart the best stability to aqueous drops containing low salt concentrations. By contrast, surfactants whose ratio of the radii of gyration is between 0.34 and 0.37 impart the best stability to aqueous drops containing high salt concentrations. Hence, the choice of the best surfactant strongly depends on the composition of the fluids.

3.2 Introduction

Aqueous drops are often used as pico- or even femtoliter sized vessels for conducting chemical reactions, [133] polymerase chain reactions (PCRs), [134] manipulating genes, [99, 135]

cells, [69, 75, 136, 137] viruses, [138–141] or small organisms, [75] and as templates for the production of microparticles of well-defined size and composition. [133] Drops can be stabilized with commercially available poly(perfluoropropylene glycol)-carboxylates; however, the charged carboxy group can interact with biomacromolecules, risking a change in their conformation and therefore a loss in their function. [77] To overcome this limitation, perfluorinated polyether blocks have been covalently linked to uncharged hydrophilic blocks, such as poly(ethylene glycol) (PEG) [83] or poly(methyl glycerol). [111] The resulting block copolymers impart good stability to aqueous drops at room temperature. However, the stability of drops coated with this surfactant is significantly lower if kept at elevated temperatures. As a result, in many cases, drops coalesce at elevated temperatures even though, under certain conditions, some drops remain intact. The reduced drop stability at elevated temperatures can be assigned to the decrease in the solubility of PEG with increasing temperature, which leads to a change in its conformation that negatively affects the surfactant quality. [142, 143] This is inconvenient because common applications, such as PCR, [143] or in some cases the conversion of drops into particles [144] require heating drops to elevated temperatures. Moreover, in many cases, this surfactant fails to stabilize drops containing high salt concentrations because the solubility of PEG also decreases with increasing salt concentrations. [143] This is inconvenient because salts are required for experiments conducted under physiologic conditions, making the use of these drops for many biological applications difficult. To improve the stability of drops subjected to these demanding conditions, more efficient surfactants must be developed. The efficiency of nonionic amphiphilic block copolymer surfactants to stabilize aqueous drops in hydrocarbon-based oils has been shown to depend on the length of the PEG block. [83] Whether similar principles also apply for fluorinated surfactants remains to be determined. A better understanding of this correlation would facilitate the choice of an appropriate surfactant and enable tuning the drop stability to the requirements of the specific application.

In this chapter, we describe the influence of the length of the PEG block of nonionic diblock and triblock copolymer surfactants on their ability to stabilize aqueous drops in fluorinated oils. Surfactants whose ratio of radii of gyration of the PEG to the hydrophobic block (FSH) is between 0.54 and 0.67 impart the highest stability to drops containing no salt. By contrast, surfactants whose ratio of radii of gyration of PEG to the hydrophobic block is between 0.34 and 0.37 impart the highest stability to salt-containing drops. Remarkably, drop stability cannot unequivocally be related to the interfacial tension or surfactant packing density: While the stability of drops coated with triblock copolymers increases with decreasing interfacial tension, that of drops coated with diblock copolymers increases with increasing packing density. Thus, the choice of the surfactant that results in the highest drop stability strongly depends on the exact composition of the fluids.

3.3 Experimental Section

3.3.1 Surfactant Synthesis

Details to the surfactant synthesis are shown in section 2.1 on page 26. To determine if the coupling was successful, we measure FTIR as described in section 2.2.2.

3.3.2 Interfacial Tension Measurements

The interfacial tension is quantified using the pendant drop method as described in section 2.2.3 on page 29. A drop composed of fluorinated oil Novec HFE-7500 (3M, USA) containing 1 wt% of surfactant is formed in Millipore water (Synergy, Merck Millipore, Germany) that optionally contains 150×10^{-3} M or 1 M NaCl (Sigma-Aldrich, USA).

3.3.3 Packing Density Measurements

The mean molecular area of the surfactants adsorbed on the air-water interface is determined with a Langmuir trough (KN2002, KSV Nima, Biolin Scientific, Finland). We approximate it to be similar to that at the oil-water interface. We employ Millipore water, water containing 150×10^{-3} M and 1 M NaCl as liquids. To measure the surface pressure, we use a platinum Wilhelmy plate. To test if the trough and the Wilhelmy plate are clean, it was made sure the surface pressure stays below 0.3 mN/m when closing the barriers without adding any surfactant. 0.1 wt% of the surfactant is dissolved in Novec HFE-7100 and 50 μL of this solution is slowly added to the water–air interface. To ensure all the HFE-7100 is evaporated and the surfactants attained their equilibrium conformation, we wait for 8 h if pure water was used, for 3 h if water containing 150×10^{-3} M NaCl, and for 1 h if water containing 1 M NaCl before the experiments are performed by closing the barriers at a speed of 5 mm/min. The area where the slope of the surface pressure against the mean molecular area clearly decreasing for the first time is assigned to the minimum area the surfactant occupies without external pressure, A_m, and this value is used to calculate the surfactant packing density, $\rho = A_m^{-1}$.

3.3.4 Production of Drops

Aqueous drops are produced using PDMS-based microfluidic devices, as described in section 2.3. They are dispersed in HFE-7500 or FC-40 (3M, USA) containing 1 wt% of surfactant. Drops are composed of pure water (MilliQ, Merck, Germany), water containing 20 wt% PEG 6000 g/mol (Rotipuran, Carl Roth, Germany), water containing 150×10^{-3} M NaCl, 1 M NaCl, or a mixture of 1 M NaCl and 20 wt% PEG.

3.3.5 Mechanical Stability of Emulsion Drops

To test the mechanical stability of drops, 30 μL of densely packed drops dispersed in HFE-7500 are added into a 1 mL Eppendorf tube (VWR, USA). The samples are accelerated for 1 min at room temperature using a centrifuge (VWR microstar 12, Labogene, Denmark) and the drop integrity is monitored using optical microscopy. If some of the drops retain their integrity, the acceleration is repetitively increased by 50 g up to a total acceleration of 250 g. If drops still retain their integrity, the acceleration is further increased in steps of 1000 g until all the drops coalesce. The acceleration at which all the drops coalesced is reported, because this transition is easier to quantify than the acceleration where the first drops start to coalesce. Each measurement is repeated at least three times, each time using a different batch of drops to calculate an average and standard deviation.

3.3.6 Temperature Stability of Emulsion Drops

To test the temperature stability of drops, 30 μL of densely packed drops dispersed in HFE-7500 are added into a 1 mL Eppendorf tube (VWR, USA) and the sample are incubated at 30 °C for 10 min (Thermal Shake Touch, VWR, Denmark). The drop integrity is monitored using optical microscopy. If some drops remain intact, the temperature is increased by 5 °C and drops are incubated at this increased temperature for 10 min. This procedure is repeated until all drops coalesced and this temperature is reported. To obtain statistics, each data point is measured at least three times, each time using a different batch of drops.

3.4 Results and Discussion

To test the influence of the surfactant composition on the drop stability, we produce aqueous drops with a diameter of 160 μm, using PDMS-based microfluidic flow-focusing devices, [83] as shown in Figure 3.1a. We use fluorinated oil, HFE-7500, containing 1 wt% surfactant as an outer phase and water containing 20 wt% of PEG6000 as an inner phase; PEG is added to the inner phase to increase its viscosity, thereby facilitating drop formation. To quantify the mechanical stability of drops, we centrifuge them and measure the minimum acceleration that causes all drops to coalesce within 1 min. To quantify the thermal stability of drops, we heat them and measure the minimum temperature where all drops coalesce within 10 min.
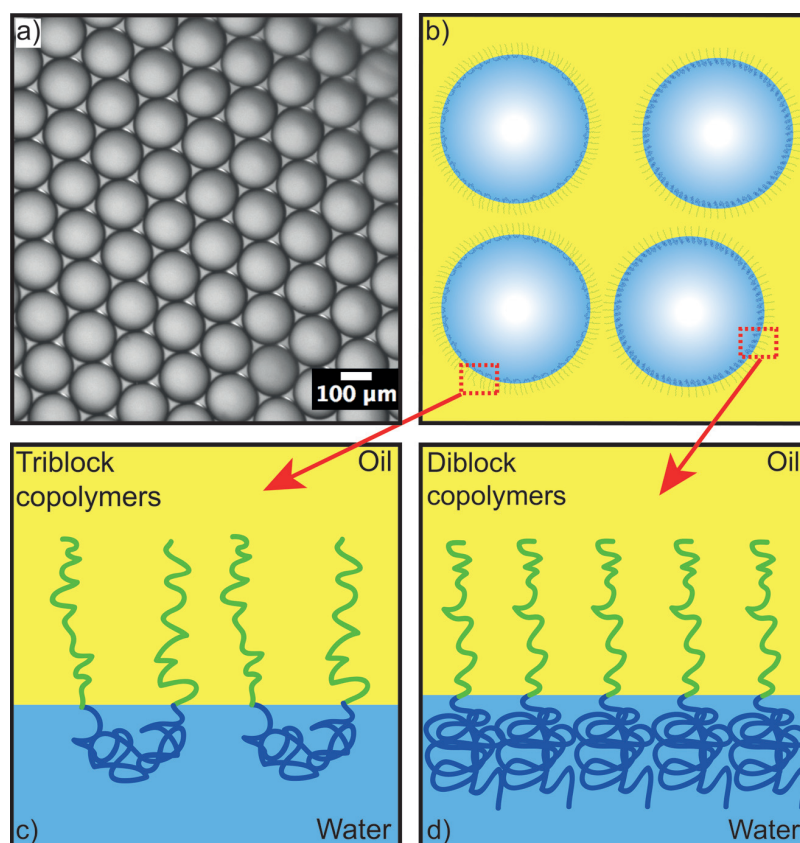
Figure 3.1: (**a**) Microscope image of water in oil emulsion drops made by a microfluidic flow-focusing device. (**b**) Overview and (**c,d**) close-up schematic illustrations of water drops dispersed in oil stabilized by (**c**) triblock and (**d**) diblock copolymer surfactants.

3.4.1 Triblock Copolymer Surfactants

Influence of the PEG Length on Drop Stability

To test if the stability of drops coated with fluorinated block copolymer surfactants depends on the PEG block length, we synthesize two different triblock copolymers. Each of them contains two fluorinated blocks (FSH_2) that are separated by a hydrophilic PEG block, FSH_2-PEG, as shown schematically in Figure 2.1 on page 27. One surfactant contains a PEG with a molecular weight of 310 g/mol, the other one with a molecular weight of 594 g/mol, as summarized in Table 2.1 on page 28. The second surfactant closely resembles FSH_2-PEG600, the surfactant, which has been reported to stabilize aqueous drops in fluorinated oils efficiently. [83] Indeed, this surfactant imparts a higher stability to drops than FSH_2-PEG310, as shown in Figure 3.2a, suggesting that drop stability increases with increasing PEG molecular weight. To test if we can increase drop stability even more by increasing the PEG length, we synthesize FSH_2-PEG5000. Unfortunately, the solubility of this surfactant in HFE-7500 is so low that it precipitates if dispersed at 1 wt% in HFE-7500 at room temperature, resulting in very low drop stability.

To vary the PEG length over a wider range, we exchange the PEG block with Jeffamine, which is composed of a linear PEG whose two ends are covalently linked to two polypropylene oxide (PPO) blocks, as shown in Figure 2.1 on page 27. Jeffamine is contained in many of the fluorinated block copolymer surfactants used to stabilize aqueous drops. [130,145,146] To test the influence of the PPO blocks on the drop stability, we synthesize a triblock copolymer surfactant with a Jeffamine whose molecular weight is 640 g/mol; this Jeffamine contains a 400 g/mol-sized PEG block. Drops coated with this surfactant display a lower stability than those coated with FSH$_2$-PEG600, as shown in Figure 3.2a. This result suggests that the volume ratio of PEG to FSH must be optimized to achieve maximum drop stability. To test this suggestion, we synthesize a surfactant containing Jeffamine900 that encompasses a PEG block with a molecular weight of 550 g/mol, which is very similar to the PEG contained in FSH$_2$-PEG600. Indeed, drops coated with this surfactant also display a very high stability; these drops do not coalesce if accelerated up to 11 400 g, which is the highest acceleration our centrifuge can be operated at, as shown in Figure 3.2a. To test the influence of the PEG length on the drop stability over a wider range, we synthesize surfactants with longer PEG blocks. Drops coated with these surfactants display an inferior stability, as shown in Figure 3.2a, indicating that there is an optimum PEG length for triblock surfactants, where they stabilize drops most efficiently.
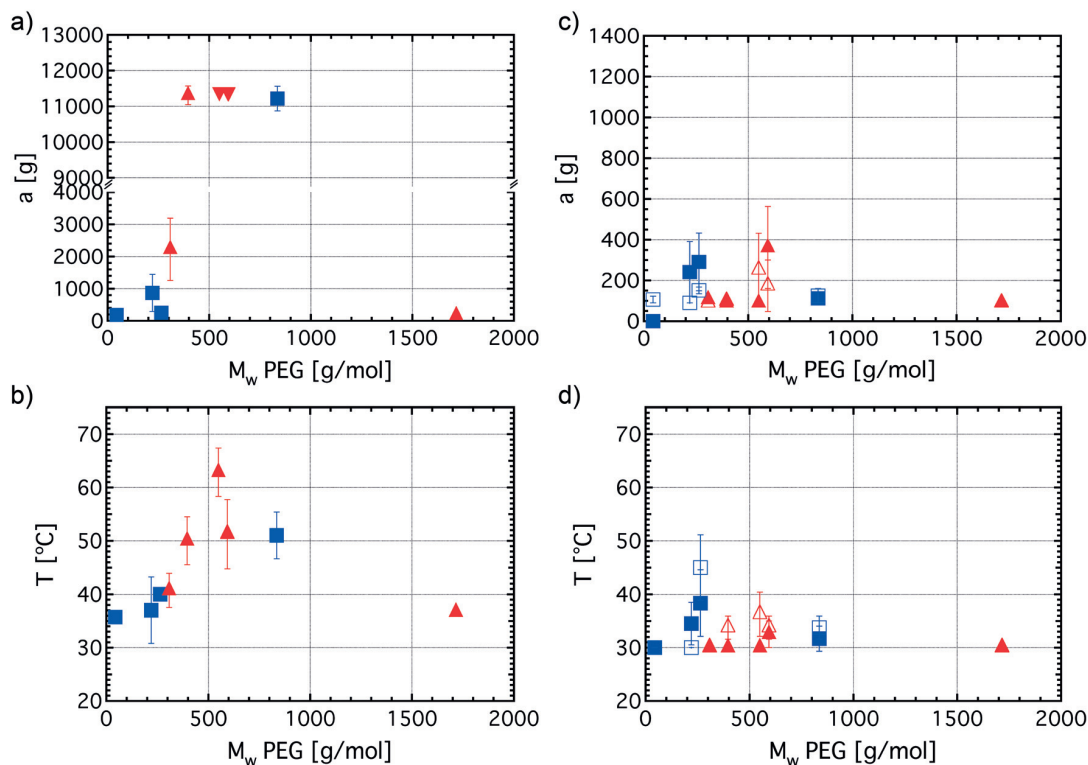
Figure 3.2: Stability of drops coated with surfactants containing PEG blocks with different molecular weights if (**a,c**) accelerated and (**b,d**) stored at elevated temperatures. Aqueous drops containing (**a,b**) 20 wt% PEG6000 and (**c,d**) 1 M NaCl (filled symbols) or 150×10^{-3} M NaCl (empty symbols) are stabilized with triblock (▲) and diblock (■) copolymers. Drops that did not coalesce at 11 400 g, the maximum achievable acceleration, are indicated with the triangles pointing down (▼).

Drop Stability at Elevated Temperatures

Many biological applications require drops to be stable at elevated temperatures. To test if good mechanical drop stability translates into good temperature stability, we visualize drops after they have been stored at different temperatures for 10 min using optical microscopy. Drops stabilized with FSH_2-Jeffamine900 display the highest stability if stored at elevated temperatures: They only coalesce when stored for 10 min at 62 °C or above, as shown in Figure 3.2b. By contrast, drops stabilized with FSH_2-600 and FSH_2-Jeffamine600 only remain intact up to 50 °C and those stabilized with all the other tested surfactants already coalesce at 40 °C or below. These results indicate that drops that display a high mechanical stability also display a high-temperature stability. Moreover, the PPO blocks contained in Jeffamine900 positively affect drop stability if the volume ratio of PEG to FSH is optimized.

To relate the optimum hydrophilic block length to the length of the entire surfactant, we compute the ratio of the radius of gyration of PEG, $R_g(PEG)$, to that of the hydrophobic block, $R_g(FSH)$, assuming both blocks are dispersed in theta solvents using equation 3.1.

$$< R_g >^2 = \frac{< r >^2}{6} = \frac{(N \times a^2 \times \frac{1+cos(\theta)}{1-cos(\theta)})^2}{6} \qquad (3.1)$$

Here, N is the number of repeat units (see Table 2.1, page 28), a the length of a repeat unit and θ the angle between the C-C bond, which we take as 109.5°. We calculate a as follows:

$$a = 0.154nm \times sin(54.75) + 2 \times 0.143nm \times sin(54.75) = 0.359nm \qquad (3.2)$$

We use this ratio instead of the hydrophilic–lipophilic balance (HLB) value because HLB values are measures for the weight percentage of the hydrophilic block in relation to the total molecular weight of the surfactant. Because the molecular weight of a fluorinated block is much higher than that of a hydrocarbon-based block with a similar number of carbon atoms, the HLB value will be much lower than that of hydrocarbon-containing surfactants with similar volume ratios. We find that triblock surfactants with a ratio $R_g(PEG)/R_g(FSH)$ of 0.56 impart the best stability to drops, as shown in Figure 3.3.
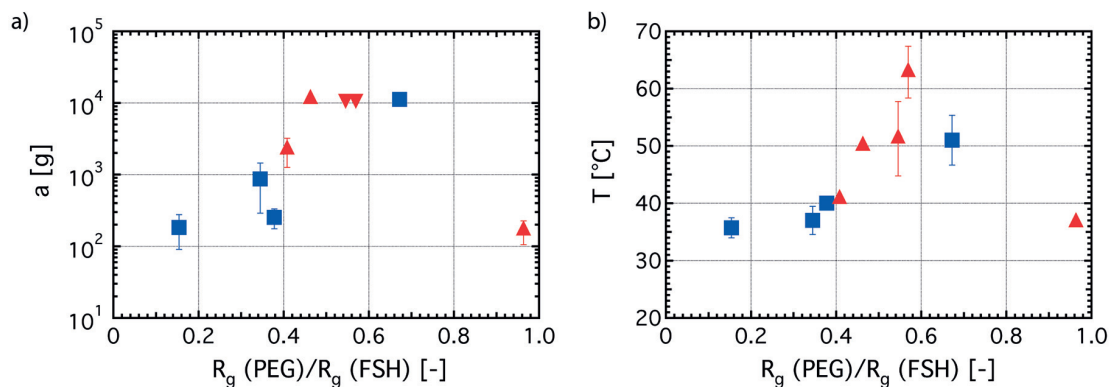
Figure 3.3: Influence of the ratio of the radii of gyration, R_g, of PEG to FSH on the stability of aqueous drops containing 20% PEG coated with diblock (■) and triblock (▲) copolymers. (**a**) The mechanical stability of drops coated with different surfactants, measured at the maximum acceleration, a, drops can sustain. Drops that did not coalesce at the maximum acceleration we could achieve are represented by triangles that point down (▼). (**b**) Temperature, T, when all drops coalesced as a function of the ratio of the radii of gyration of PEG to FSH.

Influence of Fluid Viscosity on Drop Stability

If drops are employed as vessels to conduct polymerase chain reactions (PCR) or for cell encapsulation, they often contain no or low concentrations of polymers. In these cases, the viscosity of the aqueous phase is lower than what we studied so far. To investigate the influence of the viscosity of the inner phase on the drop stability, we produce aqueous drops that do not contain any free PEG or any other additives. Pure aqueous drops, whose viscosity is three times lower than that of drops containing 20 wt% PEG, also display the highest stability if coated with FSH$_2$-Jeffamine900, as shown in Figure 3.4. This suggests that the viscosity of the inner phase does not strongly influence drops stability.

a)

b)
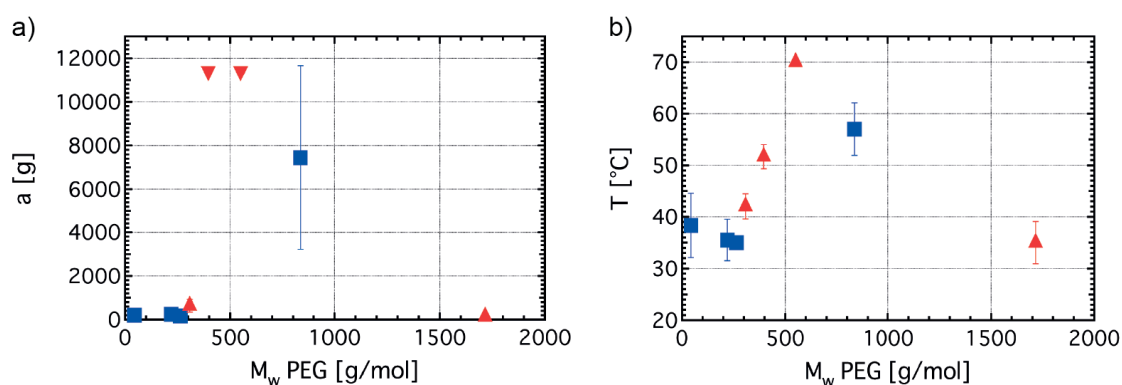
Figure 3.4: The stability of aqueous drops not containing any free PEG or salt, coated with triblock (▲) or diblock (■) surfactants if (**a**) accelerated and (**b**) stored at elevated temperatures as a function of the PEG molecular weight. Drops coated with triblock copolymer surfactants that did not coalesce at the maximum speed our centrifuge could achieve are indicated with triangles that point down (▼).

Indeed, the stabilities for pure aqueous drops coated with any of the tested surfactants are very similar to those of PEG-containing drops, indicating that the viscosity of the inner phase does not significantly influence the drop stability. To test if the viscosity of the outer phase affects drop stability, we produce aqueous drops contained in another fluorinated oil, FC-40 (3M, USA), as schematically shown in Figure 3.5, whose viscosity is almost three times higher than that of HFE-7500.

a)

b)
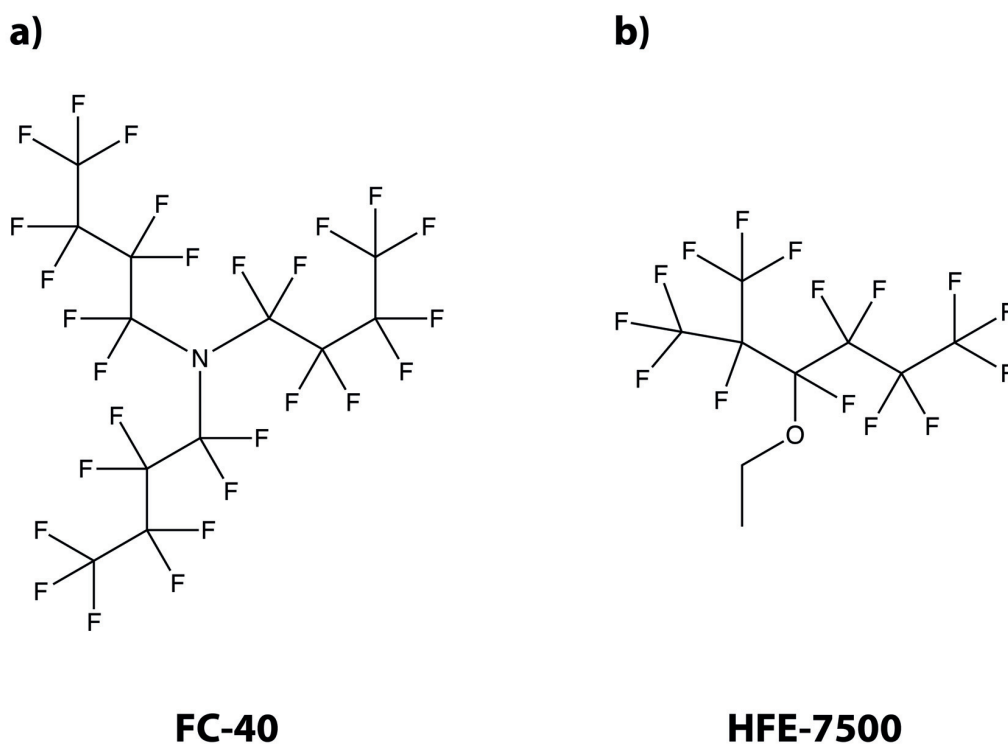
FC-40

HFE-7500

Figure 3.5: Chemical structure of (**a**) FC-40 and (**b**) HFE-7500.

In this case, the emulsion drops seem to be slightly more stable, as shown in Figure 3.6.
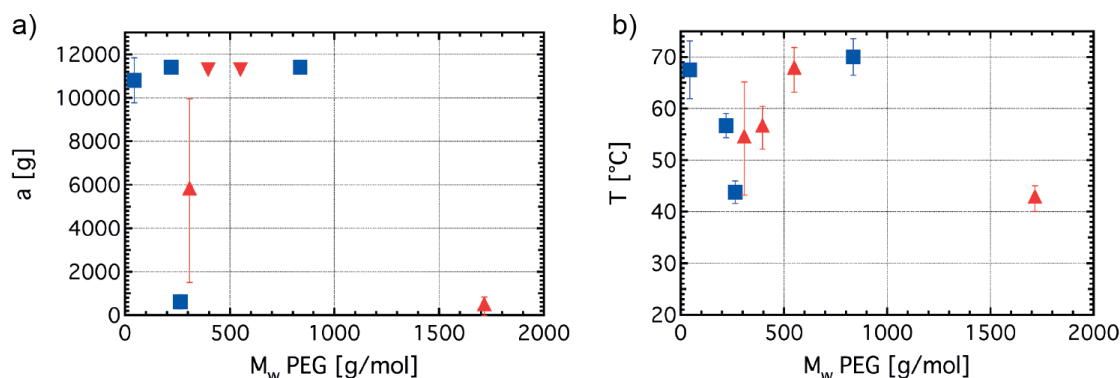
Figure 3.6: Stability of aqueous drops dispersed in FC-40. The stability of aqueous drops containing 20 wt% PEG, coated with triblock (▲) and diblock (■) surfactants dispersed in FC-40 is shown if (**a**) accelerated and (**b**) stored at elevated temperatures.

Influence of Salt on Drop Stability

Solutions that mimic physiologic conditions contain salts. Salts only weakly affect the fluid viscosity, but they lower the solubility of PEG in water, [147] thereby often reducing the effectiveness of PEG-containing surfactants to stabilize emulsion drops. To test the influence of salt on the stability of drops coated with fluorinated surfactants, we produce aqueous drops containing 150×10^{-3} M NaCl. Salt-containing drops display a much lower stability than their salt-free counterparts: Most of them rupture at accelerations below 400 g and at temperatures below 50 °C, as shown in Figures 3.2c and d. We expect this reduced drop stability to be a result of reduced PEG solubility. To test if PEG further collapses if dissolved in aqueous solutions containing higher salt concentrations, we produce aqueous drops containing 1 M NaCl. Interestingly, the stability of these drops is very similar to that of drops containing 150×10^{-3} M NaCl, as shown in Figure 3.2c. These results suggest that PEG is already strongly collapsed in the presence of 150×10^{-3} M NaCl, such that drops are unstable. The drop stability significantly increases, if they contain next to 1 M NaCl also 20 wt% of free PEG6000, as shown in Figure 3.7.
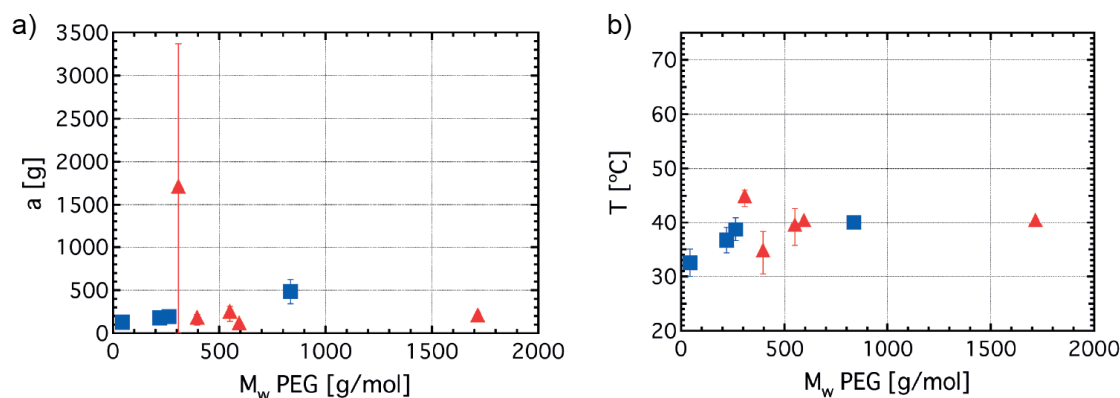
Figure 3.7: The stability of aqueous drops containing 20 wt% free PEG and 1M NaCl, coated with triblock (▲) and diblock (■) copolymers if (**a**) accelerated and (**b**) stored at elevated temperatures as a function of the PEG molecular weight.

These results indicate that free PEG reduces the collapse of the PEG contained in the surfactants and therefore increases the stability of salt-containing drops. Nevertheless, their stability is much lower than that of salt-free drops. Remarkably, drops containing high salt concentrations display the best temperature stability if coated with the surfactant that has the shortest PEG block we tested, as shown in Figure 3.2. These results indicate that the optimum ratio of the radii of gyration of PEG to FSH depends on the conformation of the blocks.

Influence of Salt on the Interfacial Tension

Salts reduce the stability of drops coated with any of the tested triblock copolymer surfactants. However, the extent to which they reduce drop stability depends on the composition of the surfactant. To understand the reason for the different behaviors of surfactants in the presence of salts, we quantify the interfacial tension between aqueous drops containing 1 M NaCl and HFE-7500 in the presence of the different surfactants. The tension of interfaces coated with FSH_2-Jeffamine2000 decreases by 61% if salt is added, as a comparison between Figure 3.9 and Figure 3.8 reveals. By contrast, the tension of water-HFE-7500 interfaces coated with FSH_2-Jeffamine900 remains nearly the same upon salt addition. This could indicate that the changes in the conformation of PEG upon salt addition depend on its length. However, this hypothesis needs to be further investigated.
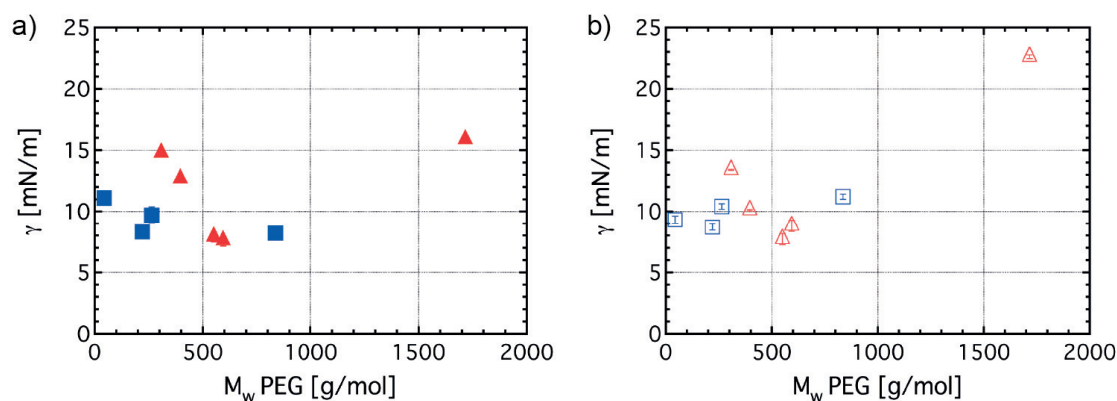
Figure 3.8: Interfacial tension, γ, between HFE-7500 and water containing (a) 1M NaCl (filled symbols) and (b) 150 mM NaCl (empty symbols) in the presence of triblock (▲) and diblock (■) copolymers.

Influence of the PEG Length on the Interfacial Tension

To investigate the reason for the different stabilities of drops coated with different surfactants, we quantify the tension of water-HFE-7500 interfaces, γ, in the presence of the different triblock copolymer surfactants. Emulsion drops tend to coalesce to reduce the interfacial area, A, and thereby the interfacial energy $E_\gamma = \gamma \times A$. Because E_γ scales with γ, the drop stability often scales with γ. [148, 149] To test if this is also the case for the surfactants investigated here, we measure γ as a function of the PEG molecular weight of the different surfactants, as shown in Figure 3.9a.
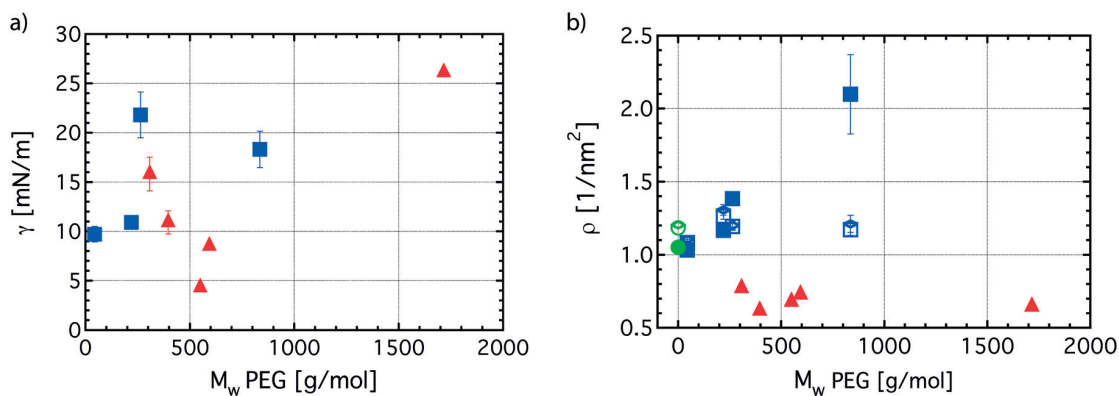
Figure 3.9: Influence of the PEG molecular weight on the interfacial tension, γ, and the surfactant packing density, ρ. (**a**) The interfacial tensions between HFE-7500 and drops composed of pure water stabilized with triblock (▲) and diblock (■) surfactants are shown as a function of the molecular weight of PEG contained in the surfactants. (**b**) Packing densities of triblock (▲) and diblock (■) surfactants at the interface of water without any salt with air (filled symbols) and that of water containing 150×10^{-3} M NaCl (◇) and 1 M NaCl (□) with air are shown as a function of the PEG molecular weight. As a reference, we include the packing density of pure Krytox FSH, at the interface of air with pure water (●), water containing 150×10^{-3} M NaCl (◇), and 1 M NaCl (○)

The interfacial tension decreases with increasing PEG molecular weight until it reaches a minimum of 4.3 mN/m for surfactants comprising Jeffamine900, which contains PEG with a molecular weigh of 550 g/mol. If the PEG molecular weight is further increased, the interfacial tension strongly increases, as shown in Figure 3.9a. Remarkably, γ is two times lower if interfaces are coated with FSH_2-Jeffamine900 than if they are coated with FSH_2-PEG600, even though these two surfactants have the same PEG length and hence the same ratio of the radii of gyration of PEG to FSH. These results indicate that the PPO blocks contribute to the reduction of the interfacial tension. The minimum tension of interfaces coated with Jeffamine900 correlates well with the highest stability measured for drops coated with this surfactant, as shown in Figure 3.10. Indeed, the stability of salt-free drops coated with triblock copolymers scales with interfacial tension, as shown in Figure 3.10.
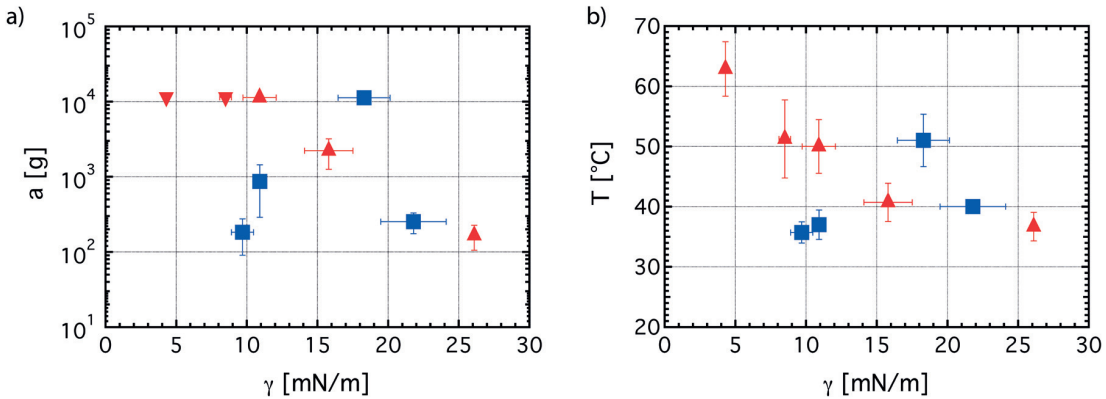
Figure 3.10: Interfacial tension, γ, of diblock (■) and triblock (▲) copolymer surfactants as a function of (**a**) the mechanical and (**b**) temperature stability of drops. Drops that did not coalesce at the maximum acceleration we could achieve are represented by triangles that point down (▼).

Influence of the PEG Length on Surfactant Packing Density

The interfacial tension is usually thought to scale with the surfactant packing density. [15] To test if this correlation also holds for the triblock copolymers investigated here, we quantify the surfactant packing density at the water–air interface using a Langmuir trough. We assume the surfactant packing density at the water–air interface to be similar to that at the water–HFE-7500 interface if the PEG is the packing density-limiting block. By contrast, if FSH is the packing density-limiting block at the water–air, we do not expect to see any influence of the PEG molecular weight on the surfactant packing density. In this case, we cannot correlate the surfactant packing density measured with the Langmuir trough to that at the water–HFE-7500 interface. By measuring the packing density as a function of the PEG molecular weight, we should be able to distinguish these two cases clearly. We measure the surface pressure as a function of the area occupied by a surfactant molecule and convert it into a packing density, assuming the surface pressure scales with the surfactant packing density. The surface pressure increases with increasing surfactant packing density until it reaches a plateau. Upon further

compression, the surface pressure usually rapidly decreases, which is assigned to a collapse of the monolayer. [150] However, in our case, the surface pressure remains almost constant, as shown in Figure 3.11.
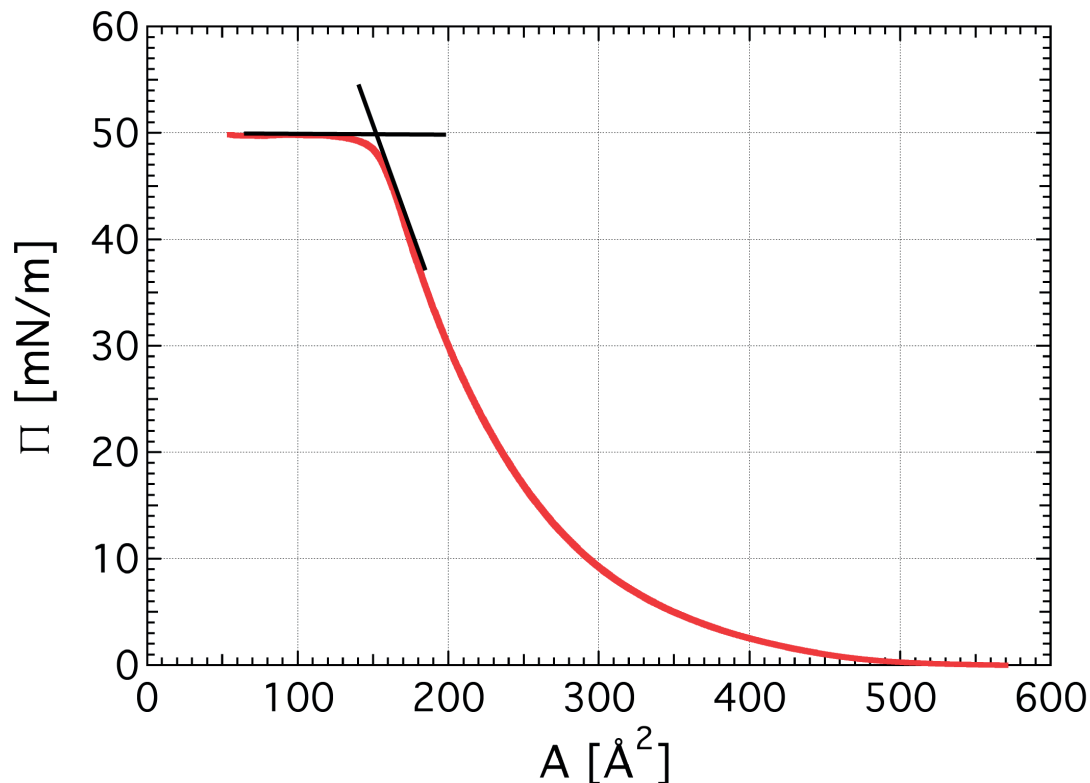
Figure 3.11: Surface pressure, Π, of FSH_2-Jeffamine900, adsorbed at the water-air interface as a function of the mean molecular area, A, measured with a Langmuir trough. To determine the minimum area occupied by a block-copolymer, we extrapolate the plateau value and the final part of the curve where the monolayer is still compressed, as indicated by the black lines. We take the value of the area of the intersection point as the minimum area occupied by a block-copolymer.

This could indicate that at this pressure, some of the surfactants form water-soluble aggregates, that can diffuse into the bulk water. We approximate the molecular area at the onset of this plateau as the minimum area a surfactant occupies at the water–air interface and use this value to calculate the maximum packing density. The packing density of triblock copolymers at the water–air interface is independent of the PEG molecular weight, as shown by the red triangles in Figure 3.9b. These results indicate that the collapsed FSH blocks are limiting the packing density. Hence, for triblock copolymers, the correlation between interfacial tension and surfactant packing density at the water–HFE-7500 interface remains unclear.

3.4.2   Diblock Copolymer Surfactants

Influence of PEG Length on Drop Stability

The surfactant packing density at liquid–liquid interfaces is usually higher for diblock than triblock copolymers, [151] as schematically illustrated in Figures 3.1c and d. To test, if we can increase drop stability by increasing the surfactant packing density, we synthesize diblock copolymers composed of an FSH block covalently linked to a hydrophilic block and vary the PEG molecular weight between 40 g/mol and 840 g/mol. From all the tested diblock copolymers, FSH-Jeffamine 1000, which has a PEG molecular weight of 840 g/mol, imparts the highest stability to drops, as shown in Figure 3.2. Interestingly, this surfactant has a ratio of the radii of gyration of PEG to FSH of 0.67, a value that is very similar to the optimum value determined for triblock copolymers. However, the stability of drops coated with diblock copolymer surfactants is in all cases inferior to that of drops coated with triblock copolymer counterparts that have a similar PEG length, as shown in Figure 3.2.

Influence of PEG Length on Interfacial Tension

To investigate the reason for the lower stability of drops coated with diblock copolymers we quantify the water-HFE-7500 interfacial tension using pendant drop measurements. Diblock copolymers lower the interfacial tension to a smaller extent than triblock copolymers with a similar PEG molecular weight, as shown in Figure 3.9. This might be a contributing reason for the lower stability of drops coated with diblock surfactants. Interestingly, the stability of drops coated with diblock surfactants does not scale with the interfacial tension, as shown in Figure 3.10. This is in strong contrast to the commonly assumed direct correlation between the interfacial tension and drop stability. This result indicates that there is another parameter that more strongly influences the stability of drops coated with diblock copolymers.

Influence of the PEG Length on Surfactant Packing Density

Block copolymer surfactants self-assemble at liquid–liquid interfaces of drops, thereby imparting a steric stabilization layer to them. The thickness of this steric stabilization layer scales with the surfactant packing density. [152] Hence, we would expect the drop stability to scale with the surfactant packing density. To test this expectation, we quantify the packing density of diblock copolymers at the water–air interface. For diblock copolymers, the surfactant packing density at the water–air interface increases with decreasing PEG molecular weight and reaches the lowest value for FSH-Jeffamine600, which contains the shortest PEG we tested; this surfactant contains only a single ethylene glycol repeat unit, whose molecular weight is 44 g/mol. Indeed, the packing density of FSH-Jeffamine600 is very similar to that of pure FSH, as shown in Figure 3.9b. These results indicate that for diblock copolymers containing more than one ethylene glycol unit, PEG is the packing density limiting block. Thus, we expect the packing density of these diblock

copolymers at the water–HFE-7500 interface to be similar to that measured at the water–air interface. Interestingly, the stability of drops coated with diblock copolymers increases with increasing surfactant packing density, as shown in Figure 3.12. These results indicate that for these diblock copolymer surfactants, a high surfactant packing density is more important than a low interfacial tension for obtaining good drop stability.
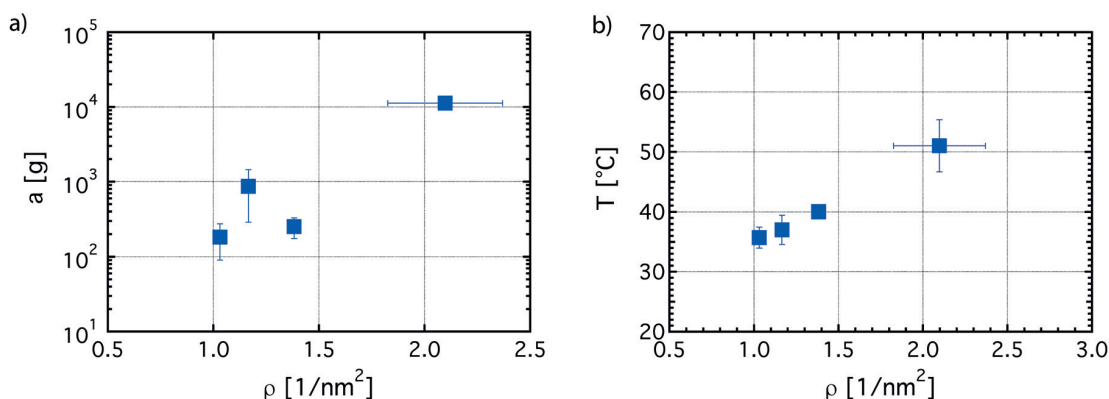
Figure 3.12: The stability of drops coated with diblock surfactants if (**a**) accelerated, a, and (**b**) subjected to elevated temperatures, T as a function of the surfactant packing density, ρ.

Influence of Salt on Drop Stability

To test the influence of salts on the stability of drops coated with diblock copolymers, we produce aqueous drops containing 150×10^{-3} M NaCl. Also in this case, salts strongly reduce the drop stability, as shown by the empty symbols in Figures 3.2c and d. The drop stability remains nearly unchanged if the salt concentration is increased to 1 M, by analogy to the stability of drops coated with triblock copolymers. The correlation of the drop stability with the dispersant packing density, observed for salt-free drops, also holds for drops containing 1 M NaCl, as shown in Figure 3.13. These results indicate that salt-containing drops are most efficiently stabilized with surfactants that pack most densely.
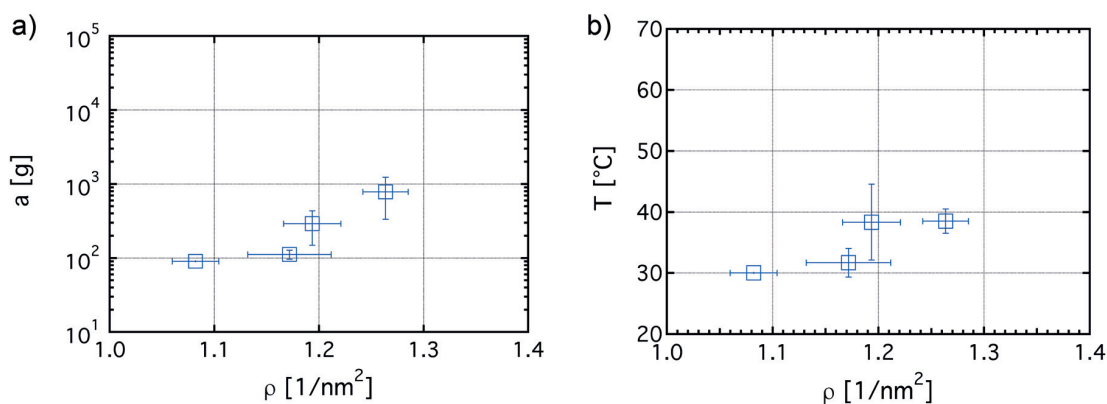
Figure 3.13: (**a**) The maximum acceleration drops containing 1 M NaCl can sustain and (**b**) the maximum temperature they can sustain is shown as a function of the surfactant packing density, ρ.

3.5 Conclusion

We study the influence of the PEG molecular weight of nonionic diblock and triblock copolymer surfactants on their ability to stabilize aqueous drops in fluorinated oils. The stability of drops coated with triblock copolymers scales inversely with the interfacial tension whereas that of drops coated with diblock copolymers scales with the surfactant packing density. The stability of aqueous, salt-free drops is highest if coated with the triblock copolymer FSH$_2$-Jeffamine900, whose ratio $R_g(PEG)/R_g(FSH)$ is 0.56; this surfactant lowers the water–HFE-7500 interfacial tension most. By contrast, the stability of salt-containing drops is highest if coated with the diblock copolymer FSH-Jeffamine2000, the surfactant that packs most densely. These results indicate that the choice of the most appropriate surfactant depends on the exact composition of the fluids. Our results provide guidelines for the synthesis of new surfactants that impart good stability to drops if subjected to demanding conditions.

Chapter 4

Cross-talk between emulsion drops: How are hydrophilic reagents transported across oil phases?

Gianluca Etienne, Antoine Vian, Marjan Biočanin, Bart Deplancke, Esther Amstad

In this chapter, we investigate the mechanism underlying the transport of hydrophilic reagents across the shell of w/o/w double emulsions. We find that small aqueous drops spontaneously form in the oil phase. These drops act as transport vehicles for encapsulants, and thereby strongly increase the permeability of these double emulsions. We demonstrate different methods to reduce the leakage.

Gianluca Etienne performed all the experiments, except for the fabrication of the aspiration device and leakage studies of the double emulsions with thin shells which were performed by Antoine Vian. The DNA and Plasmid reagents were provided by Marjan Biočanin and Bart Deplancke.

Contents

4.1 Abstract

Emulsion drops are frequently used as vessels, for example, to conduct biochemical reactions in small volumes or to perform screening assays at high throughputs while consuming minimal sample volumes. These applications typically require drops that do not allow an exchange of reagents such that no cross-contamination occurs. Unfortunately, in many cases, reagents are exchanged between emulsion drops even if they have a low solubility in the surrounding phase, resulting in cross-contamination. Here, we investigate the mechanism by which hydrophilic reagents are transported across an oil phase using water-oil-water double emulsion drops as a model system. Remarkably, even large objects, including 11000 base pair double-stranded circular DNA are transported across oil shells. Importantly, this reagent transport, that is to a large extent caused by aqueous drops that spontaneously form at the water-oil interface, is not limited to double emulsions but also occurs between single emulsion drops. We demonstrate

that the uncontrolled reagent transport can be decreased by at least an order of magnitude if appropriate surfactants that lower the interfacial tension only moderately are employed or if the shell thickness of double emulsions is decreased to a few hundreds of nanometers.

4.2 Introduction

Emulsion drops are often used as vessels to conduct chemical, [72, 84] biochemical, [66, 153] and biological screening assays at high throughputs. [66, 73, 84, 86–88, 154] To achieve a high accuracy, drops must display a narrow size distribution. The throughput achieved in these drop-based screening assays is orders of magnitude higher than that of assays performed in bulk and therefore costs are much lower. [66] These drop-based screening assays, that allow miniaturization and automation of biological assays, are frequently employed to characterize cells on a single cell level, [60, 155, 156] to perform directed evolution of enzymes, [66, 68] single cell transcriptomics, [69, 70] drug screening, [63, 104] or biomarker analysis. [157–159] Fluorinated polyether surfactants impart good stability to emulsion drops if they are composed of solutions with low salt concentrations. [1] However, they are prone to coalescence if drops are made of solutions containing high salt concentrations, which is often the case in biological and biochemical screening assays. In these cases, it is beneficial to employ water-oil-water double emulsions that are more stable and can be stored in an aqueous environment, facilitating their handling. [119] Irrespective of the type of emulsion drops employed, the use of surfactants comes with an important disadvantage: Surfactants contribute to spontaneous exchanges of reagents between different drops that are dispersed in perfluorinated [51, 108, 118, 160–164] and hydrocarbon-based oils. [163, 165]

This cross-contamination reduces the accuracy of drop-based screening assays [118] and therefore limits their performance and usefulness. The degree to which reagents are exchanged depends on their composition. [131, 164, 166, 167] Cross-contamination can be reduced if the viscosity of the oil is increased, [51] if sugar, [165] or bovine serum albumin (BSA) [163] is added to the aqueous phase, by lowering the surfactant concentration, [160, 163] or by replacing surfactants with nanoparticles. [11] The exact mechanism by which reagents are exchanged remains to be determined. Reagents might be transported across the oil by aggregates or inverse micelles that spontaneously form if surfactants self-assemble. [118, 160, 163] Reagents might also be transported across the oil by aqueous drops that spontaneously form at liquid–liquid interfaces. [20, 22, 23, 168] A better understanding of the mechanism that causes reagent exchange between emulsion drops would open up new possibilities to control it. This understanding might enable the design of tight, surfactant-stabilized emulsion drops that do not suffer from a spontaneous reagent exchange. This would result in a much higher accuracy of drop-based screening assays, thereby enabling their use for many more applications than what is currently possible.

In this chapter, we investigate the exchange of reagents across the shell of water-oil-water double emulsions stabilized with different amphiphilic block copolymers. Remarkably, even reagents as large as 11000 base pair DNA strands or 100 nm diameter poly(styrene) particles are transported across a perfluorinated oil phase despite their very low solubility in the oil. Importantly, this transport is not limited to double emulsion drops but also occurs between single emulsion drops. We find that the transport rate of reagents across the oil phase scales inversely with the interfacial tension. These results suggest that small aqueous drops with diameters of the order of 100 nm spontaneously form in the oil phase and transport hydrophilic reagents across it. Because these aqueous drops are much larger than micelles, they can also carry bigger reagents across the shell of double emulsions. We demonstrate that the spontaneous formation of aqueous drops can be reduced by at least an order of magnitude if appropriate surfactants are employed or if the thickness of double emulsion shells is reduced to dimensions that are of the same order of magnitude as the diameter of the small aqueous drops. These measures significantly reduce cross-contamination, thereby opening up new possibilities to use drops as vessels for example for conducting high throughput screening assays with a significantly increased accuracy.

4.3 Experimental Section

4.3.1 Fabrication of the Microfluidic Device

The microfluidic device is fabricated as described in section 2.3 on page 30.

4.3.2 Surfactant Synthesis

The surfactants are synthesized as described in section 2.1 on page 26.

4.3.3 Production of Double Emulsions

Water-oil-water double emulsions are produced as described in section 2.4.3 on page 33. The inner phase is composed of water containing 15 wt% PEG with a molecular weight of 6000 g/mol (Carl Roth, Germany) and 0.1 wt% fluorescein disodium salt (Carl Roth, Germany). The middle phase is composed of HFE-7500 (0.77 cSt) containing different concentrations of a surfactant. The outer aqueous phase is composed of water containing 10 wt% polyvinyl alcohol (PVA) 13000-18000 g/mol (Sigma-Aldrich, USA). The osmolarity of the two aqueous phases are measured using an osmometer (Advanced Instruments, Fiske 210) and matched by adding D(+)-Saccharose (Carl Roth, Germany).

To study the transport of the polystyrene beads, we add FITC-labeled polystyrene beads with a diameter of 100 nm (Nanocs, USA) to an aqueous solution containing 15% PEG 6000 g/mol and study the release from double emulsions. For studying the transport of DNA, we used 11000 base pair long pSIN-TRE-GW-3HA plasmid prepared using Qiagen plasmid MIDI kit and concentrate

at 1 μg/μL. For the leakage experiment, we stain the plasmid with the SYBR gold double strand specific DNA intercalating dye by adjusting the final concentration on 39X (Invitrogen 10 000X concentrate in DMSO) and we adjust the plasmid concentration to 12 ng/μL in water and PEG before producing double emulsions. For single-stranded DNA leakage experiments, we use fluorescein labeled 17 base pair long ssDNA (FAM) ordered from IDT (standard desalting) that are dissolved in distilled water and PEG to 2 μM.

4.3.4   Production of Submicron Shell Double Emulsions

Double emulsions with shells whose thickness is below 1 μm are produced using the microfluidic aspiration device. [169] In brief, double emulsions with diameters of 92 μm and shell thicknesses of 8.4 μm are injected in the microfluidic aspiration device at 900 μL/h. Oil is withdrawn through the shunt channels at a rate of 800 μL/h. To spatially separated double emulsions with thin shells, an additional aqueous phase containing PVA is injected downstream the aspiration section at 800 μL/h.

4.3.5   Leakage Measurements

To minimize the influence of PVA on the transport of encapsulants, double emulsions are washed with an osmotically balanced aqueous solution containing sucrose to remove the PVA. To wash the sample, 10 μL double emulsions are added to 1 ml of water, double emulsions sediment and the supernatant is removed. This procedure is repeated three times. Double emulsions are added into PDMS wells that have previously been filled with the aqueous washing solution. Wells are sealed with mineral oil (Sigma-Aldrich, USA) to prevent evaporation of the water. Fluorescent microscopy images are recorded every 10 min and analyzed using a custom-made MATLAB code that detects the double emulsions and quantifies the intensity inside each double emulsion over time.

4.3.6   Quantification of the cmc

The critical micelle concentration is measured with dynamic light scattering where the count rate is quantified as a function of the surfactant concentration contained in the fluorinated oil Novec HFE-7500. In addition, the interfacial tension of aqueous drops in HFE-7500 containing different surfactants is quantified with a drop shape analyzer (DSA 30, Krüss, Germany).

4.3.7   Temperature Stability of Double Emulsions

To quantify the stability of double emulsions if stored at elevated temperatures, they are added into PDMS wells that have previously been bonded to a glass slide. The double emulsions are imaged at room temperature. The sample is subsequently heated to 95°C for 10 min using a

hotplate. After the sample is cooled to room temperature it is again imaged to quantify the percentage of double emulsions that remain intact during the incubation.

4.4 Results and Discussion

4.4.1 Permeability of Water-Oil-Water Double Emulsions

Water-oil-water double emulsion drops with a diameter of 90 μm and a shell thickness of 12 μm are produced in poly(dimethyl siloxane)-based microfluidic devices [170] that are fabricated using soft lithography, [39] as shown in the optical micrographs in Figures 4.1a and b.
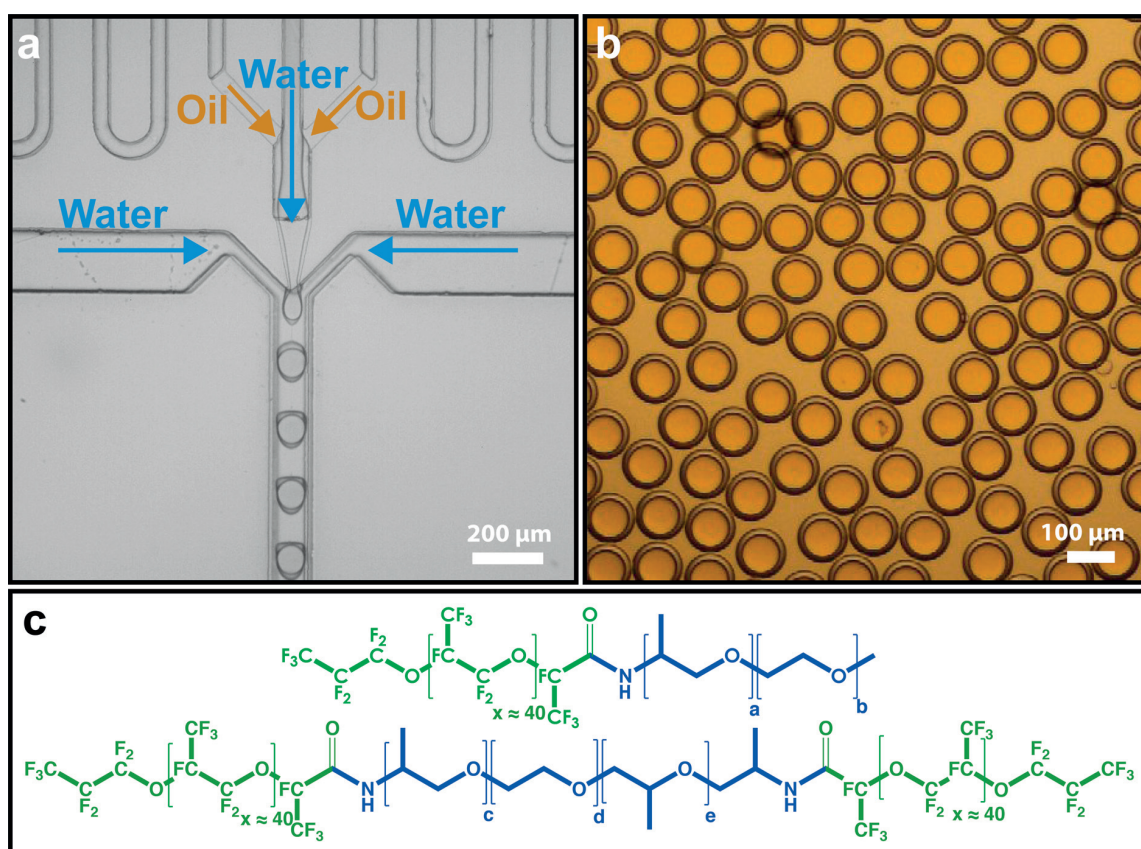
Figure 4.1: Production of water-oil-water double emulsions. (**a** and **b**) Optical microscope images of (**a**) a microfluidic double emulsion device in operation and (**b**) the resulting water-oil-water double emulsions. (**c**) Chemical structure of diblock (top) and triblock (bottom) copolymer surfactants with varying lengths of the hydrophilic block, as summarized in Table 2.1 on page 28.

We employ an aqueous solution containing 15 wt% poly(ethylene glycol) (PEG) 6000 g/mol and 0.1 wt% fluorescein sodium salt as an inner phase, a perfluorinated oil, HFE-7500, containing block copolymer surfactants as a middle phase, and an aqueous solution with 10 wt% polyvinyl alcohol (PVA) as an outer phase. The structure of the surfactant molecules are shown in Figure

4.1c. PVA is required to impart stability to the double emulsions during their collection and is subsequently removed by thoroughly washing the double emulsions with a PVA-free aqueous solution. To prevent osmotic pressure gradients that would change the dimensions of the double emulsions during their collection and storage, we balance the osmolarities of the two aqueous phases using D-saccharose. To stabilize double emulsion drops, we employ diblock copolymers composed of a perfluorinated block that is covalently linked to a PEG-based hydrophilic block. Alternatively, we stabilize double emulsion drops with triblock copolymers composed of two perfluorinated blocks that are interspaced by a PEG-based block, as shown schematically in Figure 4.1c.

We systematically change the length of the hydrophilic block to vary the inverse packing parameter (α') of the block copolymer surfactant, defined as the ratio of the cross-sections of the hydrophilic to the hydrophobic tail,

$$\alpha' = \frac{v}{a_0 \times l_h} \tag{4.1}$$

here v is the volume of the hydrophilic chain, a_0 the area of the hydrophobic group, and l_h the length of the hydrophilic block. [6] Because the head group and the tail of our surfactants are polymer blocks, we calculate α' as

$$\alpha' = \frac{< R_g >_{(hydrophilic)}^2}{< R_g >_{(hydrophobic)}^2} \tag{4.2}$$

here R_g is the radius of gyration of the respective block. To account for the fact that triblock copolymers have two hydrophobic blocks, we divide α' of triblock-copolymer surfactants by two and obtain the inverse packing parameters summarized in Table 2.1 on page 28. [1] To maximize the accuracy of screening assays, double emulsions should be impermeable to encapsulants. To test if encapsulants are transported across the shell of double emulsions, we encapsulate fluorescein and monitor the fluorescence inside the double emulsions as a function of time. The vast majority of fluorescein is released within 7 h if double emulsions are stabilized with 1 mM of the triblock copolymer surfactant FSH$_2$-Jeffamine900, as shown in the top panel of Figure 4.2a. Similarly, if empty double emulsions are incubated in a fluorescein-containing continuous phase, fluorescein is transported into empty cores, as shown in Figure 4.2b, indicating that reagent exchange occurs in both directions.
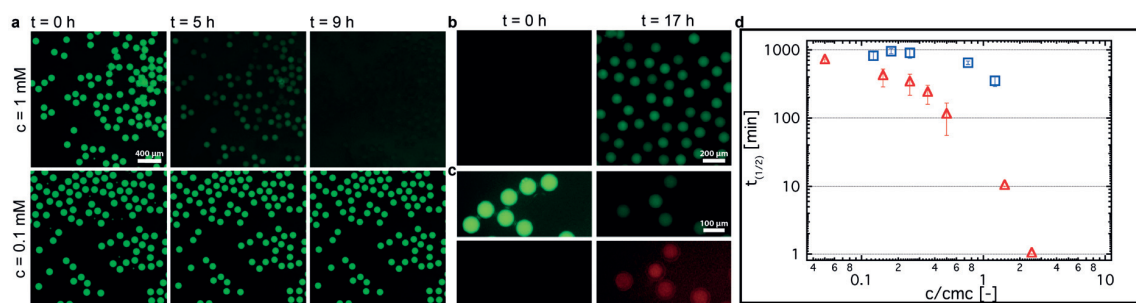
Figure 4.2: Permeability of double emulsions. (a) Time-lapse fluorescent microscope images of double emulsions with 12 μm thick shells containing 1 mM (top) and 0.1 mM (bottom) FSH$_2$-Jeffamine900. (b) Double emulsions stabilized by 1 mM FSH$_2$-Jeffamine600 containing no dye before and after storage in an aqueous solution containing 0.025 wt% fluorescein. (c) Double emulsions stabilized by 1 mM FSH$_2$-Jeffamine600 containing fluorescein in the core, before and after storage for 17 h in an aqueous solution containing cresyl violet perchlorate. Fluorescein diffuses from the core into the continuous phase whereas cresyl violet perchlorate diffuses from the continuous phase into the core of double emulsions. (d) Time until 50% of fluorescein is released ($t_{1/2}$), as a function of the concentration of FSH$_2$-Jeffamine900 ($\triangle$) and FSH-Jeffamine1000 ($\square$), contained in the double emulsion shells. The surfactant concentrations are normalized by their respective cmcs.

To test if this exchange is driven by differences in the chemical potential of the two aqueous phases, we incubate fluorescein-loaded drops in an aqueous solution containing cresyl violet perchlorate. Also in this case, fluorescein diffuses from the double emulsion core into the continuous phase while cresyl violet perchlorate is transported from the continuous phase into the double emulsion core, as shown in Figure 4.2c. This result indicates that reagents are simultaneously transported into and out of the core of double emulsions. To test the influence of the pH on the leakage of water-perfluorinated oil-water double emulsions, we produce fluorescein-loaded double emulsions stabilized with FSH$_2$-Jeffamine900 and measure the fluorescence of their cores in function of time for when they are stored in an aqueous solution whose pH is 7 and pH=8.5. The leakage is significantly retarded if the pH is increased to 8.5, as shown in Figure 4.3. However, we still observe a continuous leakage even at higher pHs as shown by the red curve. Because most of the high throughput screening experiments are performed under physiologic conditions, we investigate the permeability of double emulsions at neutral pH.
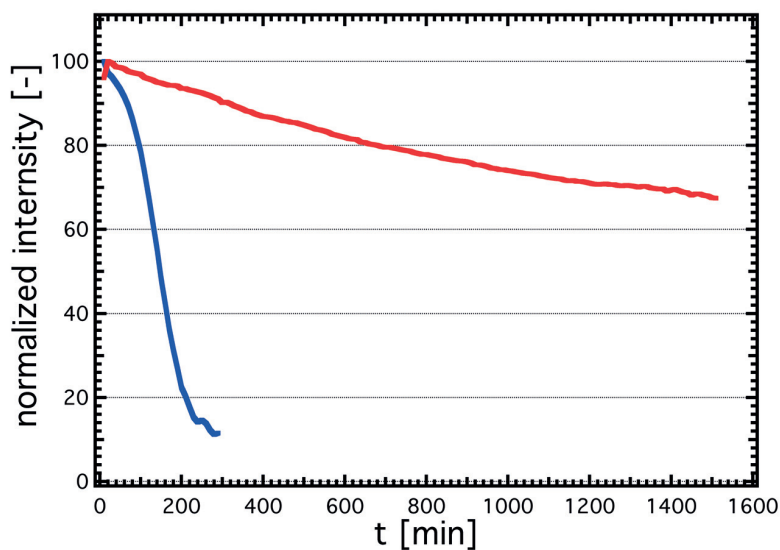
Figure 4.3: Influence of the pH on the leakiness of double emulsions. Water-perfluorinated oil-water double emulsions stabilized with FSH_2-Jeffamine900 and loaded with fluorescein are incubated in an aqueous solution at pH = 7 (blue curve) and pH=8.5 (red curve)

This reagent exchange is remarkable because the solubility of fluorescein in the oil phase is very low, such that this transport cannot be solely explained by diffusion. If the transport of fluorescein across the oil shell was caused by surfactants that form inverse micelles, we would expect this leakage to decrease with decreasing surfactant concentration, by analogy to what has been observed for single emulsion drops. [160,163] In this case, there should be a strong decrease in the leakage, if the surfactant concentration falls below the critical micelle concentration (cmc). To test this hypothesis, we quantify the cmc for each surfactant using interfacial tension and dynamic light scattering (DLS) measurements, as detailed in Figure 4.4 and summarized in Table 2.1 on page 28. For the DLS measurement, we measure the mean count rate of HFE-7500 containing different concentrations of surfactants, as exemplified for FSH_2-Jeffamine900 in Figure 4.4a. Additionally, we measure the interfacial tension between the surfactant containing HFE-7500 and water at different surfactant concentrations using pendant drop measurements, as shown in Figure 4.4b. The results are summarized in Table 2.1 on page 28.
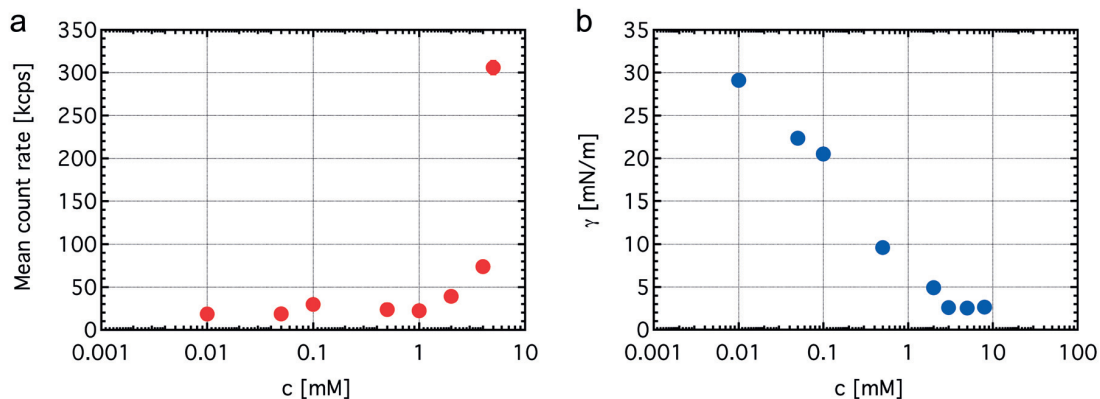
Figure 4.4: Quantification of the critical micelle concentration. (**a**) The mean count rate, determined with DLS, is shown as a function of the concentration of FSH_2-Jeffamine900 contained in HFE-7500. (**b**) The interfacial tension, γ, is measured as a function of the concentration of FSH_2-Jeffamine900 contained in HFE-7500.

We monitor the fluorescence inside double emulsions stabilized with FSH_2-Jeffamine900 and quantify the time required to release 50% of the fluorescein, $t_{1/2}$, as summarized in Figure 4.2 and detailed in Figure 4.5.
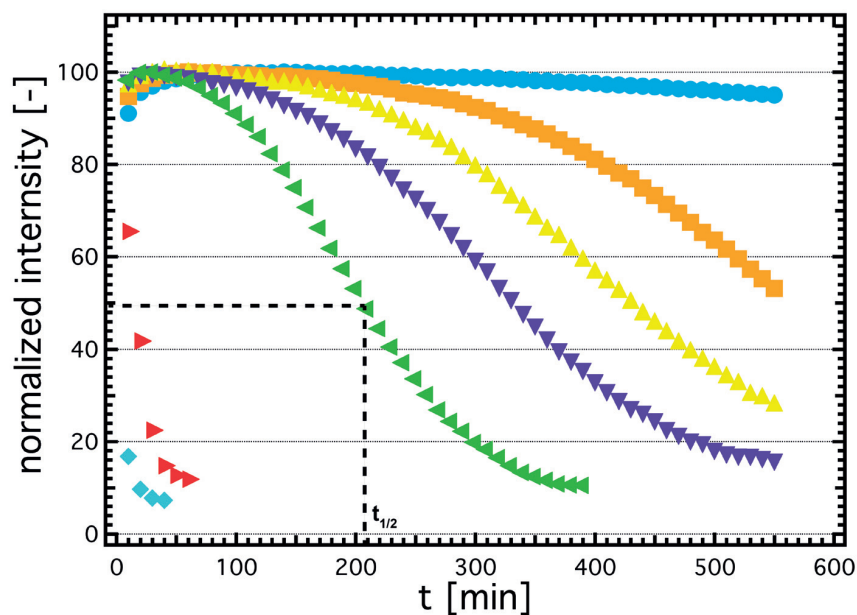
Figure 4.5: Quantification of the permeability of double emulsions. The normalized fluorescence intensity of cores of double emulsions stabilized with 5 mM (♦), 3 mM (▶), 1 mM (◀), 0.7 mM (▼), 0.5 mM (▲), 0.3 mM (■), and 0.1 mM (●) FSH_2-Jeffamine900 is shown as a function of time. The time when 50% of the fluorescein is released, $t_{1/2}$, is shown.

Indeed, the leakiness strongly decreases with decreasing surfactant concentration. However, we still observe a significant leakage, even if the surfactant concentration is below the cmc, as

shown by the red triangles in Figure 4.2d. This finding suggests that other factors might also contribute to the transport of reagents across the oil shell.

Our results suggest that inverse micelles are not the sole reason for the observed transport of reagents across the oil shell. To test if larger objects can spontaneously form and act as carrier vehicles, we cover a solution of HFE-7500 containing FSH_2-Jeffamine900 with a layer of water. Immediately after the sample is prepared, we cannot observe any objects that scatter visible light in the oil phase. However, the turbidity of the surfactant-containing oil strongly increases over time even though the sample is not mechanically agitated, as shown in Figure 4.6a. This behavior is in stark contrast to that observed for pure oil that does not contain any surfactant and is also in contact with water: the turbidity of this surfactant-free oil remains unchanged, as shown in Figure 4.6b. These results indicate that in the presence of triblock-copolymer surfactants, small aqueous drops form at the liquid–liquid interface, by analogy to what has been reported for osmotically stressed double emulsions. [23,168] Hence, our results suggest that these small water drops also form in the absence of osmotic pressure gradients and if block copolymers are used as surfactants.
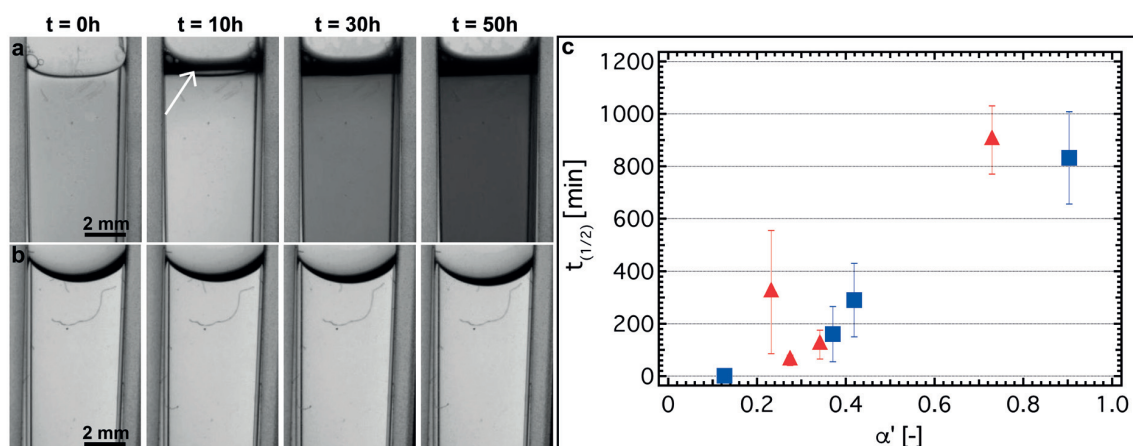
Figure 4.6: Spontaneous formation of small aqueous drops in perfluorinated oils. Time-lapse photographs of fluorinated oil (HFE-7500) (a) with 5 mM FSH_2-Jeffamine900 and (b) without surfactant. In both cases, the oil is covered with a layer of water. Samples are imaged after 0, 10, 30 and 50 hours. (a) The increase in turbidity observed in the oil phase, that starts in proximity to the liquid-liquid interface, as indicated by the white arrow, can be attributed to the spontaneous formation of aqueous drops. (c) Influence of the inverse packing parameter, α', on the leakage of fluorescein from double emulsions stabilized with 1 mM of diblock (■) or triblock (▲) copolymers.

To exclude that the increase in turbidity is caused by the hydration of the PEG-based blocks contained in the surfactants, we dissolve FSH_2-Jeffamine2000, a surfactant with a much higher PEG molecular weight than that of FSH_2-Jeffamine900, in the oil. The turbidity of this sample

remains unchanged even though the oil encompasses an equal molar concentration of FSH_2-Jeffamine2000 whose PEG molecular is much higher, as shown in Figure 4.7.

t = 0h   **t = 10h**   **t = 30h**   **t = 50h**

2 mm
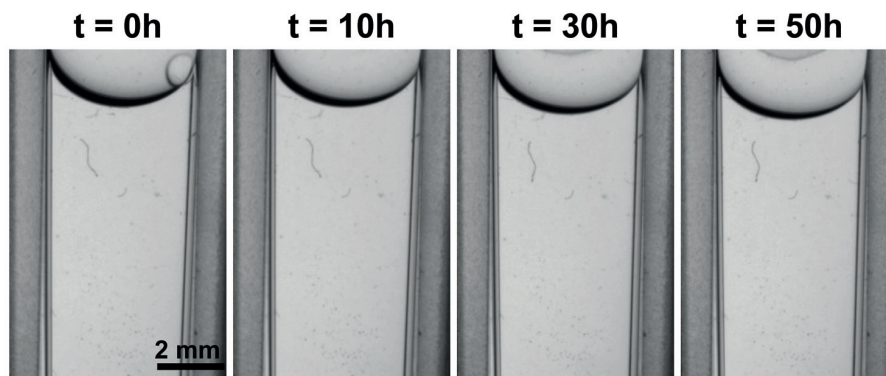
Figure 4.7: Time-lapse photographs of a cuvette containing HFE-7500 encompassing 5 mM FSH_2-Jeffamine2000 and a layer of water. Images are acquired 0, 10, 30 and 50 h after the sample was prepared. We cannot observe any significant changes in the turbidity of the oil indicating that only very small amounts of aqueous drops with diameters similar to the wavelength of the visible light spontaneously form.

This result indicates that the light scattering observed for samples encompassing FSH_2-Jeffamine900 cannot solely be caused by the hydration of PEG. To further test this indication, we quantify the size of the scattering objects with dynamic light scattering measurements. This analysis reveals objects with diameters in the order of 100 nm, a size much larger than that of individual surfactant molecules, as detailed in Figure 4.8 and summarized in Table 4.1. These results confirm our hypothesis that the scattering objects are small water drops.
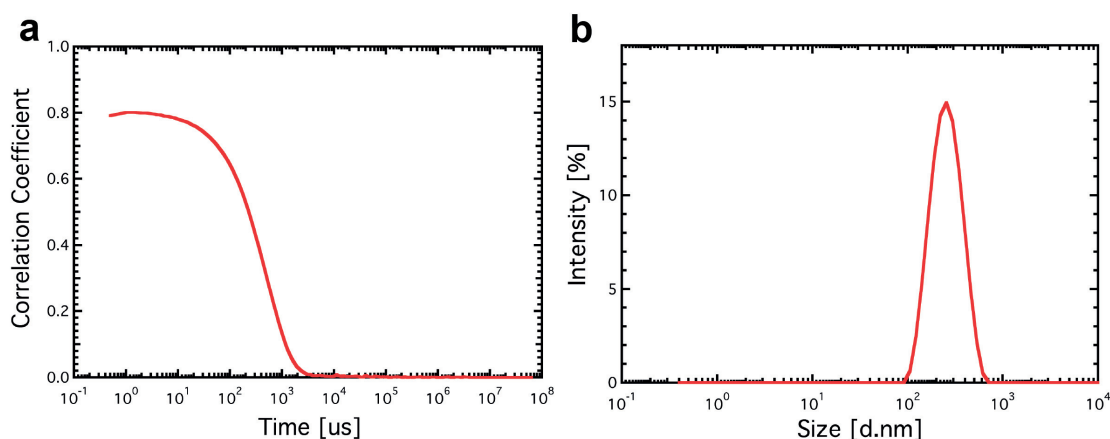
Figure 4.8: Average size of scattering objects formed in a solution containing 4 mM of a surfactant FSH_2-Jeffamine900. Typical (a) correlation function and (b) intensity average measured with DLS.

Name	Size at 4 mM [d.nm]
FSH-PEG220	189
FSH-Jeffamine600	100
FSH-Jeffamine1000	143
FSH-Jeffamine2000	34
FSH_2-PEG310	171
FSH_2-Jeffamine600	67
FSH_2-Jeffamine900	114
FSH_2-Jeffamine2000	21

Table 4.1: Average diameter of scattering objects formed in HFE-7500 containing 4 mM of different surfactants.

4.4.2   Influence of the Interfacial Tension on the Permeability

If small aqueous drops form in the oil phase, new water-oil interfaces must be produced. This process is energetically expensive. We therefore expect the formation of these drops to decrease with increasing interfacial energy and hence, with increasing interfacial tension. To test this expectation, we analyze the permeability of double emulsions stabilized with an equal concentration of surfactants having different compositions and plot it as a function of the interfacial tension. Indeed, the leakiness decreases with increasing interfacial tension for emulsions stabilized with di- and triblock copolymers, as summarized in Figure 4.10a. Similarly, if double emulsions are stabilized with the same type of surfactant, their leakiness decreases with decreasing surfactant concentration and hence with increasing interfacial tension, as summarized in Figure 4.10b. Our results suggest that with increasing interfacial tension, fewer drops form. This suggestion is well in agreement with the observation that the turbidity of the oil remains unchanged if it contains FSH_2-Jeffamine2000, a surfactant that only moderately lowers the interfacial tension, as shown in Figure 4.7. These results further support our hypothesis that the transport of encapsulants across the shell of double emulsions is mainly caused by aqueous drops that spontaneously form in proximity to the liquid-liquid interface, as schematically illustrated in Figure 4.10c. The leakiness of double emulsions can be reduced by increasing the interfacial tension. However, if the interfacial tension is increased, the stability of single emulsion drops usually decreases. [1] This trade-off would limit the use of surfactant stabilized single emulsion drops for high accuracy screening assays. To test, if the stability of double emulsions also inversely scales with the interfacial tension, we quantify their stability by incubating them at 95°C for 10 min. We determine the fraction of double emulsions that remains intact during this incubation using optical microscopy. The majority of double emulsion drops stabilized with any of the tested surfactants remains intact during this incubation, as shown in Figure 4.9. Remarkably, we cannot observe

any clear correlation between the drop stability and the surfactant composition, even though the surfactant composition influences the interfacial tension, as summarized in Table 2.1 on page 28.
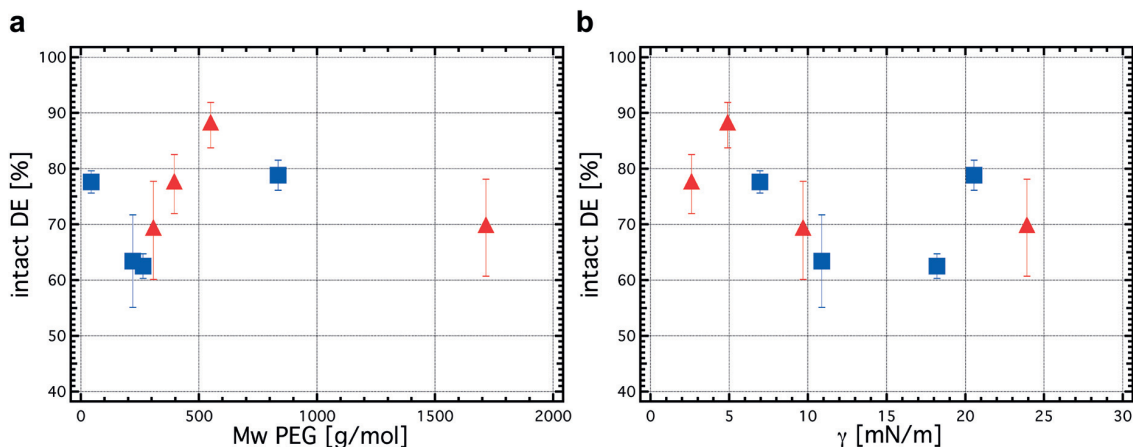
Figure 4.9: Influence of surfactant composition on the stability of double emulsions. (a) Influence of the PEG molecular weight of diblock (■) and triblock (▲) copolymer surfactants (Mw PEG) and (b) the interfacial tension, γ, on the stability of double emulsions, measured as the percentage of intact double emulsions after they have been incubated at 95°C for 10 min. Double emulsions are stabilized with 1 mM of the respective surfactant.

These results suggest that for double emulsions, a good stability must not be traded off with a low permeability such that they have the potential to be well-suited tight vessels for screening assays.
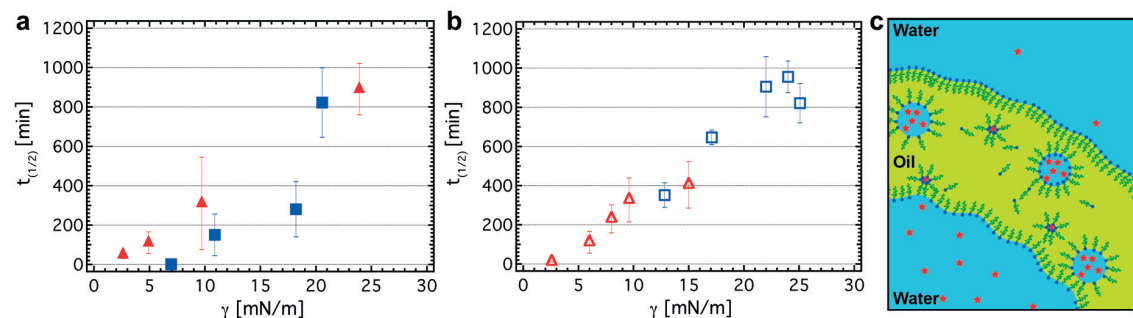
Figure 4.10: Leakage of double emulsions. (a) Influence of the interfacial tension, γ, on the transport of fluorescein across the oil shell of double emulsions stabilized with 1 mM of diblock (■) and triblock (▲) copolymer surfactants, measured as $t_{1/2}$. (b) Influence of γ on $t_{1/2}$ of double emulsion stabilized with different concentrations of FSH$_2$-Jeffamine900 (△) and FSH-Jeffamine1000 (□). (c) Schematic illustration of a water-oil-water double emulsion drop with the suggested mechanism by which encapsulants (red stars) are transported across their oil shell (green): Small aqueous drops (blue) act as carriers for encapsulants.

4.4.3   Influence of Surfactant Structure on the Permeability

Our results indicate that small aqueous drops spontaneously form in close proximity to the liquid-liquid interface. If these drops are formed at the liquid-liquid interface, this interface

must deform. Surfactants with small inverse packing parameters increase the local curvature of liquid-liquid interfaces, [171, 172] thereby likely facilitating the formation of small drops in the presence of convective flows. [19, 25] Indeed, our results suggest that the formation of these drops, and hence the transport of reagents across the oil shell, increases with decreasing inverse packing parameter of the surfactant, as indicated in Figure 4.6c. Surfactants with small inverse packing parameters also more easily assemble into inverse micelles that can grow into drops, by analogy to emulsion polymerization processes; [173–175] this could be another contributing reason for the spontaneous formation of drops. The exact mechanism by which these small drops form remains to be determined.

4.4.4   Transport of Large Reagents Across the Oil Phase.

If small aqueous drops spontaneously form in the shell of double emulsions, we expect them also to transport large encapsulants across the shell. Many of the drop-based screening assays are employed for biological applications. To test if also biologically relevant encapsulants are transported across oil phases, we load double emulsions with fluorescently labeled single strand DNA composed of 17 base pairs. These DNA strands are rapidly transported across the shell, as shown by the yellow triangles in Figure 4.11a. Even plasmids containing up to 11000 base pairs are transported across the shell of these double emulsion drops, as shown by the orange circle in Figure 4.11a. These results demonstrate that double emulsions are highly permeable also towards large encapsulants.
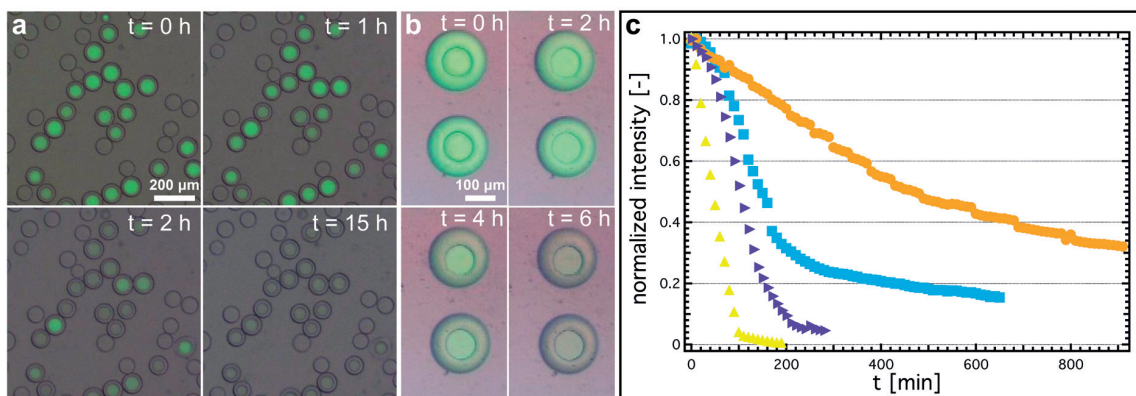
Figure 4.11: Transport of encapsulants across the shell of double emulsions. (**a**) Time-lapse fluorescent micrographs of double emulsions stabilized with 1 mM FSH$_2$-Jeffamine900 that encompass fluorescently labeled 100 nm polystyrene beads in their cores. (**b**) Trapped single emulsion drops containing 100 nm polystyrene beads imaged over time. A decrease in fluorescence intensity is observed. (**c**) Normalized fluorescent intensity of the double emulsion cores as a function of the incubation time if the cores contain 100 nm polystyrene beads (■), 11000 base pairs long plasmid (●), 17 base pair long single strand DNA (▲) and fluorescein (▶). All double emulsions are stabilized with 1 mM FSH$_2$-Jeffamine900.

To test if also large solid objects can be transported across the oil phase, we produce double emulsions that contain fluorescently labeled 100 nm diameter polystyrene (PS) beads in their cores; these double emulsions are stabilized with 1 mM FSH_2-Jeffamine900. To quantify the size of the fluorescently labeled PS-beads size, we image them with scanning electron microscopy (SEM) and measure their hydrodynamic diameter using dynamic light scattering (DLS). The average diameter of these particles is approximately 100 nm as shown in the SEM image and the DLS results in Figure 4.12a and 4.12b.
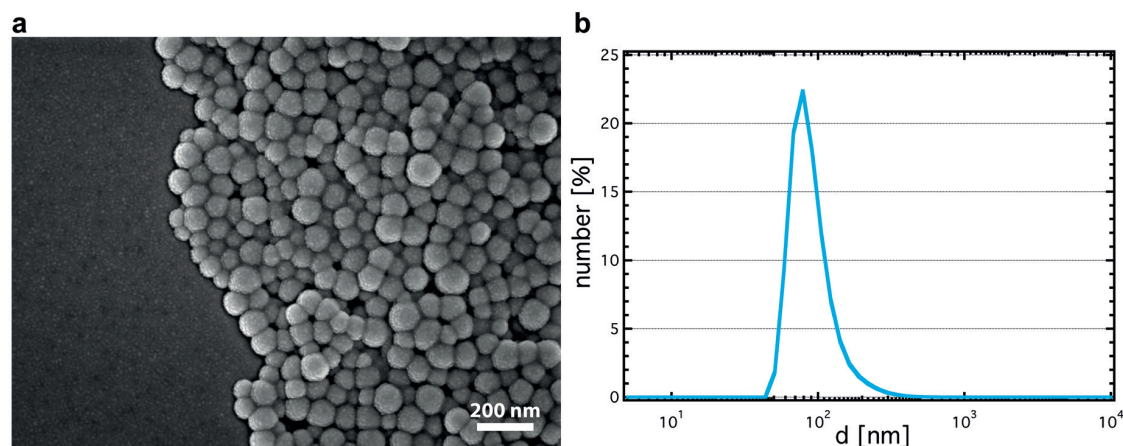
Figure 4.12: Characterization of fluorescently labeled polystyrene beads. (**a**) Scanning electron microscopy (SEM) image of the fluorescently labeled polystyrene beads and (**b**) the size distribution of these beads measured with DLS.

Indeed, also these PS beads are transported across the oil shell, as indicated by the decrease in fluorescence over time shown by the blue squares in Figure 4.11a and in the microscope image in Figures 4.11b and c.

To test if this transport is limited to double emulsions, we produce two batches of water in oil single emulsion drops, one where drops are loaded with PS beads and one with empty drops. Upon mixing of the two batches, the fluorescence of the PS-loaded single emulsion drops decreases over time, as shown in Figure 4.11c. By contrast, if only single emulsions containing PS beads are dispersed in the oil phase and these drops are imaged under the same conditions, the fluorescence of the drops remains unchanged, as shown in Figure 4.13. These results indicate that the decrease in fluorescence, observed in Figure 4.11b, is related to an exchange of PS beads between PS-loaded and empty drops and it is not related to bleaching.
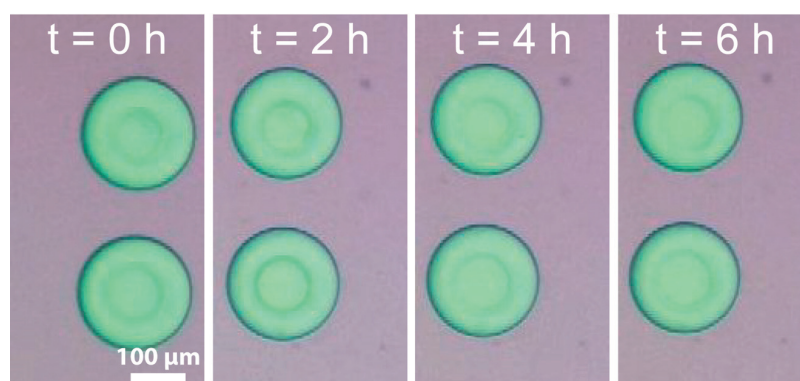
Figure 4.13: Time lapse microscopy images of trapped single emulsion drops containing 100 nm polystyrene beads. Compared to Figure 4.11, where a mixture of empty and PS bead-loaded drops was incubated, here only drops containing the fluorescently labeled PS beads are incubated and no leakage is visible.

These results indicate that the transport of reagents, that can be as large as 100 nm in diameter, is not limited to oil shells of double emulsions but also occurs across bulk oil phases.

4.4.5   Influence of Shell-Thickness on the Permeability

The permeability of double emulsions can be reduced if they are stabilized with an appropriate surfactant. For the system tested here, the triblock copolymer surfactant FSH$_2$-Jeffamine2000 results in the lowest permeability. However, this reduction in permeability requires surfactants that are not commercially available and hence, that are more difficult to access. For many applications, it would be beneficial to reduce the leakiness of double emulsion drops without changing the surfactant composition. If the transport of reagents is caused by 100 nm diameter drops, we expect it to be slowed down if we reduce the shell thickness to values that are similar to those of the diameter of the small drops. To test this expectation, we produce double emulsions with different shell thicknesses; all these double emulsions are stabilized with FSH$_2$-Jeffamine900. To produce double emulsions with shell thicknesses below 4 μm, we employ the microfluidic aspiration device that can reduce the shell thickness of double emulsions down to 330 nm. [169] Indeed, the transport of fluorescein across a shell as thin as 0.33 μm is much slower than that across a 8.4 μm thick shell, as a comparison of time-lapse fluorescence micrographs in Figure 4.14a reveals. If the shell thickness is reduced from 13.5 μm to 0.33 μm, $t_{1/2}$ increases from 118 min to 1679 min, as shown in Figure 4.14b. We assign the decrease in permeability to the steric hindrance that delays or even suppresses drop formation. In addition, the thinner shells have a higher hydrodynamic resistance that slows down the convective flow of the oil, thereby reducing the propensity for small aqueous drops to form at the liquid-liquid interface. These results demonstrate that the permeability of double emulsions can be reduced by more than an order of magnitude without changing the composition of the surfactants by simply reducing the thickness of the oil shell. This reduction in shell thickness constitutes an elegant way to

minimize the transport of reagents across the shell of double emulsion drops, and thereby offers new ways to improve the accuracy of screening assays.
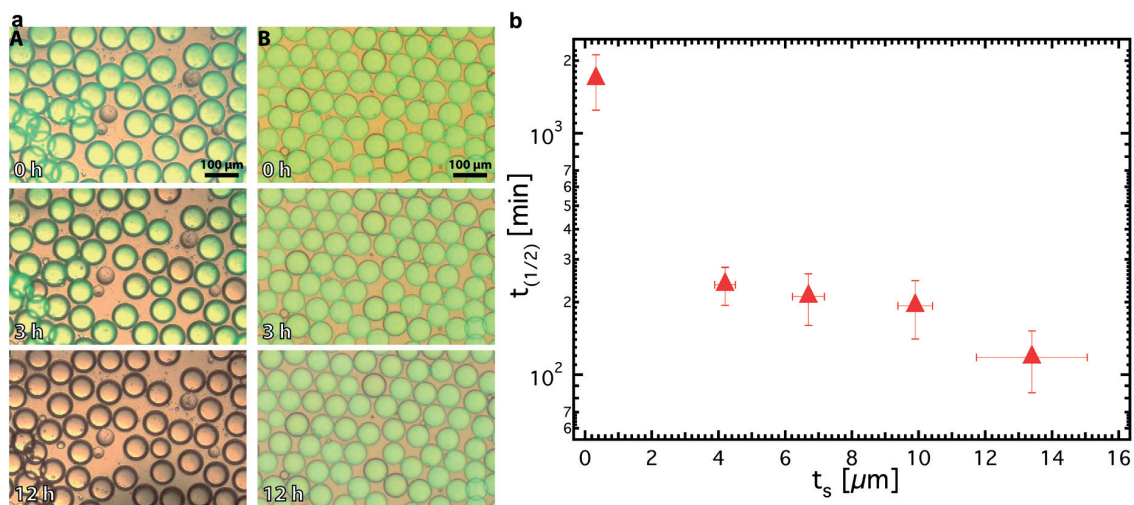
Figure 4.14: Influence of shell thickness on leakiness. (**a**) Overlay time-lapse optical and fluorescence micrographs of double emulsions whose cores contain fluorescein and whose shell thickness is (A) $t_s = 8.4$ μm and (B) $t_s = 0.33$ μm. (**b**) Influence of the shell thickness, t_s, on $t_{1/2}$ for double emulsions stabilized with 1 mM FSH$_2$-Jeffamine900.

4.4.6 Leakage of Double Emulsions Stabilized by Commercial Oils

To test if the leakage from double emulsions is related to surfactants we synthesized, we stabilize double emulsions with commercially available surfactants, as shown in Figure 4.15. Double emulsions whose shell is composed of the droplet generation oil EvaGreen (BioRad, USA) display a similar leakage as that observed with our FSH$_2$-Jeffamine900 surfactant, as shown in Figure 4.15. By contrast, drops whose shell is composed of the partitioning oil (10X Genomics, USA) are less leaky and the transport of fluorescein across this shell is similar to the transport observed with our optimized surfactant FSH$_2$-Jeffamine2000, shown by the diamonds, or if we reduce the shell thickness to 0.33 μm, as shown by the triangles in Figure 4.15.
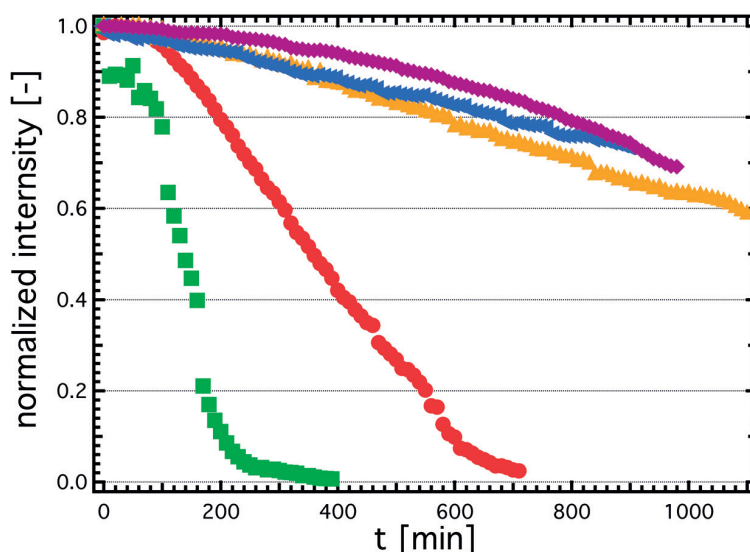
Figure 4.15: Transport of encapsulants across the shell of water-oil-water double emulsions whose shell is composed of commercial oils. Evolution of the fluorescence intensity of the core of double emulsions with shells composed of the droplet generation oil Eva Green (BioRad). Double emulsions contain fluorescein (●), or fluorescently labeled DNA with 17 base pairs (■) in the core. In addition, the permeability of double emulsions with shells composed of a surfactant-containing fluorinated oil from 10X genomics that contain fluorescein in their cores (▲) is shown. The permeability is compared to optimized double emulsions, namely double emulsions with shell thicknesses of 0.33 μm (◄) and those with 12 μm thick shells that are stabilized with FSH$_2$-Jeffamine2000 (♦).

4.5   Conclusion

Emulsion drops are frequently employed as reaction vessels to conduct high throughput screening assays. The accuracy of these assays is often compromised by the exchange of reagents contained in different drops that causes cross-contamination. Here, we demonstrate that the transport of reagents across the oil phase is primarily caused by aqueous drops with diameters of the order of 100 nm that spontaneously form in the oil phase. The propensity of these small drops to form and hence, the leakiness of large emulsion drops can be reduced by at least an order of magnitude if they are stabilized with surfactants that only moderately lower the interfacial tension. Because the stability of double emulsions only weakly depends on the interfacial tension, it must not be traded-off with their leakiness such that mechanically stable double emulsions with a very low permeability can be produced. However, this approach requires optimized surfactants. The leakiness of double emulsions can also be strongly decreased if their shell thickness is reduced to values similar to the diameter of the small drops that spontaneously form in the oil. In this case, the formation of these drops is sterically hindered such that almost no encapsulants are transported across thin oil shells. From these mechanistic insights, design rules for the synthesis of optimized surfactants and emulsion fabrication processes can be derived that offer a tighter control over the leakiness of emulsion drops. This understanding might open

up new possibilities to use drop-based screening assays also for applications that require a high accuracy, including applications in pharmacy and food industries.

Chapter 5

Bio-inspired self-healing capsules: Delivery vehicles and beyond

Gianluca Etienne, Esther Amstad

In this chapter, we introduce novel microcapsules with viscoelastic shells, that are made of surfactants containing a metal binding moiety, that can be ionically cross-linked at the drop surface. These capsules show high mechanical stability and can be printed into 3D structures.

This chapter is adapted from the paper entitled **"Bio-inspired self-healing capsules: Delivery vehicles and beyond"**, authored by Gianluca Etienne, Esther Amstad, submitted in 2018.

Contents

5.1   Abstract

Microcapsules are often used as individually dispersed carriers of active ingredients to prolong their shelf life or to protect premature reactions with substances contained in the surrounding. Here, we go beyond this application and employ microcapsules as principal building blocks of macroscopic 3D materials with well-defined structures. To achieve this goal and inspired by nature, we fabricate capsules from surfactants that are functionalized with catechols, a metal-coordinating motif. These surfactants self-assemble at the surface of emulsion drops where they are ionically crosslinked to form viscoelastic capsules that display a low permeability even towards small encapsulants. These mechanically robust catechol-functionalized capsules have a high affinity to each other such that they can be 3D printed into macroscopic viscoelastic structures without the need for additional crosslinking agents. Thereby, these capsules open up new opportunities for additive manufacturing of soft, self-healing materials composed of individual compartments that can be functionalized with different types of spatially separated reagents.

5.2   Introduction

Polymer microcapsules are often used as individually dispersed carriers to control the timing and location of the release of active ingredients [176] for example in food, [177, 178] cosmetic, [179, 180] and pharmaceutical [181, 182] applications. Key to a successful application of these capsules is a good control over their mechanical stability and permeability. [183] These parameters can be tuned with the composition and dimensions of the capsule shells. Capsules composed of thin polymeric shells that display a low permeability towards charged encapsulants are frequently made through layer-by-layer deposition of oppositely charged polyelectrolytes onto solid cores. [184–187] Once polyelectrolyte multilayers are formed, the core is dissolved such that capsules result. To reduce the number of deposition steps, capsules have been fabricated from covalently or ionically crosslinked reagents including polydopamines [188] or tannic acid. [189, 190] The solid particles that are used as templates offer a good control over the size of the capsules. However, they limit the amount of encapsulants that can be loaded into the capsule core. This limitation can be overcome if emulsion drops are employed as templates. Indeed, capsules composed of a wide range of materials have been produced from double emulsion templates by solidifying their shells. [191, 192] The flexibility in the materials choice enables the fabrication of capsules that offer triggered release of encapsulants in response to various stimuli, including changes in temperature, [193] pH, [194, 195] ionic strength, [196] oil composition, [192] and the presence of enzymes. [122] However, the resulting capsules typically have rather thick shells, rendering them stiff. Their stiffness hampers their flow through narrow orifices, which would typically be required if they want to be used as principal building blocks of inks that can be 3D printed. Moreover, the high volume fraction occupied by the shell limits the amount of encapsulants that can be loaded into their cores. Feasibility to use double emulsions as templates to produce capsules with thin polymeric shells that occupy less than 2% of the capsule volume has been shown. [197] However, these capsules were rather stiff such that they broke if mechanically deformed, hampering their further processing into macroscopic materials. Capsules with much thinner, flexible shells that can be loaded with significantly higher quantities of encapsulants can be fabricated if reagents are solidified at the drop surface. This can be achieved, for example, if reagents dispersed in the drop meet appropriate reagents dispersed in the oil at the drop surface where a polymerization reaction occurs. [198–200] Capsules with charged polymeric shells can be formed through coacervation reactions where oppositely charged macromolecules are dissolved in the drop and the continuous phase respectively. [201, 202] Similarly, polyelectrolyte multilayer-based capsules can be assembled from emulsion drops if they are stabilized with charged surfactants and dispersed in a solution containing oppositely charged reagents. [203, 204] Capsules with thin shells can also be produced from chemically reactive surfactants that are directly crosslinked at the drop surface. [205–209] However, the number of reagents that can be employed to form thin polymeric capsules through these approaches is limited. Flexible capsules that display a narrow size distribution, low permeability towards encapsulants, allow controlled

repetitive exchanges of reagents, and are mechanically sufficiently stable to withstand significant shear stresses such that they can be further processed into macroscopic materials through additive manufacturing techniques remain to be established. These capsules would open up a new field of their use as principal building blocks of macroscopic materials with well-defined structures and locally varying compositions that goes far beyond their current use as individually dispersed delivery vehicles. Here, we introduce a new type of viscoelastic, mechanically stable capsule that are composed of bio-inspired ionically crosslinked catechol-functionalized block copolymer surfactants. Because of the viscoelastic properties, capsules are self-healing such that they can be merged and split at will. These capsules present a high concentration of Fe^{3+}-complexed catechols at their surface such that they have a high affinity to each other. Therefore, they cannot only be used as individually dispersed mobile carrier vehicles that display a low permeability even towards small encapsulants, but also as principal building blocks of macroscopic soft materials. We demonstrate for the first time that these capsules are mechanically sufficiently stable to serve as principal building blocks of inks that can be 3D printed into macroscopic granular materials with well-defined structures.

5.3 Materials and Methods

5.3.1 Surfactant Synthesis

Chemicals: All chemicals, namely fluorinated oils HFE-7100 and HFE-7500 (3M, USA), the fluorinated block of the surfactant FSH (Krytox 157 FSH, Chemours, USA), polypropylene glycol (PPG 2000 g/mol, Acros Organics), thionyl chloride and chloroform (Merck, Germany), dichloromethane (DCM), anhydrous ethyl acetate (EtAc), methanol (MeOH), triethylamine, dopamine hydrochloride (Dopa), N,N-dicyclohexylcarbodiimide (DCC) (Sigma-Aldrich), anhydrous N,N-Dimethylformamide (DMF) and 3-(3,4,-Dihydroxyphenyl)propionic acid (Hydrocaffeic acid, HA) (Abcr, Germany), and N-Hydroxysuccinimide (NHS) and stearoyl chloride (TCI, Japan) were used as received.

FSHDopa Synthesis

All the reactions are performed under argon atmosphere using dry glassware. 1 mol equivalent of FSH is dissolved at 0.2 g/mL in HFE-7100, dried with molecular sieves, and the solution is degassed with argon. 10 mol equivalents of thionyl chloride is added to the solution under argon atmosphere to activate the carboxylic end group of the FSH. This reaction is refluxed at 65°C for 2 hours. Under reduced pressure and at 90°C the excess thionyl chloride is removed, resulting in the pure activated FSH. The FSH is subsequently re-dissolved in HFE-7100. 2.5 mol equivalents of dopamine is dissolved in DMF and the solution is degassed with argon before it is mixed with activated FSH. 2.5 mol equivalents of triethylamine is added to the reaction to drive

the reaction to completion. The reaction is refluxed overnight at 65°C. The solution is filtered through a filter paper, and all the solvents are removed under reduced pressure. The product is purified using a mixture of water and HFE-7100 and subsequently washed using a mixture of HFE-7100 and methanol. The precipitates are removed through centrifugation at 3000 g for 15 min (Mega Star, 1.6R, VWR). This washing step is repeated three times before the product is dried using a rotary evaporator (Hei-VAP, Heidolph, Germany) and freeze dryer (FreeZone 2.5, Labconco, USA).

FSHPEG900HA Synthesis

1 mol equivalent of hydrocaffeic acid is dissolved in dry ethyl acetate at 0.04 g/mL and 1 mol equivalent NHS is added to the reaction. 1 mol equivalent of DCC is dissolved in ethyl acetate and added to the NHS HA mixture that is stirred overnight under inert atmosphere. The product HA-NHS is filtered through a filter paper and dried under reduced pressure. 1 mol equivalent of HA-NHS is dissolved at 0.11 g/mL in dry ethyl acetate and bubbled with argon. 0.95 mol equivalent of the polyethylene glycol Jeffamine ED-900 (Huntsman, USA) is dissolved in dry ethyl acetate, added to the HA-NHS solution, and stirred overnight. The solvent is removed using a rotary evaporator, resulting in the intermediate product H_2N-PEG-HA. FSH is activated as described for the synthesis of FSHDopa. 1.5 mol equivalent of H_2N-PEG-HA is dissolved in DCM and added to the activated FSH. 1 mol equivalent of triethylamine is added to drive the reaction to completion, and everything is refluxed overnight at 65°C. The solvent is removed and the product is washed using a mixture of HFE-7100 and methanol and they are centrifuged at 3000 g. This washing step is repeated three times. The final product is dried using a rotary evaporator and a freeze dryer.

SADopa Synthesis

1 mol equivalent of stearyl chloride is dissolved in anhydrous DMF under argon at 0.2 g/mL. 1.5 mol equivalents of dopamine is dissolved at 0.06 g/mL in DMF and cooled to 0°C. 3 mol equivalents of triethylamine is added to the dopamine and mixed with stearyl chloride. The mixture is heated to 65°C and stirred overnight under argon atmosphere. The reaction product is extracted with water and ethyl acetate. This cleaning step is repeated three times before everything is dried in a rotary evaporator and a freeze dryer.

DiDopaPPG Synthesis

1 mol equivalent of propyleneglycol is dissolved in chloroform and 10 mol equivalent of thionyl chloride is added. The solution is refluxed at 65°C for 2 hours. The excess thionyl chloride is removed under reduced pressure at 90°C. 4 mol equivalents of dopamine is dissolved in DMF, 1.5 mol equivalents of triethylamine is added, and the mixture is stirred overnight. The product

is extracted with diethylether and water. Extraction is repeated three times before the solvents are removed using a rotary evaporator and freeze dryer.

5.3.2 Buckling Test

To test the buckling of the capsules we use a pendant drop setup (DSA-30 Krüss, Germany) to image the drops and to controllably retract the fluid contained in them.

5.3.3 Fabrication of Microfluidic Device

We produce flow-focusing microfluidic devices from PDMS, as described in section 2.3 on page 30.

5.3.4 Production of Emulsion Drops

Emulsion drops are produced using microfluidic flow-focusing devices as described in section 2.4.2 on page 32.

To produce double emulsions, an aqueous phase containing 6 wt% PEG 6000 Da, 0.01 wt% Fluorescein Na salt, 0.3 M BICINE buffered at pH=8.5, and 0.02 mM Fe^{3+} is employed. The middle phase consists of HFE-7500 or HFE-7100 containing 2 mM of a surfactant. The outer phase is an aqueous solution containing 10 wt% partially hydrolyzed polyvinyl alcohol (PVA) 13-18 kDa (Sigma-Aldrich, USA). Double emulsions are produced by injecting the inner phase at around 1000 μl/h, the middle phase at 1000-1300 μl/h and the outer phase at around 6000 μl/h. To avoid osmotic pressure gradients, that would result in a change in the dimensions of the double emulsions, the osmolarity of the inner and outer phase is matched using D(+)-saccharose (Carl Roth, Germany); the osmolarity of the solutions is quantified with an osmometer (Advanced Instruments, Fiske 210).

5.3.5 Quantification of the Leakage

To minimize the risk that the permeability of double emulsions is influenced by PVA present in the outer phase, double emulsions are washed three times using an osmotically balanced aqueous solution. 1 μl of washed double emulsions is added to 1.5 mL of an osmotically balanced aqueous solution and emulsions are imaged every 10 min using a fluorescent microscope (Eclipse Ti-S, Nikon). The fluorescence images are analyzed using a custom-made MATLAB code that quantifies the evolution of the fluorescent intensity of double emulsion cores over time.

5.3.6 3D printing of Capsules

2 mM FSHPEG900HA are dissolved in HFE-7100 containing Fe^{3+} ions at a 3:1 ratio. Iron is added to HFE-7100 from an ethanol-based solution containing 1M $FeCl_3$ (Sigma-Aldrich, USA).

Single water in oil emulsions are produced using a PDMS microfluidic flow-focusing device. An HFE-7100-based solution containing surfactants and Fe^{3+} is used as the continuous phase.

5.4 Results

5.4.1 Production of Capsules

Emulsion drops are often stabilized with polymeric surfactants that are crucial during the drop production and storage. However, once the drops are converted into capsules, surfactants are usually superfluous or even devastating because they irreproducibly change the surface wettability of the capsules. Instead of identifying protocols that efficiently remove surfactants from the capsule surface, we introduce surfactants that serve as building blocks to form viscoelastic capsules. To achieve this goal, we synthesize a new amphiphilic block copolymer surfactant that is end-functionalized with catechol, a metal-coordinating motif, as shown in Figure 5.1a. We employ a diblock copolymer surfactant composed of a perfluoropolyether block that is covalently linked to a poly(ethylene glycol) (PEG)-based block as a model surfactant; this surfactant has proven to stabilize water in perfluorinated oil drops efficiently. [1] To enable the formation of metal-coordination bonds between adjacent surfactants, we functionalize their PEG-ends with catechol, a molecule that strongly complexes certain metal ions such as Fe^{3+}, [210–212] as shown schematically in Figures 5.1b and c.
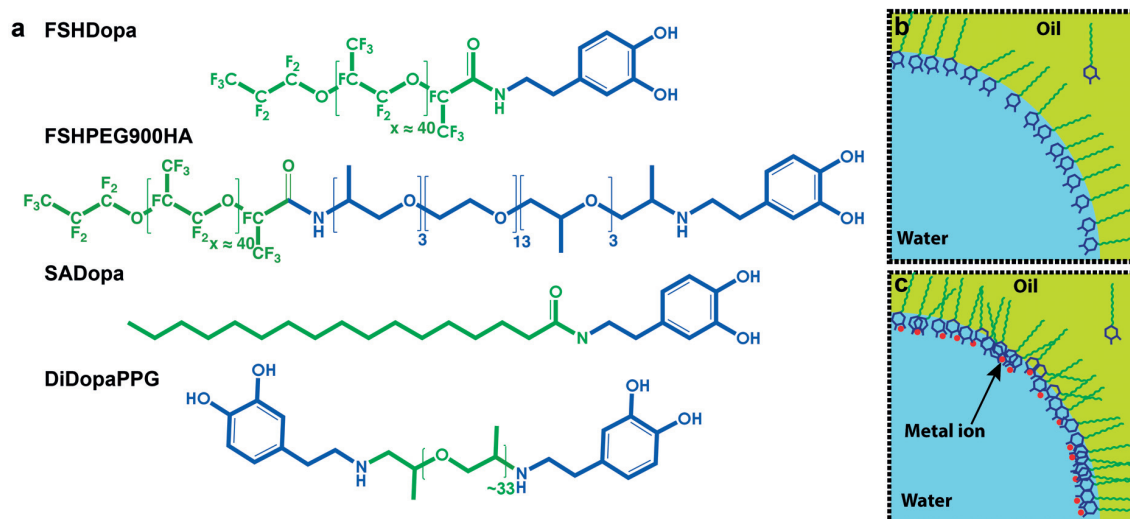

Figure 5.1: Catechol-functionalized surfactants. (**a**) Chemical structure of different catechol-functionalized surfactants. (**b,c**) Schematic illustrations of emulsion drops stabilized with catechol-functionalized surfactants in the (**b**) absence and (**c**) presence of Fe^{3+} ions that cross-link the surfactants at the interface.

To test if we can convert emulsion drops stabilized with our catechol-functionalized surfactants into viscoelastic shells, we form perfluorinated drops using a pendant drop set-up. Fluorinated drops encompassing 2 mM of the catechol-functionalized surfactant FSHPEG900HA are formed in an aqueous solution containing 1 mM $FeCl_3$. We expect catechol-Fe^{3+} complexes to form if the pH is increased to basic values where catechols are deprotonated. [211] To test this expectation, we increase the pH of the surrounding using NaOH. Indeed, under basic conditions, we observe the formation of thin solid shells at the drop surface within 30 s. These shell starts to buckle if liquid is retracted, as shown in the time-lapse micrographs in Figure 5.2a. A similar behavior is observed if drops are stabilized with 2 mM FSHDopa that lacks the PEG-based block, indicating that shells form even in the absence of any hydrophilic spacer, as shown in the Figure 5.2e. By contrast, if the pH is adjusted to 3, where the hydroxyl groups of catechols are protonated, we cannot observe any sign of a shell, even if the liquid is completely retracted from the drop, as shown in Figure 5.2b. Similarly, no signs of a shell formation can be observed within the investigated timeframe if drops do not encompass any surfactants, as shown in Figure 5.2c, or if catechol-free surfactants are used, as detailed in the Figure 5.2f. These results suggest that catechol-functionalized amphiphilic block copolymers can indeed be converted into thin shells if catechols are deprotonated such that they form multivalent complexes with Fe^{3+}.
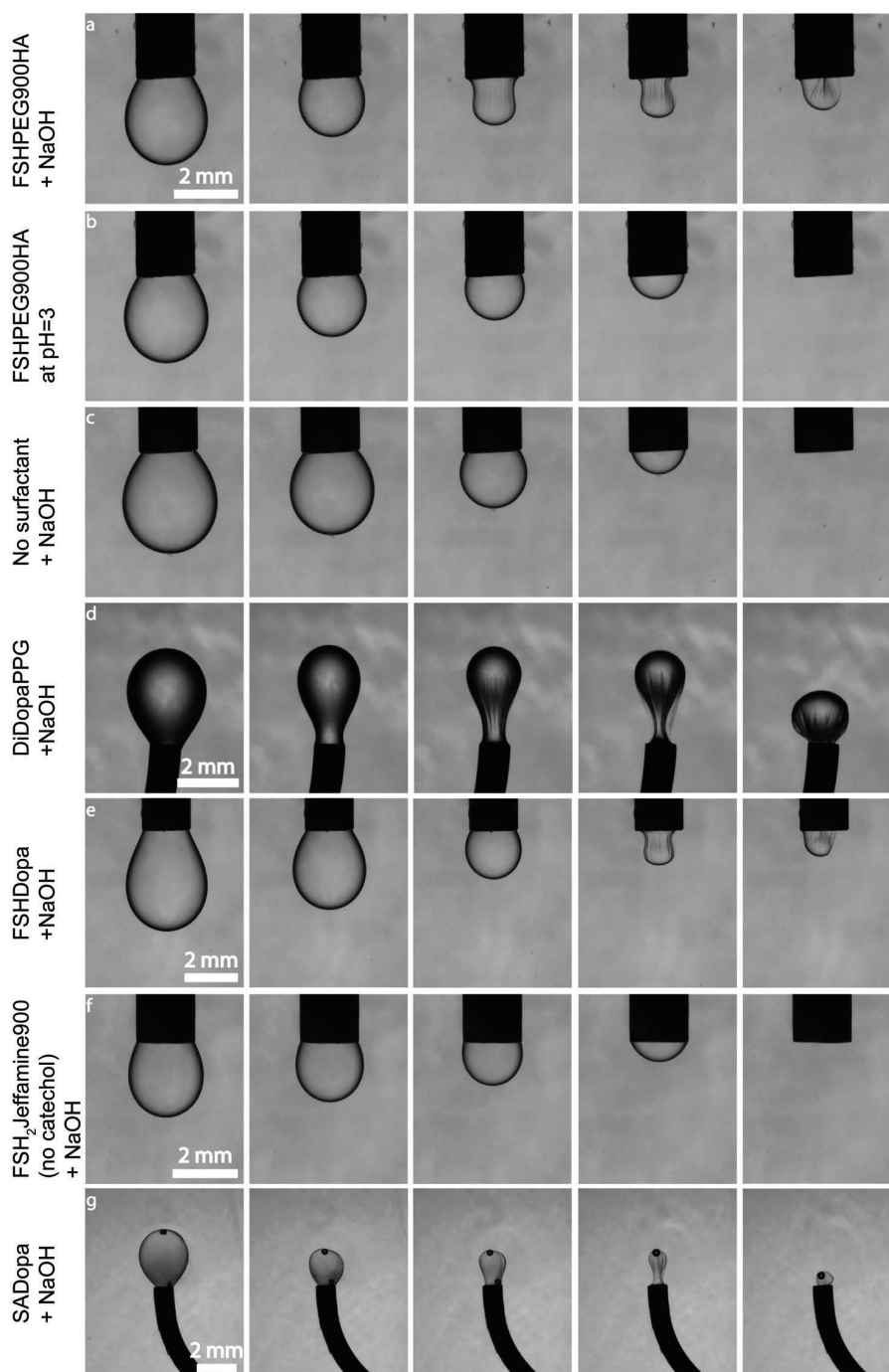
Figure 5.2: Time-lapse optical micrographs of oil drops containing catechol surfactants that are dispersed in aqueous solutions containing 1 mM $FeCl_3$ acquired during the retraction of the oil phase. (**a,b**) Drops composed of HFE-7500 containing 2 mM FSHPEG900HA (**a**) with and (**b**) without 0.01 M NaOH in the continuous phase. (**c**) Control experiments of HFE-7500-based drops containing no surfactant. Drops are formed inside an aqueous solution containing 1 mM $FeCl_3$. (**d**) Drop composed of toluene, containing 2 mM DiDopaPPG dispersed in an aqueous solution containing 1mM $FeCl_3$ and 0.01 M NaOH. (**e**) Drop composed of 2 mM FSHDopa with 0.01 M NaOH added to the continuous phase. (**f**) Control experiment with 2 mM FSH_2-Jeffamine900, an unfunctionalized surfactant. (**f**) Ethyl acetate based drop containing 2 mM SADopa containing Fe^{3+} in an aqueous solution where the pH is 8.

Our results indicate that perfluorinated surfactants can be converted into viscoelastic shells if they are functionalized with catechols and ionically crosslinked. By crosslinked in this work we mean that two or three catechol groups can bind to one metal ion but that it is very likely we have further entanglement of the polymer chains, therefore, forming a network of surfactant molecules at the interface. To test the generality of our approach, we synthesize a non-fluorinated hydrocarbon-based surfactant composed of polypropylene glycol whose two ends are functionalized with catechols (DiDopaPPG), as shown in Figure 5.1a. We form toluene drops encompassing 2 mM of DiDopaPPG and 1 mM Fe^{3+} in an aqueous solution and increase the pH of the surrounding aqueous phase using NaOH. Also in this case, we observe the formation of a thin shell at the drop surface that starts buckling if fluid is retracted, as shown in Figure 5.2d. Similar behavior is observed for drops stabilized with dopamine-functionalized stearic acid (SADopa), as shown in Figure 5.2g. These results indicate that the formation of viscoelastic shells is not limited to fluorinated surfactants but also occurs if hydrocarbon-based catechol-functionalized surfactants are employed. Note that if the amount of added base is increased, thin, rather fragile shells become apparent, even for drops that do not encompass any surfactant or those that contain catechol-free surfactants. This shell formation most likely is caused by Fe^{3+} ions that aggregate. The resulting particles accumulate at the surface, thereby forming Pickering emulsions.

To test if catechol-functionalized surfactants are indeed ionically crosslinked, we perform UV-VIS spectroscopy on SADopa that is dissolved in ethanol at 4 mM. In the absence of any Fe^{3+} ions, an absorption peak at 280 nm, typical for catechols, [213] is observed. Upon addition of Fe^{3+} the absorption peak shifts to 246 nm, as shown in Figure 5.3. The observed shift is much smaller than that measured for catechol/Fe^{3+} complexes formed in aqueous solutions. [214] We assign this difference to the different solvent we use. These results indicate that catechol-functionalized surfactants are ionically crosslinked at the drop surface.
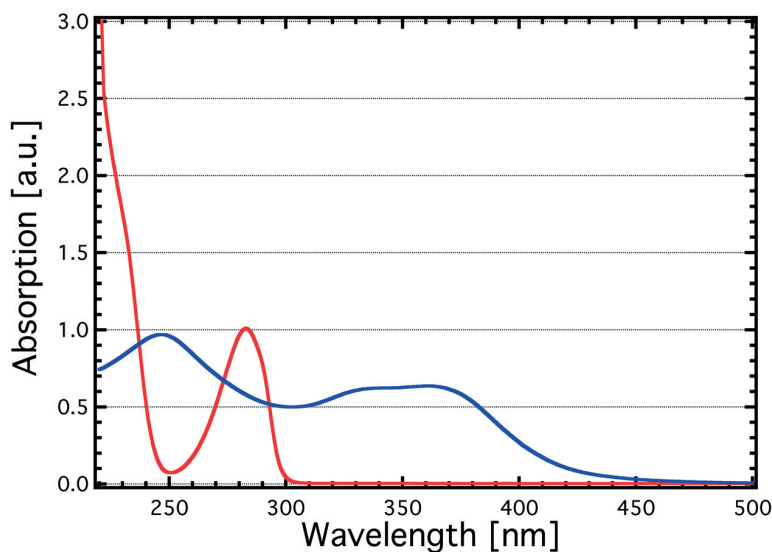
Figure 5.3: UV/VIS spectra of the catechol-functionalized surfactant SADOPA. UV/VIS traces of SADopa dissolved in ethanol with (blue line) and without (red line) Fe^{3+}.

5.4.2 Merging of Capsules

If catechols are ionically crosslinked, the capsules should display a viscoelastic behavior, by analogy to the catechol-functionalized hydrogels that are crosslinked with Fe^{3+} ions. [211, 215, 216] In this case, we expect them to merge if they are in contact with each other. To test this expectation, we form a drop composed of HFE-7100 containing 2 mM FSHDopa and 0.6 mM Fe^{3+} in a basic aqueous solution (pH = 8.5). We deposit this drop on a glass substrate and form a second fluorinated drop that is attached to a steel needle. When the two drops come in contact, they strongly adhere to each other, as shown in Figure 5.4a. If the shells are elastic, we expect the two drops to remain intact even if they are in contact with each other. By contrast, if the shells are viscoelastic, we expect them to merge such that encapsulants can be exchanged between the two drops. To qualitatively assess the mechanical properties of these shells, we form a first fluorinated drop that encompasses a 1.5 mm diameter air bubble and deposit it on a substrate. When a second drop is brought in contact with the first one, a connecting neck forms. When the diameter of the formed connection reaches values similar to the diameter of the air bubble, the air bubble starts to rise into the pendant drop, as shown in the time-lapse micrographs in Figure 5.4b. These results indicate that the two shells merged to form a connecting neck, which can only occur if the shells are viscoelastic. As a result of the viscoelastic behavior, the two merged drops can be separated after the air bubble is exchanged, resulting in two separate intact capsules, as shown in the last two frames in Figure 5.4b.
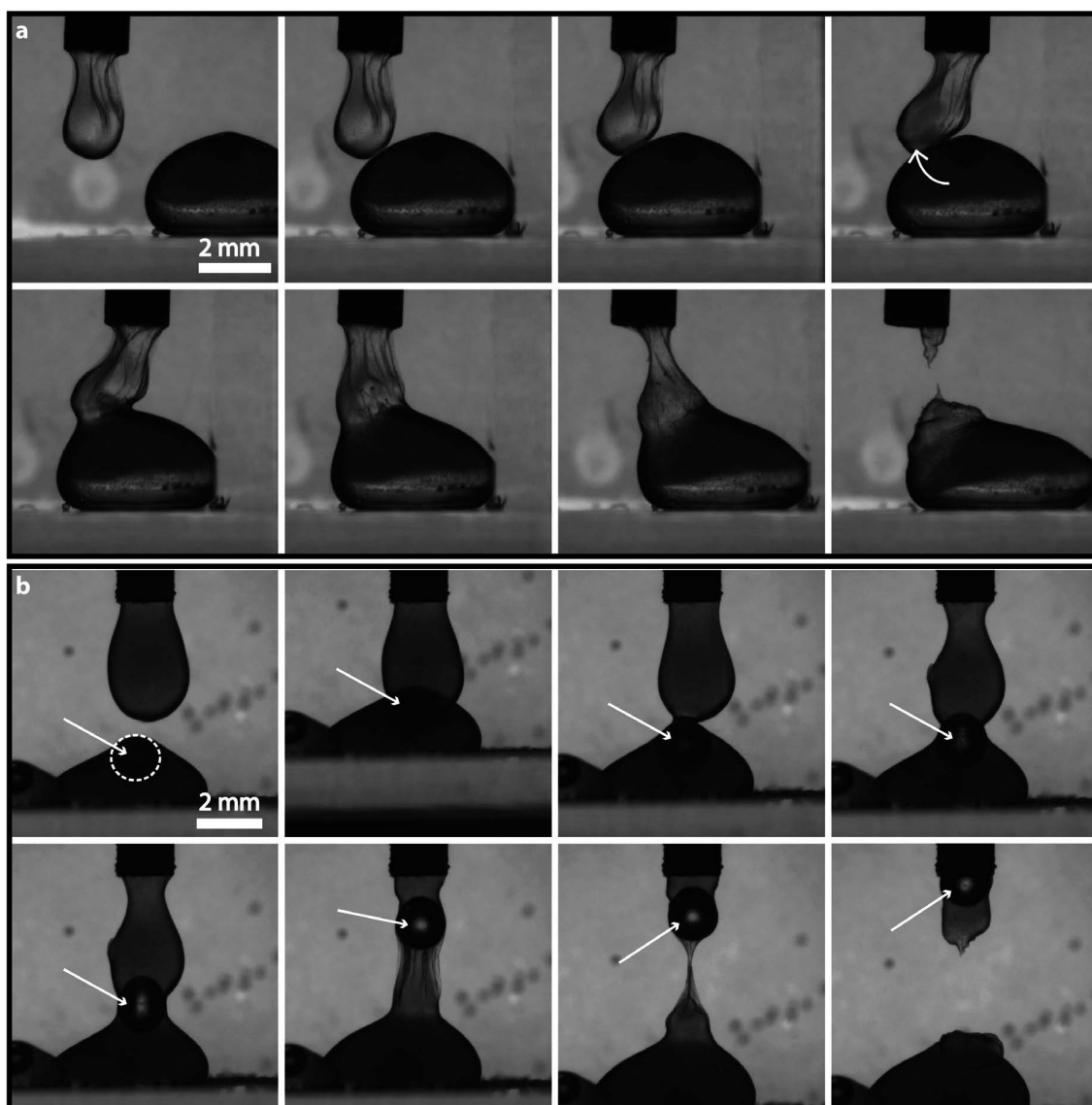
Figure 5.4: Time-lapse photographs of fluorinated drops stabilized with ionically crosslinked catechol-functionalized surfactants. Drops composed of HFE-7100 are loaded with 6 mM Fe^{3+} and 2 mM FSHDOPA and surrounded by a buffered aqueous solution. Catechol-functionalized surfactants are crosslinked with Fe^{3+} to form viscoelastic shells that (**a**) can be merged if two drops come in contact and (**b**) allow exchanging even large encapsulants, as exemplified by a 1.5 mm diameter air bubble that is initially trapped in the sessile drop and transferred to the pendant drop, as indicated by the white arrows.

5.4.3   Mechanical Stability of Capsules

Catechol-functionalized materials have a high affinity towards iron-presenting surfaces. [143] We therefore expect capsules presenting Fe^{3+} complexed catechols at their surfaces to have a high affinity to each other if not all catechols are complexed to Fe^{3+} ions. To test this expectation, we produce aqueous drops (pH = 8) that are dispersed in HFE-7100 containing 2 mM of the catechol-functionalized FSHPEG900HA surfactant and 0.6 mM Fe^{3+}. To closely control the size

of the drops, they are formed in polydimethylsiloxane (PDMS)-based microfluidic flow focusing devices. These monodisperse drops with a diameter of 114 μm are deposited onto a layer of an aqueous solution (pH = 8) where they self-assemble into a densely packed monolayer, as shown in the optical micrograph in Figure 5.5a. Interestingly, individual capsules with aqueous cores do not coalesce but adhere to each other to form an integral monolayer, as indicated by the collective movement of the layer. If adjacent capsules are linked through ionic bonds, the films should be self-healing. Indeed, when ruptured interfaces are brought in contact, they self-heal, as shown in the time-lapse optical micrographs in Figure 5.5a. These results indicate that a significant fraction of free catechols are present at the drop surface.
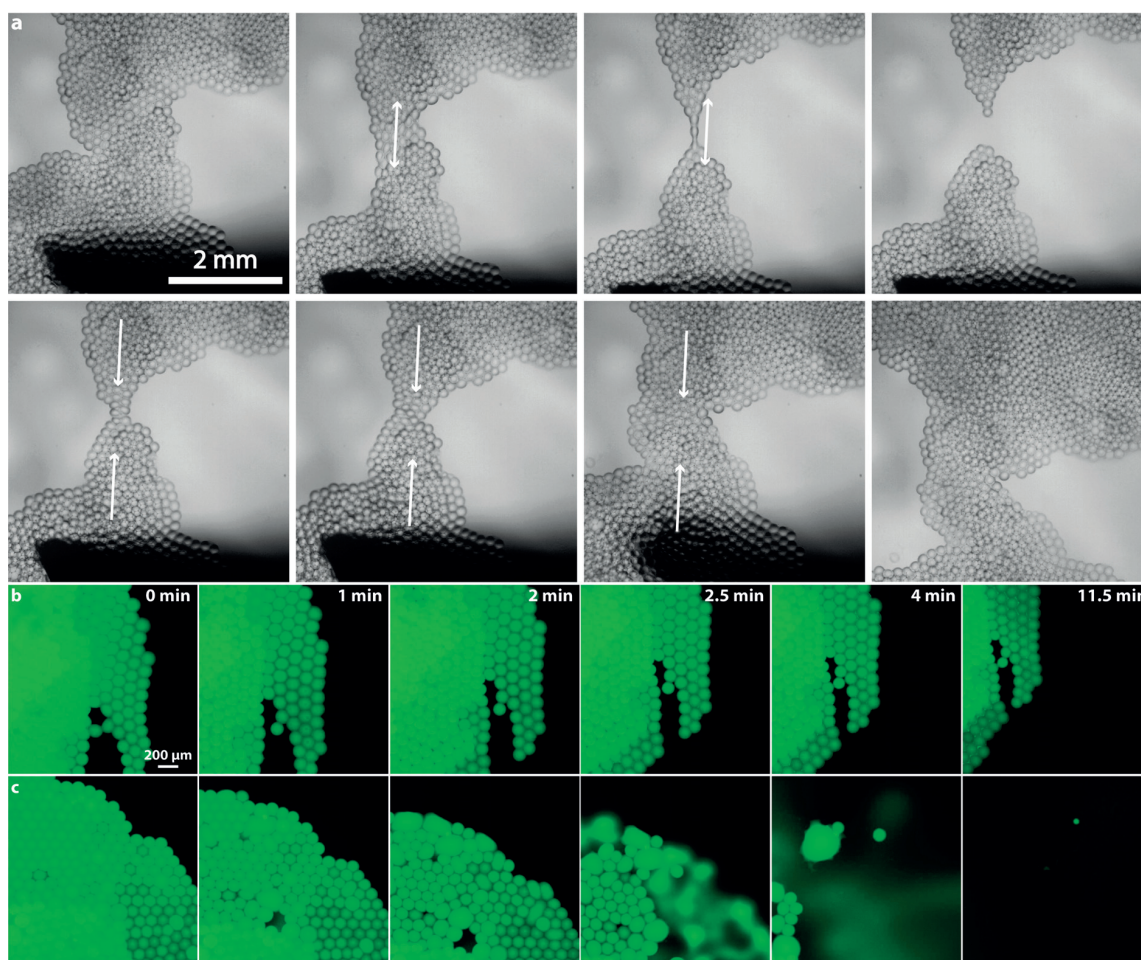
Figure 5.5: (**a**) Time-lapse optical micrographs of self-healing films composed of viscoelastic capsules. Aqueous drops (pH=8) dispersed in HFE-7100 containing FSHPEG900HA and Fe^{3+} are deposited onto an aqueous solution (pH=8). When the oil evaporates, a film composed of individual capsules form. These plastically deformable films self-heal when broken parts are brought in contact. Arrows indicate the direction of force applied on the film (**b,c**) Fluorescence microscopy images of fluorescently labeled single emulsion drops floating on a buffered Fe^{3+}-containing water solution (pH=8.5). Drops are stabilized with (**b**) catechol-functionalized FSHPEG900HA and (**c**) unfunctionalized FSH-Jeffamine2000. Drops stabilized with unfunctionalized surfactants rupture during the evaporation of the oil whereas those stabilized with catechol-functionalized surfactants remain intact.

We expect ionic bonds to increase the stability of emulsion drops against rupture. To assess the stability of these capsules if mechanically compressed, we centrifuge them at 13500g. We do not observe any significant rupture or merging, indicating that these capsules are at least as mechanically stable as drops stabilized with optimized unfunctionalized surfactants. [1] To test the stability of capsules against rupture if dried, we produce 114 μm diameter water drops that encompass fluorescein. Drops are deposited onto an aqueous solution containing 0.6 mM Fe^{3+} that is buffered to pH = 8.5 using BICINE. Drops stabilized with the catechol-functionalized FSHPEG900HA surfactant self-assemble into a hexagonal close-packed monolayer. Even though they are in direct contact with their neighbors, these aqueous drops retain their integrity even if the surrounding oil is evaporated, as shown in Figure 5.5b. By contrast, drops stabilized with unfunctionalized FSH-Jeffamine2000 surfactants rupture during the evaporation of the oil, thereby releasing fluorescein to the surrounding, as shown in Figure 5.5c. These results indicate that the stability of emulsion drops increases upon ionic crosslinking.

5.4.4 Leakage from Capsules

The vast majority of emulsion drops are stabilized with polymeric surfactants. These surfactants typically impart stability to emulsion drops. However, they come at an important expense: Free surfactants spontaneously form micelles and small aqueous drops that carry reagents across oil phases, resulting in cross-contamination between different drops. [2, 51, 118, 160, 161, 163, 164] This cross-contamination limits the use of surfactant-stabilized emulsion drops as picoliter-sized vessels for conducting sensitive high-throughput screening assays. This reagent transport also reduces the encapsulation efficiency if such drops are used as templates to form capsules. We expect this exchange of reagents to be delayed or even suppressed, if surfactants are ionically crosslinked such that their mobility at the liquid-liquid interface is reduced. To test our expectation, we produce water-oil-water double emulsions, containing fluorescein in their cores. Indeed, the vast majority, of fluorescein contained in double emulsions stabilized with ionically crosslinked FSHPEG900HA is retained for more than 14 days, which is the duration of our experiment, as shown in the micrograph in Figure 5.6a and summarized by the blue triangles in Figure 5.6b. By contrast, fluorescein is very rapidly released if double emulsions are stabilized with catechol-functionalized surfactants, FSHPEG900HA, that are not ionically crosslinked, as shown by the orange triangles in Figure 5.6b. Even faster release of fluorescein is observed if double emulsions are stabilized with 2 mM FSH_2-Jeffamine600, a non-functionalized surfactant, as shown by the red circles in Figure 5.6b. These results demonstrate that our catechol-functionalized surfactants constitute an elegant way to overcome cross-contamination that typically occur between surfactant-stabilized emulsions. Hence, these surfactants have the potential to significantly increase the usefulness of drops as picoliter-sized tight vessels for conducting high-throughput screening assays with an unprecedented accuracy.
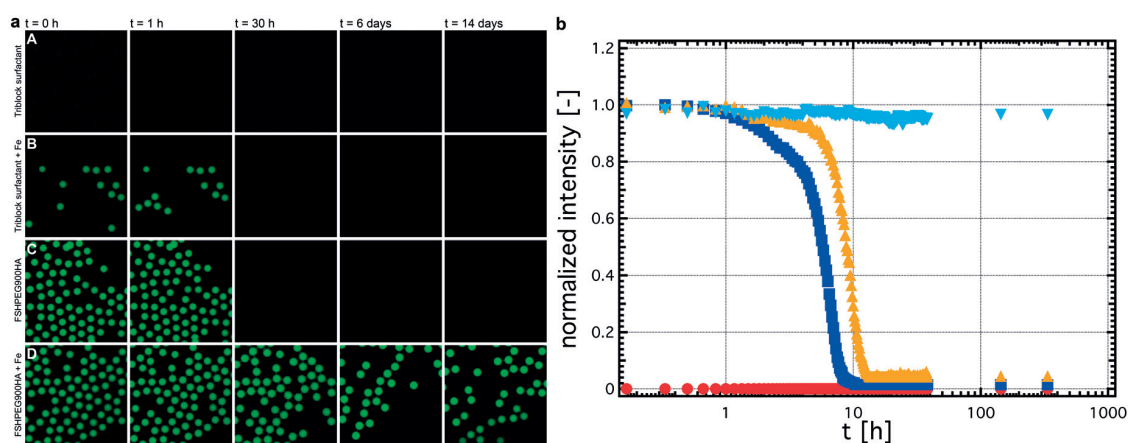
Figure 5.6: Permeability of double emulsions. (**a**) Fluorescent micrographs of double emulsions containing fluorescein acquired after they have been stored at room temperature for 0 h, 1 h, 30 h, 6 days, and 14 days. Double emulsions are stabilized with (**A,B**) 2 mM unfunctionalized FSH$_2$-Jeffamine600 and (**C,D**) the catechol functionalized FSHPEG900HA. The core of the double emulsions contains (**A,C**) water and fluorescein, (**B,D**) Fe^{3+}, fluorescein, and BICINE to buffer the pH at 8.5. (**b**) Normalized fluorescent intensity of the cores of double emulsions as a function of the incubation time at room temperature. All double emulsions are dispersed in water where the osmotic pressure is balanced. Double emulsions whose cores have a neutral pH, contain no iron and are stabilized with FSH$_2$-Jeffamine600 (●), contain BICINE, iron and stabilized with FSH$_2$-Jeffamine600 (▲), have a neutral pH, contain no iron, and stabilized with FSHPEG900HA (■) and contain BICINE, iron, and are stabilized with FSHPEG900HA (▼).

5.4.5 3D printing of Capsules

The good mechanical stability, high deformability, and stickiness of our capsules might open up a new field of their application: If up-concentrated, they have the potential to serve as inks that can be 3D printed. To test if these capsules indeed can be processed into macroscopic materials using 3D printing, we assemble aqueous drops that are dispersed in HFE-7100 containing 2 mM of the catechol-functionalized FSHPEG900HA surfactant and 0.6 mM Fe^{3+}. We up-concentrate the drops and eject them through a pipette tip at a controlled flow rate to form a 3D hydrogel, as shown in the time-lapse photographs in Figure 5.7a. Remarkably, the ejected solution is sufficiently viscoelastic to ensure good control over the shape of the processed macroscopic materials, as shown in Figure 5.7a. Indeed, even free-standing structures such as bridges can be 3D printed, as shown in Figure 5.7b. The printed materials are composed of individual compartments with well-defined sizes that are linked to their neighbors, resulting in granular structures, as shown in Figure 5.7c. These results show feasibility to not only use these capsules as individually dispersed delivery vehicles but also as building blocks of macroscopic materials with well-defined structures and locally varying compositions. However, these structures are viscoelastic such that they change their shape over time. To test if we can use the same capsules to produce mechanically stable, elastic granular hydrogels, we eject the concentrated solution into an aqueous solution whose pH is adjusted to 12 to induce covalent crosslinking of catechols, [217] as shown in Figures 5.7d and e. Indeed, if printed under these conditions, the formed threads

are much more stable, as indicated in the time-lapse photographs in Figure 5.7d, yet the regular, granular structure is preserved, as shown in Figure 5.7f. These results suggest that the capsule shells are covalently cross-linked. As a result of the covalent cross-links, adjacent layers do not stick to each other anymore, as shown in Movie S8. These results open up a new field of use of capsules with thin shells, namely their collective assembly to form macroscopic granular materials with well-defined structures and compositions that vary over short length scales.
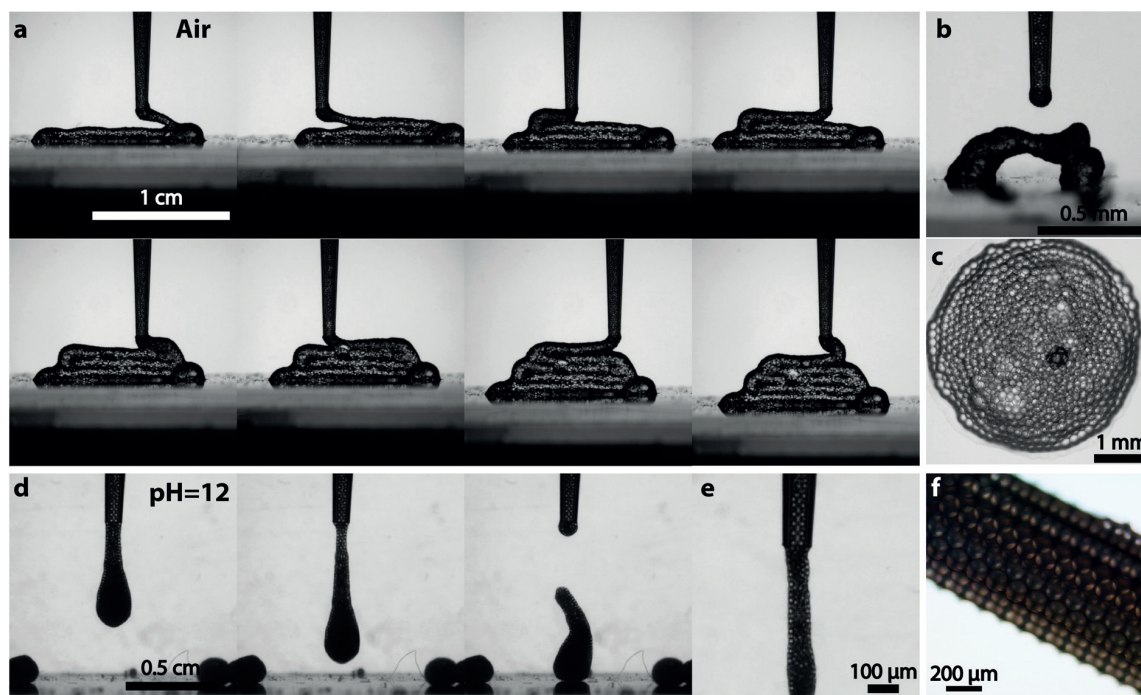

Figure 5.7: 3D printing of viscoelastic capsules in (**a-c**) air and in (**d-f**) aqueous solutions. (**a**) Time-lapse photographs of capsules whose cores are composed of an aqueous solution (pH=8.5). Capsules are made from water in HFE-7100 emulsion drops stabilized by 2 mM FSHPEG900HA and Fe^{3+}. (**b**) Photograph of a 3D printed suspended bridge composed of viscoelastic capsules. (**c**) Cross-section of a 3D printed structure revealing its granular structure. (**d**) Time-lapse photographs of densely packed capsules that are printed into an aqueous solution whose pH is 12. (**e**) Zoom-in on the ink composed of up-concentrated capsules as it is ejected. (**f**) Microscope image of the resulting printed structure composed of covalently crosslinked capsules.

5.5 Conclusion

We introduce new viscoelastic, sticky capsules that are deformable and mechanically sufficiently robust to be additive manufactured into macroscopic materials. Capsules are composed of catechol-functionalized block copolymer based surfactants that are ionically crosslinked at the drop surface to form viscoelastic shells. The resulting mechanically stable capsules are for practical purposes impermeable even towards low molecular weight encapsulants, thereby enabling the use of drops as truly closed containers that do not suffer from cross-contamination. Importantly, the mechanical stability and viscoelastic behavior of these capsules open up a new field of their

use in additive manufacturing: They can be 3D printed into proto-tissue-like cm-sized materials with well-defined structures. This feature offers new possibilities for additive manufacturing of functional soft materials with structures that are well-defined on several length scales and locally varying compositions.

Chapter 6

Conclusion and Outlook

The development of microfluidics in the past 25 years has contributed to the miniaturization and automation of biological and chemical assays. Droplet-based microfluidics has emerged as a technology to analyze samples at high-throughputs by producing emulsion drops in a controlled way. Each emulsion drop functions as a closed reaction vessel, where drops can be produced and analyzed at a rate of several thousand per second. A possibility to stabilize emulsion drops and to prevent them from coalescing, is the use of surfactants. The most common system used for biological high-throughput screening applications are water in fluorinated oil emulsions which are stabilized by fluorinated surfactants.

In the first part of this work, we studied how the length of the hydrophilic block and the block copolymer structure of fluorinated surfactants influence the mechanical and thermal stability of single emulsion drops. Therefore, we synthesized different fluorinated surfactants where we changed the length of the hydrophilic block of di- and triblock copolymer surfactants. We show that the composition of the surfactant has a big influence on the mechanical and thermal stability of emulsion drops. The stability of emulsion drops stabilized by triblock copolymers scales inversely with the interfacial tension. By contrast, the stability of drops coated with diblock copolymers scales with the surfactant packing density. We show that the performance of the surfactants strongly depends on the composition of the fluids. At low salt concentrations, surfactants with a ratio of the radii of gyration of the PEG to the hydrophobic block ranging from 0.54 to 0.67 impart the highest stability to emulsion drops (FSH$_2$-Jeffamine900 and FSH-Jeffamine1000). At high salt concentrations, FSH-PEG220 and FSH-Jeffamine2000, surfactants with a ratio of the radii of gyration of PEG to the hydrophobic block varying between 0.34 and 0.37 impart the highest stability. These guidelines help choosing what type of surfactant should be used to result in the highest stability of emulsion drops.

Surfactants are necessary to stabilize emulsion drops. However, they can also contribute to the transport of encapsulants from one drop to another. We studied this transport that results

in cross-contamination. We found that hydrophilic encapsulants can be transported through the oil shell of water in oil in water double emulsions. We demonstrate that this transport is mainly caused by emulsion drops of the order of 100 nm that spontaneously form at the water oil interface. We show that the time when 50% of encapsulants are transported across the shell only scales with the interfacial tension. The stronger a surfactant decreases the interfacial tension, the faster the leakage occurs. Since the leakage is causes by emulsion drops with diameters of the order of 100 nanometers, dyes such as plasmids with 11'000 base pairs and 100 nm polystyrene beads can leak out from emulsion drops. We show that the leakage can be reduced by applying surfactants that only moderately lower the interfacial tension, by reducing the amount of surfactant in the oil shell, or by creating double emulsion drops with sub-micrometer thin shells. These results provide guidelines for the appropriate selection of surfactants and emulsion dimensions.

To overcome the trade-off between drop stability and reagent transport between drops, we developed novel types of surfactants that can be reversibly cross-linked at the interface of an emulsion drop, resulting in capsules with a viscoelastic, self-healing shells. These surfactants contain a catechol group that can be chelated using metal ions. We demonstrate that these capsules show a high mechanical stability and that they can keep their shape even when the oil evaporates. By cross-linking surfactants at the interface we can prevent the leakage of hydrophilic dyes from double emulsion drops and by packing the capsules at high densities we can print them into 3D structures. Hence, these new surfactants might open up possibilities to build new self-healing 3D structures made out of individual compartments.

As preliminary work, we further increased the stability of these capsules by created emulsion drops containing two different catechol functionalized surfactants: one in the aqueous phase and one in the fluorinated oil phase. By adding Fe^{3+}, the two surfactants cross-linked at the interface, thereby forming a stronger capsule wall. The exact mechanism must still be determined. An example of a capsule that has been mechanically stressed with a razor blade i shown in Figure 6.1.
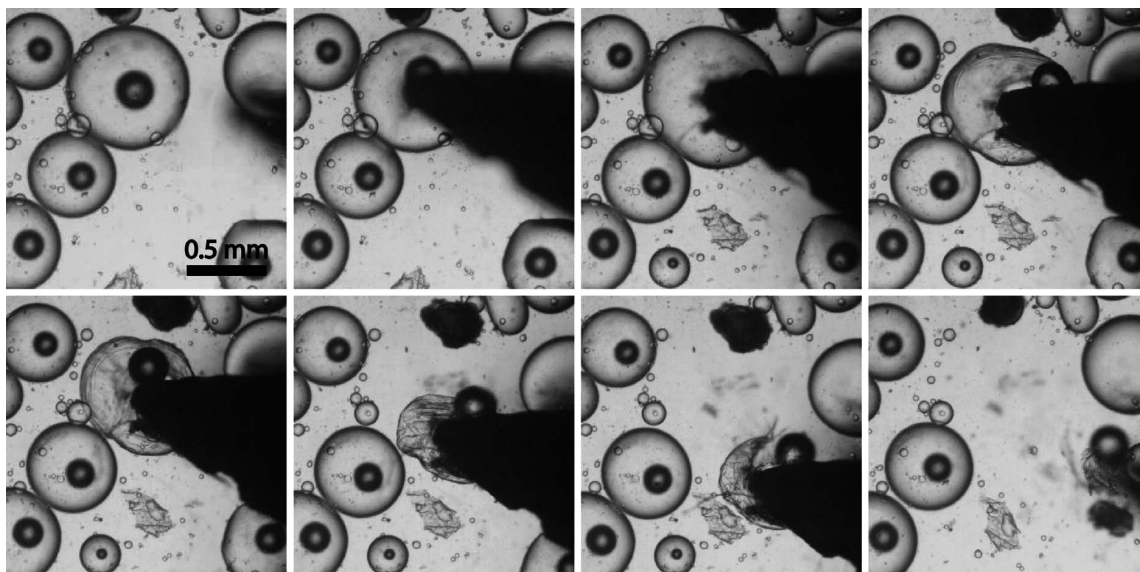
Figure 6.1: Time-lapse optical micrographs of oil in water drops stabilized with two types of catechol-functionalized surfactants. To increase the strength of the capsule wall, 4 mM SADopa is dissolved in EtOH containing Fe^{3+} and transferred to NaOH (pH=8) then they are mixed with HFE-7500 containing 2 mM FSHPEG900HA. The resulting capsules show good stability and rupture if sufficiently strongly deformed.

By replacing FSHPEG900HA with a sorter FSHDopa, we can create stable capsules that attain non-spherical shapes. This result suggests that capsules made from two different types of catechol-functionalized surfactants are mechanically more stable than those made of only one type of surfactant, as shown in Figure 6.2.
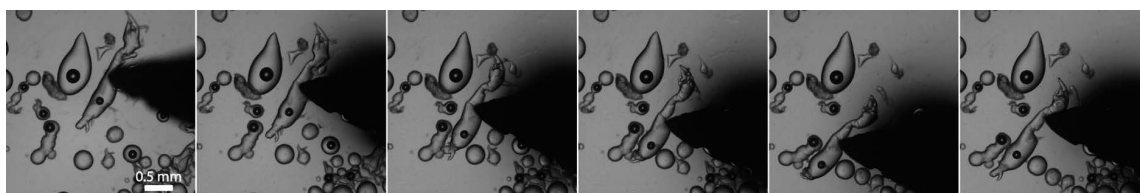
Figure 6.2: Time-lapse optical micrographs of oil in water drops stabilized with two types of catechol-functionalized surfactants. To increase the strength of the capsule wall, 4 mM SADopa is dissolved in EtOH containing Fe^{3+} and transferred to BICINE (pH=8.5) before they are mixed with HFE-7500 containing 2 mM FSHDopa. After shaking, the emulsions keep their non-spherical shapes and when mechanically stressed with a razor blade, they do not break but deform.

Appendices

Appendix A

FTIR of Fluorinated Surfactants

All the FTIR spectra measured of the different di- and triblock fluorinated surfactants are shown in Figures A.1-A.8. The FTIR were measured as described in section 2.2.2 on page 29.
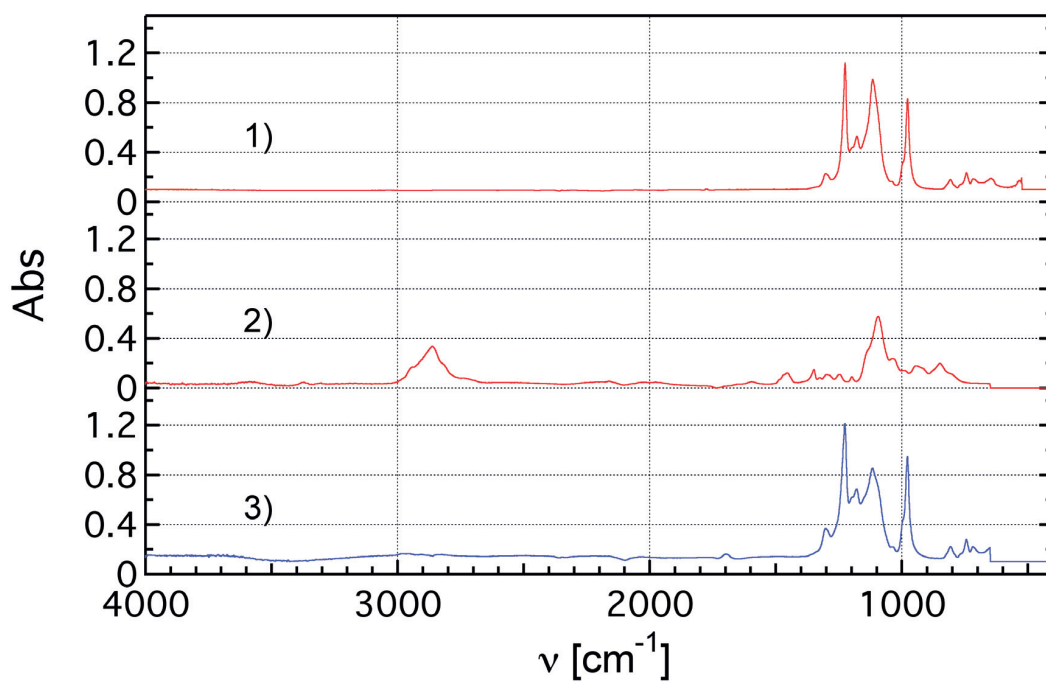
Figure A.1: FTIR spectra of (**1**) FSH, (**2**) PEG220, and (**3**) FSH-PEG220.
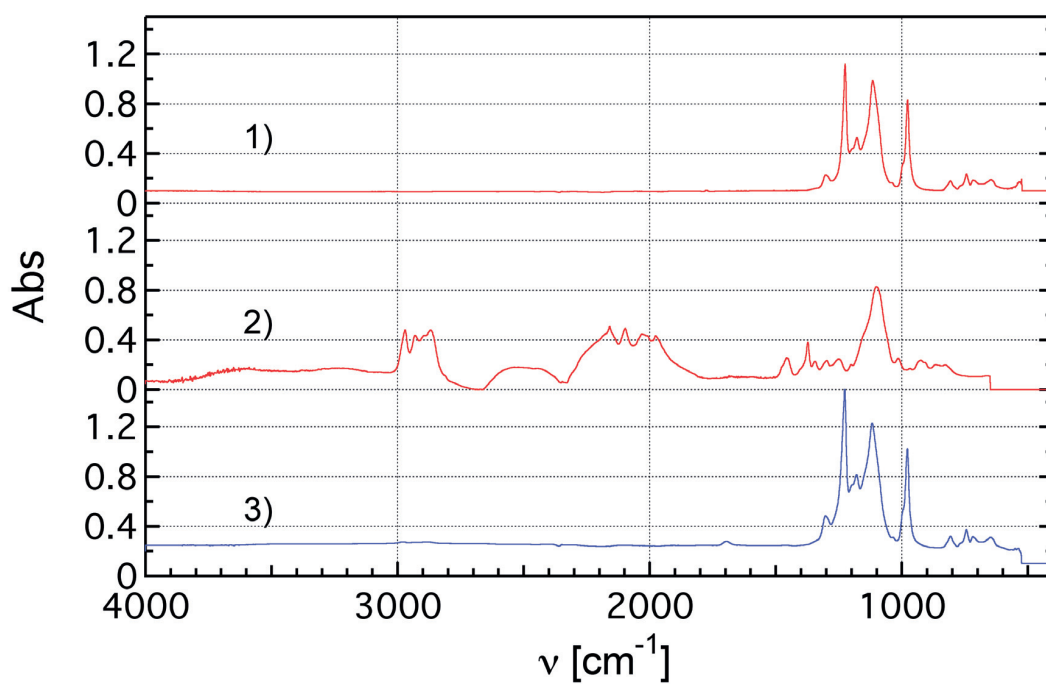
Figure A.2: FTIR spectra of (**1**)) FSH, (**2**) Jeffamine600, and (**3**) FSH-Jeffamine600.
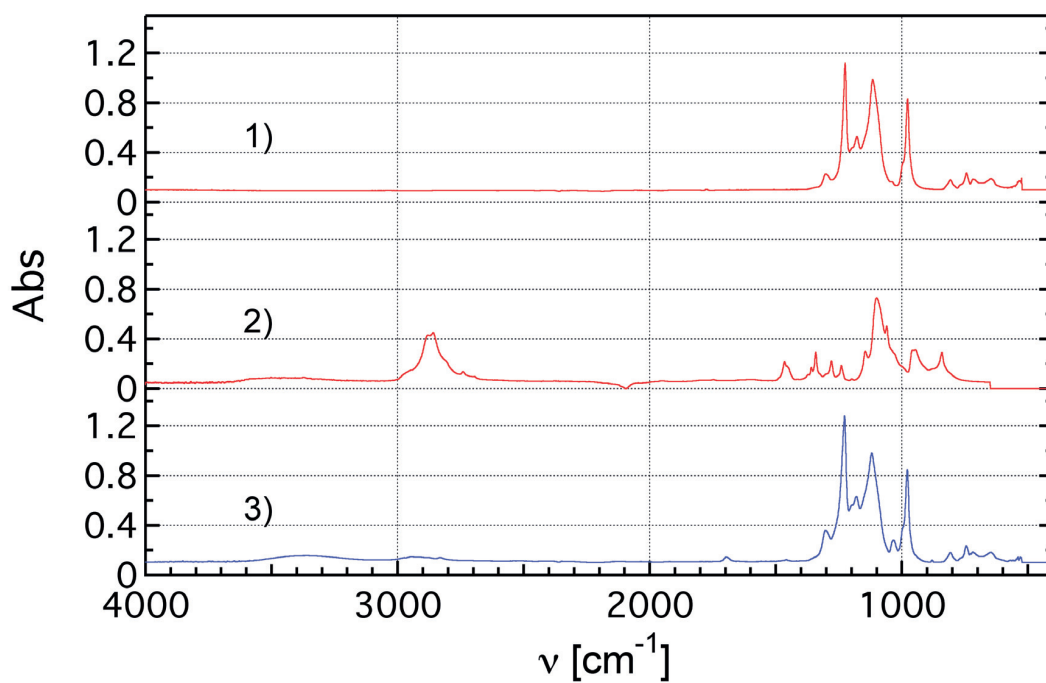
Figure A.3: FTIR spectra of (**1**) FSH, (**2**) Jeffamine1000, and (**3**) FSH-Jeffamine1000.
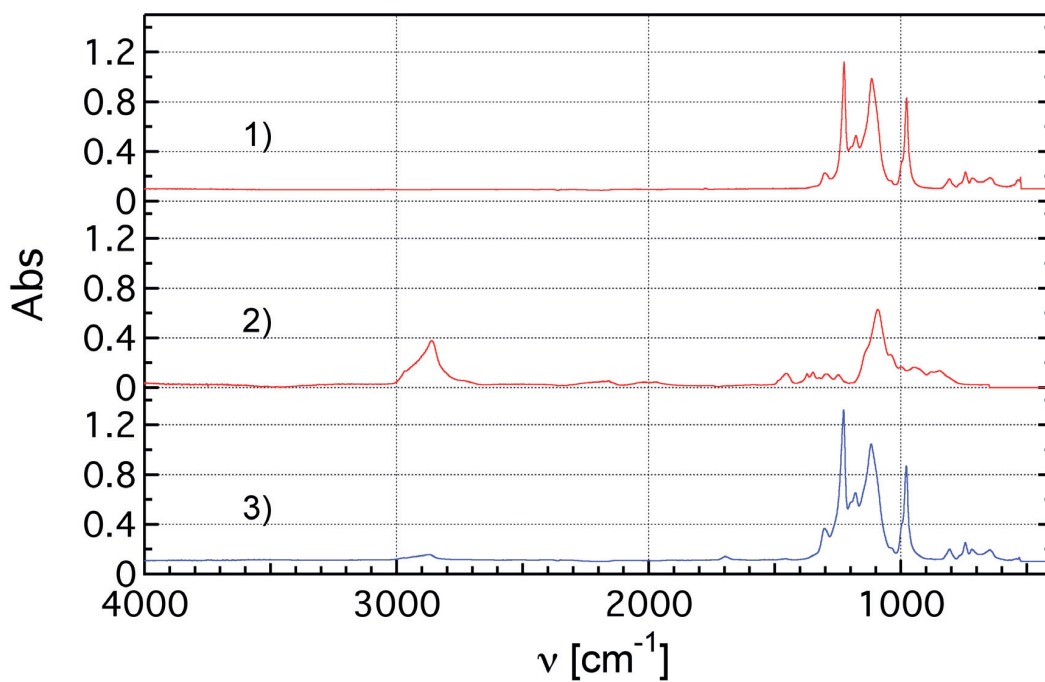
Figure A.4: FTIR spectra of (**1**) FSH, (**2**) Jeffamine2000, and (**3**) FSH-Jeffamine2000.
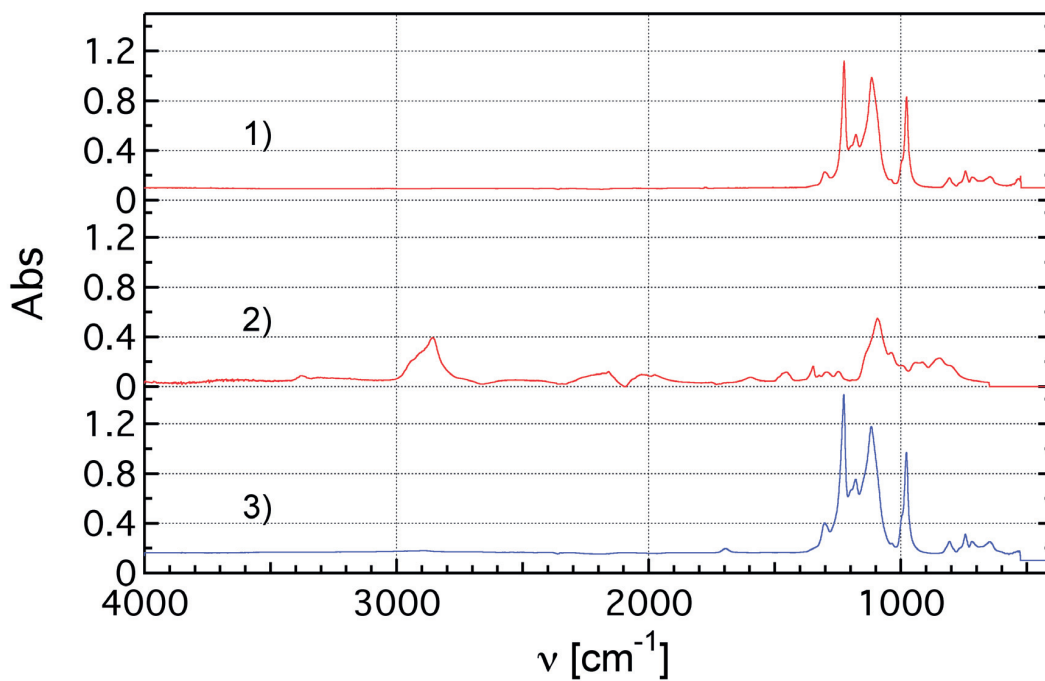
Figure A.5: FTIR spectra of FSH (**1**), PEG310 (**2**), and FSH$_2$-PEG310 (**3**).
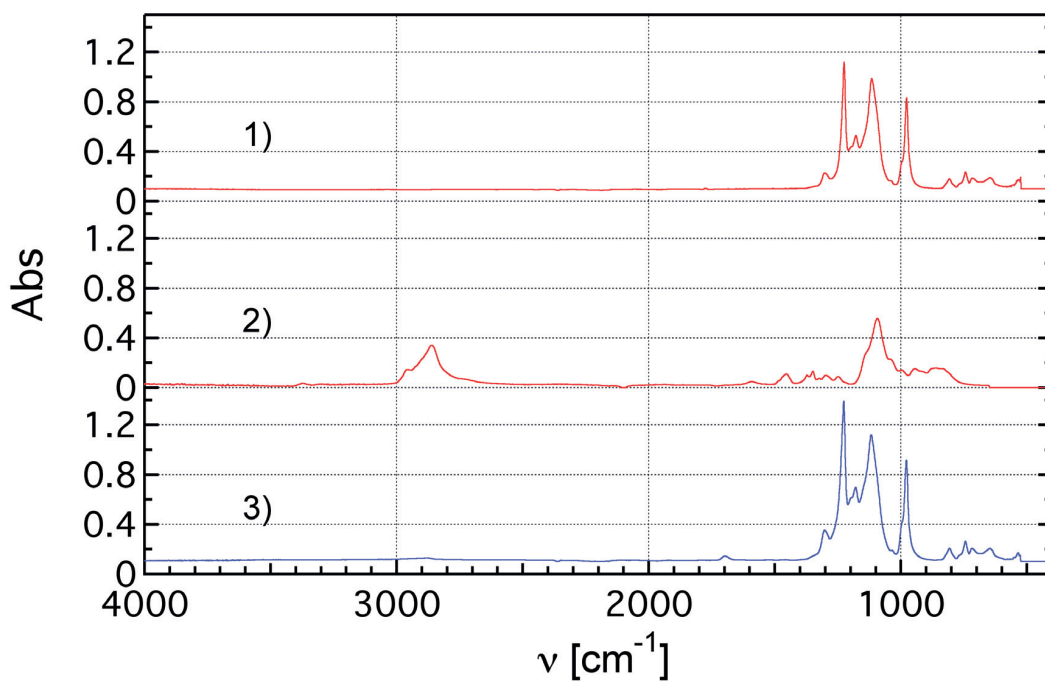
Figure A.6: FTIR spectra of FSH (**1**), Jeffamine600 (**2**), and FSH$_2$-Jeffamine600 (**3**).
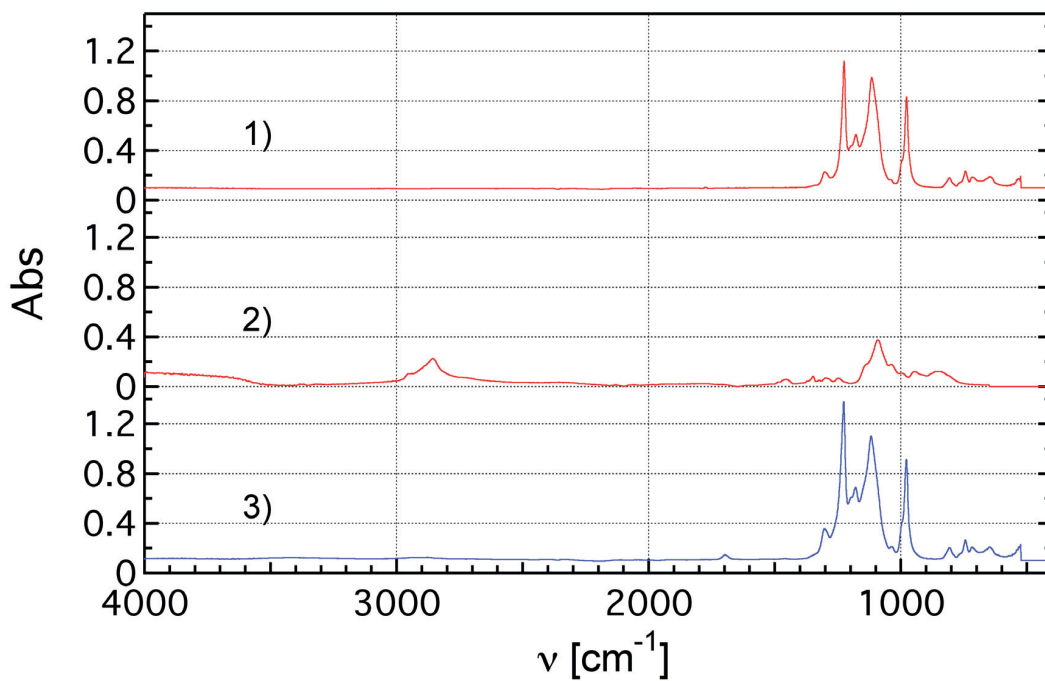
Figure A.7: FTIR spectra of FSH (**1**), Jeffamine900 (**2**), and FSH$_2$-Jeffamine900 (**3**).
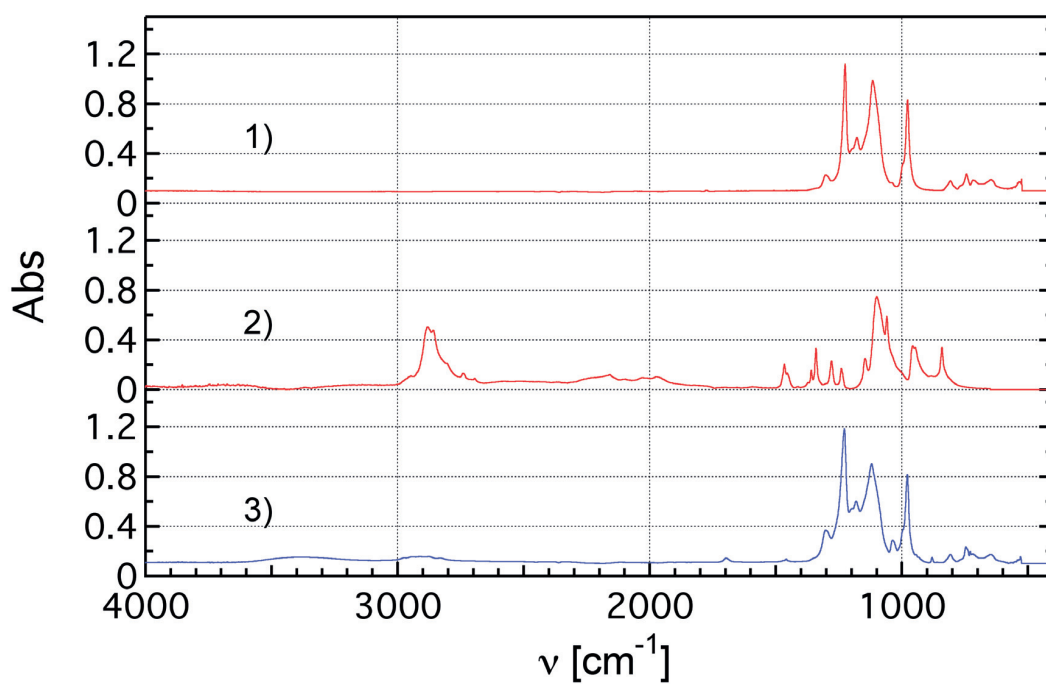
Figure A.8: FTIR spectra of FSH (**1**), Jeffamine2000 (**2**), and FSH$_2$-Jeffamine2000 (**3**).

Appendix B

Abbreviations

- **cac**: Critical aggregation concentration

- **cmc**: Critical micelle concentration

- **DLS**: Dynamic light scattering

- **DNA**: Deoxyribonucleic acid

- **Dopa**: Dopamine

- **FACS**: Fluorescence-activated cell sorting

- **FC-40**: Fluorinated solvent

- **FSH**: Commercial name of perfluorinated polyether used as hydrophobic block in fluorinated surfactants

- **HA**: Hydrocaffeic acid

- **HFE-7100**: Fluorinated solvent

- **HFE-7500**: Fluorinated solvent

- **HLB**: Hydrophilic-lipophilic balance

- **HLD**: Hydrophilic-lipophilic deviation

- **Jeffamine**: Name of commercial product of block copolymers containing mainly polyethyleneglycol and polypropylene glycol used as a building block for surfactants

- **NaCl**: Soldium chloride

- **O/W**: Oil in water emulsion

- **PEG**: Polyethylene glycol

- **PCR**: Polymerase chain reaction

- **PDMS**: Polydimethylsiloxane

- **PPG**: Polypropylene glycol

- **PS**: Polystyrene

- **PVA**: Polyvinyl alcohol

- $\mathbf{R_g}$: Radius of gyration

- **RNA**: Ribonucleic acid

- **SA**: Stearic acid

- **SEM**: Scanning Electron Microscope

- **W/O**: Water in oil emulsion

- **W/O/W**: Water in oil in water double emulsion

Appendix C

Symbols

- A: Total area

- A_L: Total area in Langmuir trough

- A_m: Mean molecular area

- a_i: Activity coefficient

- a: Length of repeat unit

- α: Packing parameter

- α': Inverse packing parameter

- a_0: Optimal area of hydrophilic group

- Ca: Capillary number

- C: Concentration

- Da: Dalton

- E_γ: Interfacial energy

- η: Viscosity

- F: Force

- G: Gibbs free energy

- g: Gravitational acceleration

- γ: Surface tension or interfacial tensions

- Γ: Surface excess concentration

- l_c: Length of hydrophobic chain

- M: Molar

- M_h: Molecular weight hydrophilic group

- M_{tot}: Total molecular weight

- μ: Chemical potential

- N: Number of repeat units

- n^{σ}: Number of molecule at interface

- ν: Wavenumber

- p: Laplace pressure

- Π: Surface pressure

- R: Gas constant coefficient

- ρ: Packing density

- ρ_i: Density

- T: Temperature

- t: Time

- $t_{1/2}$: Time until 50% of content is released

- t_s: Shell thickness

- U: Flow velocity

- v: Volume of hydrophobic chain

List of Figures

References

[1] Gianluca Etienne, Michael Kessler, and Esther Amstad. Influence of fluorinated surfactant composition on the stability of emulsion drops. *Macromolecular Chemistry and Physics*, 218(2):1–10, 2017.

[2] Gianluca Etienne, Antoine Vian, Marjan Biočanin, Bart Deplancke, and Esther Amstad. Cross-talk between emulsion drops: how are hydrophilic reagents transported across oil phases? *Lab on a Chip*, 18(24):3903–3912, 2018.

[3] Milton J. Rosen. *Surfactants and Interfacial Phenomena*. Wiley-Interscience, third edition, 2004.

[4] Drew Myers. *Surfactant Science and Technology*. Wiley-Interscience, third edition, 2006.

[5] Jérôme Bibette, Fernando Leal-Calderon, and Poulin P. Emulsions: basic principles. *Reports on Progress in Physics*, 62:969, 1999.

[6] Jacob N Israelachvili. *Intermolecular and Surface Forces*. Elsevier, third edition, 2010.

[7] Jean Christophe Baret. Surfactants in droplet-based microfluidics. *Lab on a Chip*, 12(3):422–433, 2012.

[8] Nicolas Bremond and Jérôme Bibette. Exploring emulsion science with microfluidics. *Soft Matter*, 8(41):10549–10559, 2012.

[9] Robert Aveyard, Bernard P. Binks, and John H. Clint. Emulsions stabilised solely by colloidal particles. *Advances in Colloid and Interface Science*, 100-102:503–546, 2003.

[10] B. P. Binks and S. O. Lumsdon. Pickering emulsions stabilized by monodisperse latex particles: Effects of particle size. *Langmuir*, 17(15):4540–4547, 2001.

[11] Ming Pan, Liat Rosenfeld, Minkyu Kim, Manqi Xu, Edith Lin, Ratmir Derda, and Sindy K Y Tang. Fluorinated pickering emulsions impede interfacial transport and form rigid interface for the growth of anchorage-dependent cells. *ACS Applied Materials and Interfaces*, 6(23):21446–21453, 2014.

[12] A. Witthayapanyanon, J. H. Harwell, and D. A. Sabatini. Hydrophilic-lipophilic deviation (HLD) method for characterizing conventional and extended surfactants. *Journal of Colloid and Interface Science*, 325(1):259–266, 2008.

[13] Edgar J. Acosta. The HLD-NAC equation of state for microemulsions formulated with nonionic alcohol ethoxylate and alkylphenol ethoxylate surfactants. *Colloids and Surfaces A: Physicochemical and Engineering Aspects*, 320(1-3):193–204, 2008.

[14] Steven Abbott. *Surfactant Science : Principles and Practice.* 2015.

[15] Geoffrey T. Barnes and Ian R. Gentle. *Interfacial Scinece: an introduction.* Oxford University Press, second edition, 2011.

[16] Alissa J. Prosser and Elias I. Franses. Adsorption and surface tension of ionic surfactants at the air-water interface: Review and evaluation of equilibrium models. *Colloids and Surfaces A: Physicochemical and Engineering Aspects*, 178(1-3):1–40, 2001.

[17] Esther Amstad and Laura R Arriaga. Nanoparticle actuated vesicles. In *Handbook of Functional Nanomaterials.* Nova Science, 2013.

[18] Fernando Leal-Calderon, Véronique Schmitt, and Jérôme Bibette. *Emulsion Science Basic Principles.* Springer, second edition, 2007.

[19] Jesús Santana-Solano, Carla M. Quezada, Sandra Ozuna-Chacón, and José Luis Arauz-Lara. Spontaneous emulsification at the water/oil interface. *Colloids and Surfaces A: Physicochemical and Engineering Aspects*, 399:78–82, 2012.

[20] Lixiong Wen and Kyriakos D. Papadopoulos. Visualization of water transport in W1/O/W2 emulsions. *Colloids and Surfaces A: Physicochemical and Engineering Aspects*, 174(1-2):159–167, 2000.

[21] Pedro S. Silva, Sergey Zhdanov, Victor M. Starov, and Richard G. Holdich. Spontaneous emulsification of water in oil at appreciable interfacial tensions. *Colloids and Surfaces A: Physicochemical and Engineering Aspects*, 521:141–146, 2017.

[22] Simone Bochner De Araujo, Maria Merola, Dimitris Vlassopoulos, and Gerald G. Fuller. Droplet Coalescence and Spontaneous Emulsification in the Presence of Asphaltene Adsorption. *Langmuir*, 33(40):10501–10510, 2017.

[23] Jana Bahtz, Deniz Z. Gunes, Axel Syrbe, Nicola Mosca, Peter Fischer, and Erich J. Windhab. Quantification of spontaneous w/o emulsification and its impact on the swelling kinetics of multiple w/o/w emulsions. *Langmuir*, 32(23):5787–5795, 2016.

[24] Johan Sjöblom. *Emulsions and Emulsion Stability.* CRC Press, second edition, 2006.

[25] Juan Carlos Lapez-Montilla, Paulo Emilio Herrera-Morales, Samir Pandey, and Dinesh O. Shah. Spontaneous emulsification: Mechanisms, physicochemical aspects, modeling, and applications. *Journal of Dispersion Science and Technology*, 23(1-3):219–268, 2002.

[26] James W. McBain and Ts-Ming Woo. Spontaneous Emulsification, and Reactions Overshooting E quilibrium. *Proceedings of the Royal Society A*, 163:182–188, 1937.

[27] Clarence A. Miller, Rei Nan Hwan, William J. Benton, and Tomlinson Fort. Ultralow interfacial tensions and their relation to phase separation in micellar solutions. *Journal of Colloid and Interface Science*, 61(3):554–568, 1977.

[28] Moon Jeong Rang, Clarence A. Miller, Heinz H. Hoffmann, and Christine Thunig. Behavior of hydrocarbon/alcohol drops injected into dilute solutions of an amine oxide surfactant. *Industrial and Engineering Chemistry Research*, 35(9):3233–3240, 1996.

[29] Richard W. Greiner and D. Fennell Evans. Spontaneous Formation of A Water-Continuous Emulsion from a W/O Microemulsion. *Langmuir*, 6(12):1793–1796, 1990.

[30] N. Shahidzadeh, D. Bonn, and J. Meunier. A new mechanism of spontaneous emulsification: Relation to surfactant properties. *Europhysics Letters*, 40(4):459–464, 1997.

[31] Chien Hsiang Chang and Elias I. Franses. Adsorption dynamics of surfactants at the air/water interface: a critical review of mathematical models, data, and mechanisms. *Colloids and Surfaces A: Physicochemical and Engineering Aspects*, 100:1–45, 1995.

[32] Kai Urban, Gerhard Wagner, David Schaffner, Danny Röglin, and Joachim Ulrich. Rotor-stator and disc systems for emulsification processes. *Chemical Engineering and Technology*, 29(1):24–31, 2006.

[33] Stefan Schultz, Gerhard Wagner, Kai Urban, and Joachim Ulrich. High-pressure homogenization as a process for emulsion formation. *Chemical Engineering and Technology*, 27(4):361–368, 2004.

[34] Simon M Joscelyne and Gun Trägårdh. Membrane emulsification — a literature review. *Journal of Membrane Science*, 169:107–117, 2000.

[35] G. T. Vladisavljević, Isao Kobayashi, and Mitsutoshi Nakajima. Production of uniform droplets using membrane, microchannel and microfluidic emulsification devices. *Microfluidics and Nanofluidics*, 13(1):151–178, 2012.

[36] A. S. Utada, L.-Y. Chu, A. Fernandez-Nieves, D. R. Link, C. Holtze, and D. A. Weitz. Dripping, jetting, drops, and wetting: The magic of microfluidics. *MRS Bulletin*, 32(9):702–708, 2007.

[37] George M Whitesides. The origins and the future of microfluidics. *Nature*, 442(7101):368–373, 2006.

[38] Todd M Squires and Stephen R. Quake. Microfluidics: Fluid physics at the nanoliter scale. *Reviews of Modern Physics*, 77:977–1026, 2005.

[39] Younan Xia and George M Whitesides. Soft lithography. *Angewandte Chemie International Edition*, 37(5):550–575, 1998.

[40] Todd Thorsen, Sebastian J. Maerkl, and Stephen R. Quake. Microfluidic large-scale integration. *Science*, 298(5593):580–584, 2002.

[41] Piotr Garstecki, Michael J. Fuerstman, Howard A. Stone, and George M. Whitesides. Formation of droplets and bubbles in a microfluidic T-junction - Scaling and mechanism of break-up. *Lab on a Chip*, 6(3):437–446, 2006.

[42] Shelley L. Anna, Nathalie Bontoux, and Howard A. Stone. Formation of dispersions using "flow focusing" in microchannels. *Applied Physics Letters*, 82(3):364–366, 2003.

[43] Esther Amstad, Xiaoming Chen, Max Eggersdorfer, Noa Cohen, Thomas E. Kodger, Carolyn L. Ren, and David A. Weitz. Parallelization of microfluidic flow-focusing devices. *Physical Review E*, 95(4):1–6, 2017.

[44] E. Amstad, M. Chemama, M. Eggersdorfer, L. R. Arriaga, M. P. Brenner, and D. A. Weitz. Robust scalable high throughput production of monodisperse drops. *Lab on a Chip*, 16(21):4163–4172, 2016.

[45] Shinji Sugiura, Mitsutoshi Nakajima, Satoshi Iwamoto, and Minoru Seki. Interfacial tension driven monodispersed droplet formation from microfabricated channel array. *Langmuir*, 17(18):5562–5566, 2001.

[46] Takahiro Kawakatsu, Hideaki Komori, Mitsutoshi Nakajima, Yuji Kikuchi, and Toshikuni Yonemoto. Production of monodispersed oil-in-water emulsion using crossflow-type silicon microchannel plate. *Journal of Chemical Engineering of Japan*, 32(2):241–244, 1999.

[47] Tomasz S. Kaminski, Ott Scheler, and Piotr Garstecki. Droplet microfluidics for microbiology: Techniques, applications and challenges. *Lab on a Chip*, 16(12):2168–2187, 2016.

[48] Jiseok Lim, Ouriel Caen, Jérémy Vrignon, Manfred Konrad, Valérie Taly, and Jean Christophe Baret. Parallelized ultra-high throughput microfluidic emulsifier for multiplex kinetic assays. *Biomicrofluidics*, 9(3):034101, 2015.

[49] Albert Tsung Hsi Hsieh, Nicole Hori, Rustin Massoudi, Patrick Jen Hao Pan, Hirotaka Sasaki, Yuh Adam Lin, and Abraham P. Lee. Nonviral gene vector formation in monodispersed picolitre incubator for consistent gene delivery. *Lab on a Chip*, 9(18):2638–2643, 2009.

[50] D. R. Link, S. L. Anna, D. A. Weitz, and H. A. Stone. Geometrically Mediated Breakup of Drops in Microfluidic Devices. *Physical Review Letters*, 92(5):4, 2004.

[51] Linas Mazutis, Jean Christophe Baret, Patrick Treacy, Yousr Skhiri, Ali Fallah Araghi, Michael Ryckelynck, Valérie Taly, and Andrew D. Griffiths. Multi-step microfluidic droplet processing: Kinetic analysis of an in vitro translated enzyme. *Lab on a Chip*, 9(20):2902–2908, 2009.

[52] Nicolas Bremond, Abdou R. Thiam, and Jérôme Bibette. Decompressing emulsion droplets favors coalescence. *Physical Review Letters*, 100(2):1–4, 2008.

[53] Xize Niu, Shelly Gulati, Joshua B. Edel, and Andrew J. Demello. Pillar-induced droplet merging in microfluidic circuits. *Lab on a Chip*, 8(11):1837–1841, 2008.

[54] Adam R. Abate, Tony Hung, Pascaline Mary, Jeremy J. Agresti, and David A. Weitz. High-throughput injection with microfluidics using picoinjectors. *Proceedings of the National Academy of Sciences*, 107(45):19163–19166, 2010.

[55] Xize Niu, Fabrice Gielen, Joshua B. Edel, and Andrew J. DeMello. A microdroplet dilutor for high-throughput screening. *Nature Chemistry*, 3(6):437–442, 2011.

[56] Lucas Frenz, Kerstin Blank, Eric Brouzes, and Andrew D. Griffiths. Reliable microfluidic on-chip incubation of droplets in delay-lines. *Lab on a Chip*, 9(10):1344–1348, 2009.

[57] Helen Song, Michelle R. Bringer, Joshua D. Tice, Cory J. Gerdts, and Rustem F. Ismagilov. Experimental test of scaling of mixing by chaotic advection in droplets moving through microfluidic channels. *Applied Physics Letters*, 83(22):4664–4666, 2003.

[58] Heng Dong Xi, Hao Zheng, Wei Guo, Alfonso M. Gañán-Calvo, Ye Ai, Chia Wen Tsao, Jun Zhou, Weihua Li, Yanyi Huang, Nam Trung Nguyen, and Say Hwa Tan. Active droplet sorting in microfluidics: a review. *Lab on a Chip*, 17(5):751–771, 2017.

[59] Oliver J. Dressler, Xavier Casadevall i Solvas, and Andrew J. DeMello. Chemical and Biological Dynamics Using Droplet-Based Microfluidics. *Annual Review of Analytical Chemistry*, 10(1):1–24, 2017.

[60] Bachir El Debs, Ramesh Utharala, Irina V. Balyasnikova, Andrew D. Griffiths, and Christoph A. Merten. Functional single-cell hybridoma screening using droplet-based microfluidics. *Proceedings of the National Academy of Sciences*, 109(29):11570–11575, 2012.

[61] Linas Mazutis, John Gilbert, W Lloyd Ung, David A Weitz, Andrew D Griffiths, and John A Heyman. Single-cell analysis and sorting using droplet-based microfluidics. *Nat. Protocols*, 8(5):870–891, 2013.

[62] Eric Brouzes, Martina Medkova, Neal Savenelli, Dave Marran, Mariusz Twardowski, J Brian Hutchison, Jonathan M Rothberg, Darren R Link, Norbert Perrimon, and Michael L Samuels. Droplet microfluidic technology for single-cell high-throughput screening. *Proceedings of the National Academy of Sciences of the United States of America*, 106(34):14195–200, 2009.

[63] Oliver J Miller, Abdeslam El Harrak, Thomas Mangeat, Jean-Christophe Baret, Lucas Frenz, Bachir El Debs, Estelle Mayot, Michael L Samuels, Eamonn K Rooney, Pierre Dieu, Martin Galvan, Darren R Link, and Andrew D Griffiths. High-resolution dose – response screening using droplet-based microfluidics. *Proceedings of the National Academy of Sciences*, 109(2):378–383, 2012.

[64] Ashleigh B. Theberge, Estelle Mayot, Abdeslam El Harrak, Felix Kleinschmidt, Wilhelm T.S. Huck, and Andrew D. Griffiths. Microfluidic platform for combinatorial synthesis in picolitre droplets. *Lab on a Chip*, 12(7):1320–1326, 2012.

[65] Tushar D. Rane, Helena C. Zec, and Tza Huei Wang. A barcode-free combinatorial screening platform for matrix metalloproteinase screening. *Analytical Chemistry*, 87(3):1950–1956, 2015.

[66] Jeremy J. Agresti, Eugene Antipov, Adam R. Abate, Ahn Keunho, Amy C. Rowat, Jean-Christophe Baret, Manuel Marquez, Alexander M Klibanov, Andrew D. Griffiths, and David A. Weitz. Ultrahigh-throughput screening in drop-based microfluidics for directed evolution. *Proceedings of the National Academy of Sciences*, 107(14):4004–4009, 2010.

[67] Fabrice Gielen, Raphaelle Hours, Stephane Emond, Martin Fischlechner, Ursula Schell, and Florian Hollfelder. Ultrahigh-throughput–directed enzyme evolution by absorbance-activated droplet sorting (AADS). *Proceedings of the National Academy of Sciences*, 113(47):E7383–E7389, 2016.

[68] Benjamin L. Wang, Adel Ghaderi, Hang Zhou, Jeremy Agresti, David A. Weitz, Gerald R. Fink, and Gregory Stephanopoulos. Microfluidic high-throughput culturing of single cells for selection based on extracellular metabolite production or consumption. *Nature Biotechnology*, 32(5):473–478, 2014.

[69] Allon M. Klein, Linas Mazutis, Ilke Akartuna, Naren Tallapragada, Adrian Veres, Victor Li, Leonid Peshkin, David A. Weitz, and Marc W. Kirschner. Droplet barcoding for single-cell transcriptomics applied to embryonic stem cells. *Cell*, 161(5):1187–1201, 2015.

[70] Evan Z. Macosko, Anindita Basu, Rahul Satija, James Nemesh, Karthik Shekhar, Melissa Goldman, Itay Tirosh, Allison R. Bialas, Nolan Kamitaki, Emily M. Martersteck, John J. Trombetta, David A. Weitz, Joshua R. Sanes, Alex K. Shalek, Aviv Regev, and Steven A. McCarroll. Highly parallel genome-wide expression profiling of individual cells using nanoliter droplets. *Cell*, 161(5):1202–1214, 2015.

[71] Katherine S. Elvira, Xavier Casadevall I Solvas, Robert C.R. Wootton, and Andrew J. Demello. The past, present and potential for microfluidic reactor technology in chemical synthesis. *Nature Chemistry*, 5(11):905–915, 2013.

[72] Andrew J DeMello. Control and detection of chemical reactions in microfluidic systems. *Nature*, 442(7101):394–402, 2006.

[73] Nachiket Shembekar, Chawaree Chaipan, Ramesh Utharala, and Christoph A. Merten. Droplet-based microfluidics in drug discovery, transcriptomics and high-throughput molecular genetics. *Lab on a Chip*, 16(8):1314–1331, 2016.

[74] Philipp Gruner, Birte Riechers, Laura Andreina Chacòn Orellana, Quentin Brosseau, Florine Maes, Thomas Beneyton, Deniz Pekin, and Jean Christophe Baret. Stabilisers for water-in-fluorinated-oil dispersions: Key properties for microfluidic applications. *Current Opinion in Colloid and Interface Science*, 20(3):183–191, 2015.

[75] Jenifer Clausell-Tormos, Diana Lieber, Jean Christophe Baret, Abdeslam El-Harrak, Oliver J. Miller, Lucas Frenz, Joshua Blouwolff, Katherine J. Humphry, Sarah Köster, Honey Duan, Christian Holtze, David A. Weitz, Andrew D. Griffiths, and Christoph A. Merten. Droplet-Based Microfluidic Platforms for the Encapsulation and Screening of Mammalian Cells and Multicellular Organisms. *Chemistry and Biology*, 15(5):427–437, 2008.

[76] Helen Song, Delai L. Chen, and Rustem F. Ismagilov. Reactions in droplets in microfluidic channels. *Angewandte Chemie International Edition*, 45(44):7336–7356, 2006.

[77] L. Spencer Roach, Helen Song, and Rustem F. Ismagilov. Controlling nonspecific protein adsorption in a plug-based microfluidic system by controlling interfacial chemistry using fluorous-phase surfactants. *Analytical Chemistry*, 77(3):785–796, 2005.

[78] Kenneth C. Lowe. Perfluorochemical respiratory gas carriers: Benefits to cell culture systems. *Journal of Fluorine Chemistry*, 118(1-2):19–26, 2002.

[79] Marie Pierre Krafft and Jean G Riess. Chemistry, Physical Chemistry, and Uses of Molecular Fluorocarbon - Hydrocarbon Diblocks, Triblocks, and Related Compounds. *Chemical Reviews*, 109:1714–1792, 2009.

[80] David M. Lemal. Perspective on Fluorocarbon Chemistry. *Journal of Organic Chemistry*, 69(1):1–11, 2004.

[81] Kenneth C. Lowe. Fluorinated blood substitutes and oxygen carriers. *Journal of Fluorine Chemistry*, 109(1):59–65, 2001.

[82] Jessamine Ng Lee, Cheolmin Park, and George M. Whitesides. Solvent Compatibility of Poly(dimethylsiloxane)-Based Microfluidic Devices. *Analytical Chemistry*, 75(23):6544–6554, 2003.

[83] C. Holtze, A. C. Rowat, J. J. Agresti, J. B. Hutchison, F. E. Angilè, C. H.J. Schmitz, S. Köster, H. Duan, K. J. Humphry, R. A. Scanga, J. S. Johnson, D. Pisignano, and D. A.

Weitz. Biocompatible surfactants for water-in-fluorocarbon emulsions. *Lab on a Chip*, 8(10):1632–1639, 2008.

[84] Ashleigh B. Theberge, Fabienne Courtois, Yolanda Schaerli, Martin Fischlechner, Chris Abell, Florian Hollfelder, and Wilhelm T S Huck. Microdroplets in microfluidics: An evolving platform for discoveries in chemistry and biology. *Angewandte Chemie - International Edition*, 49(34):5846–5868, 2010.

[85] Ralf Seemann, Martin Brinkmann, Thomas Pfohl, and Stephan Herminghaus. Droplet based microfluidics. *Reports on Progress in Physics*, 75(1):1–41, 2012.

[86] Valerie Taly, Bernard T. Kelly, and Andrew D. Griffiths. Droplets as microreactors for high-throughput biology. *ChemBioChem*, 8(3):263–272, 2007.

[87] Sarah Köster, Francesco E. Angilè, Honey Duan, Jeremy J. Agresti, Anton Wintner, Christian Schmitz, Amy C. Rowat, Christoph A. Merten, Dario Pisignano, Andrew D. Griffiths, and David A. Weitz. Drop-based microfluidic devices for encapsulation of single cells. *Lab on a Chip*, 8(7):1110–1115, 2008.

[88] Mira T. Guo, Assaf Rotem, John A. Heyman, and David A. Weitz. Droplet microfluidics for high-throughput biological assays. *Lab on a Chip*, 12(12):2146–2155, 2012.

[89] Margaret Macris Kiss, Lori Ortoleva-Donnelly, N Reginald Beer, Jason Warner, Christopher G Bailey, Bill W Colston, Jonathon M Rothberg, Darren R Link, and John H Leamon. High-throughput quantitative polymerase chain reaction in picoliter droplets. *Analytical Chemistry*, 80(23):8975–8981, 2008.

[90] Helen Song and Rustem F. Ismagilov. Millisecond Kinetics on a Microfluidic Chip Using Nanoliters of Reagents. *Journal of the American Chemical Society*, 125(47):14613–14619, 2003.

[91] Helen Song, Joshua D. Tice, and Rustem F. Ismagilov. A microfluidic system for controlling reaction networks in time. *Angewandte Chemie - International Edition*, 42(7):768–772, 2003.

[92] Colin King, Edmond Walsh, and Ronan Grimes. PIV measurements of flow within plugs in a microchannel. *Microfluidics and Nanofluidics*, 3(4):463–472, 2007.

[93] Bo Zheng, Cory J. Gerdts, and Rustem F. Ismagilov. Using nanoliter plugs in microfluidics to facilitate and understand protein crystallization. *Current Opinion in Structural Biology*, 15(5):548–555, 2005.

[94] Luis M. Fidalgo, Graeme Whyte, Daniel Bratton, Clemens F. Kaminski, Chris Abell, and Wilhelm T.S. S Huck. From microdroplets to microfluidics: Selective emulsion separation

in microfluidic devices. *Angewandte Chemie - International Edition*, 47(11):2042–2045, 2008.

[95] Bo Zheng, Joshua D. Tice, and Rustem F. Ismagilov. Formation of droplets of alternating composition in microfluidic channels and applications to indexing of concentrations in droplet-based assays. *Analytical Chemistry*, 76(17):4977–4982, 2004.

[96] Max Chabert, Kevin D. Dorfman, Patricia De Cremoux, Johan Roeraade, and Jean Louis Viovy. Automated microdroplet platform for sample manipulation and polymerase chain reaction. *Analytical Chemistry*, 78(22):7722–7728, 2006.

[97] Delai Chen, Wenbin Du, Ying Liu, Weishan Liu, Andrey Kuznetsov, Felipe E Mendez, Louis H Philipson, and Rustem F Ismagilov. The chemistrode: A droplet-based microfluidic device for stimulation and recording with high temporal, spatial, and chemical resolution Delai. *Proceedings of the National Academy of Sciences*, 105(44):16843–16848, 2008.

[98] Liat Rosenfeld, Tiras Lin, Ratmir Derda, and Sindy K Y Tang. Review and analysis of performance metrics of droplet microfluidics systems. *Microfluidics and Nanofluidics*, 16(5):921–939, 2014.

[99] Dan S. Tawfik and Andrew D. Griffiths. Man-made cell-like compartments for molecular evolution. *Nature Biotechnology*, 16(7):652–656, 1998.

[100] Shia Yen Teh, Robert Lin, Lung Hsin Hung, and Abraham P. Lee. Droplet microfluidics. *Lab on a Chip*, 8(2):198–220, 2008.

[101] Adam R. Abate and David A. Weitz. Faster multiple emulsification with drop splitting. *Lab on a Chip*, 11(11):1911–1915, 2011.

[102] Michele Zagnoni, Guillaume Le Lain, and Jonathan M. Cooper. Electrocoalescence mechanisms of microdroplets using localized electric fields in microfluidic channels. *Langmuir*, 26(18):14443–14449, 2010.

[103] Ethan Schonbrun, Adam R. Abate, Paul E. Steinvurzel, David A. Weitz, and Kenneth B. Crozier. High-throughput fluorescence detection using an integrated zone-plate array. *Lab on a Chip*, 10(7):852–856, 2010.

[104] Jean-Christophe Baret, Yannick Beck, Isabelle Billas-Massobrio, Dino Moras, and Andrew D. Griffiths. Quantitative cell-based reporter gene assays using droplet-based microfluidics. *Chemistry & Biology*, 17(5):528–536, 2010.

[105] A. R. Abate and D. A. Weitz. High-order multiple emulsions formed in poly(dimethylsiloxane) microfluidics. *Small*, 5:2030–2032, 2009.

[106] Lucas Frenz, Abdeslam El Harrak, Matthias Pauly, Sylvie Bégin-Colin, Andrew D. Griffiths, and Jean Christophe Baret. Droplet-based microreactors for the synthesis of magnetic iron oxide nanoparticles. *Angewandte Chemie - International Edition*, 47(36):6817–6820, 2008.

[107] Paul Abbyad, Pierre Louis Tharaux, Jean Louis Martin, Charles N. Baroud, and Antigoni Alexandrou. Sickling of red blood cells through rapid oxygen exchange in microfluidic drops. *Lab on a Chip*, 10(19):2505–2512, 2010.

[108] Pierre R. Marcoux, Mathieu Dupoy, Raphael Mathey, Armelle Novelli-Rousseau, Virginie Heran, Sophie Morales, Florence Rivera, Pierre L. Joly, Jean Pierre Moy, and Frédéric Mallard. Micro-confinement of bacteria into w/o emulsion droplets for rapid detection and enumeration. *Colloids and Surfaces A: Physicochemical and Engineering Aspects*, 377(1-3):54–62, 2011.

[109] Jean Christophe Baret, Felix Kleinschmidt, Abdeslam El Harrak, and Andrew D. Griffiths. Kinetic aspects of emulsion stabilization by surfactants: A microfluidic analysis. *Langmuir*, 25(11):6088–6093, 2009.

[110] Ya Ling Chiu, Hon Fai Chan, Kyle K L Phua, Ying Zhang, Sissel Juul, Birgitta R. Knudsen, Yi Ping Ho, and Kam W. Leong. Synthesis of fluorosurfactants for emulsion-based biological applications. *ACS Nano*, 8(4):3913–3920, 2014.

[111] Olaf Wagner, Julian Thiele, Marie Weinhart, Linas Mazutis, David A. Weitz, Wilhelm T.S. Huck, and Rainer Haag. Biocompatible fluorinated polyglycerols for droplet microfluidics as an alternative to PEG-based copolymer surfactants. *Lab on a Chip*, 16(1):65–69, 2016.

[112] Randall Scanga, Lucie Chrastecka, Ridhwan Mohammad, Austin Meadows, Phenix Lan Quan, and Eric Brouzes. Click chemistry approaches to expand the repertoire of PEG-based fluorinated surfactants for droplet microfluidics. *RSC Advances*, 8(23):12960–12974, 2018.

[113] Daniel J. Holt, Richard J. Payne, Wing Ying Chow, and Chris Abell. Fluorosurfactants for microdroplets: Interfacial tension analysis. *Journal of Colloid and Interface Science*, 350(1):205–211, 2010.

[114] Daniel J. Holt, Richard J. Payne, and Chris Abell. Synthesis of novel fluorous surfactants for microdroplet stabilisation in fluorous oil streams. *Journal of Fluorine Chemistry*, 131(3):398–407, 2010.

[115] Thomas Schuster, Joseph W. Krumpfer, Steffen Schellenberger, Reiner Friedrich, Markus Klapper, and Klaus Müllen. Effects of chemical structure on the dynamic and static surface tensions of short-chain, multi-arm nonionic fluorosurfactants. *Journal of Colloid and Interface Science*, 428:276–285, 2014.

[116] K. Astafyeva, L. Somaglino, S. Desgranges, R. Berti, C. Patinote, D. Langevin, F. Lazeyras, R. Salomir, A. Polidori, C. Contino-Pépin, W. Urbach, and N. Taulier. Perfluorocarbon nanodroplets stabilized by fluorinated surfactants: characterization and potentiality as theranostic agents. *J. Mater. Chem. B*, 3(14):2892–2907, 2015.

[117] P. Verdia, H. Q. N. Gunaratne, T. Y. Goh, J. Jacquemin, and M. Blesic. A class of efficient short-chain fluorinated catanionic surfactants. *Green Chem.*, pages 1234–1239, 2016.

[118] Philipp Gruner, Birte Riechers, Benoît Semin, Jiseok Lim, Abigail Johnston, Kathleen Short, and Jean Christophe Baret. Controlling molecular transport in minimal emulsions. *Nature Communications*, 7(1):10392, 2016.

[119] Jui-Chia Chang, Zoe Swank, Oliver Keiser, Sebastian J. Maerkl, and Esther Amstad. Microfluidic device for real-time formulation of reagents and their subsequent encapsulation into double emulsions. *Scientific Reports*, 8(1):1–9, 2018.

[120] Shaun W. Lim and Adam R. Abate. Ultrahigh-throughput sorting of microfluidic drops with flow cytometry. *Lab on a Chip*, 13(23):4563–4572, 2013.

[121] Anastasia Zinchenko, Sean R A Devenish, Balint Kintses, Pierre Yves Colin, Martin Fischlechner, and Florian Hollfelder. One in a million: Flow cytometric sorting of single cell-lysate assays in monodisperse picolitre double emulsion droplets for directed evolution. *Analytical Chemistry*, 86(5):2526–2533, 2014.

[122] Sujit S. Datta, Alireza Abbaspourrad, Esther Amstad, Jing Fan, Shin Hyun Kim, Mark Romanowsky, Ho Cheung Shum, Bingjie Sun, Andrew S. Utada, Maike Windbergs, Shaobing Zhou, and David A. Weitz. 25th anniversary article: Double emulsion templated solid microcapsules: Mechanics and controlled release. *Advanced Materials*, 26(14):2205–2218, 2014.

[123] A S Utada, E Lorenceau, D R Link, P D Kaplan, H A Stone, and D A Weitz. Monodisperse double emulsions generated from a microcapillary device. *Science*, 308(5721):537–541, 2005.

[124] Valessa Barbier, Michael Tatoulian, Hong Li, Farzaneh Arefi-Khonsari, Armand Ajdari, and Patrick Tabeling. Stable modification of PDMS surface properties by plasma polymerization: Application to the formation of double emulsions in microfluidic systems. *Langmuir*, 22:5230–5232, 2006.

[125] Cheung Shum Ho, Jin Woong Kim, and David A. Weitz. Microfluidic fabrication of monodisperse biocompatible and biodegradable polymersomes with controlled permeability. *Journal of the American Chemical Society*, 130(29):9543–9549, 2008.

[126] J. Cooper McDonald and George M. Whitesides. Poly(dimethylsiloxane) as a material for fabricating microfluidic devices. *Accounts of Chemical Research*, 35(7):491–499, 2002.

[127] Hatice Ceylan Koydemir, Haluk Külah, and Canan Özgen. Solvent compatibility of parylene c film Layer. *Journal of Microelectromechanical Systems*, 23(2):298–307, 2014.

[128] Alessandro Ofner, David G. Moore, Patrick A. Rühs, Pascal Schwendimann, Maximilian Eggersdorfer, Esther Amstad, David A. Weitz, and André R. Studart. High-Throughput Step Emulsification for the Production of Functional Materials Using a Glass Microfluidic Device. *Macromolecular Chemistry and Physics*, 218(2):1–10, 2017.

[129] Wadim L. Matochko, Simon Ng, Mohammad R. Jafari, Joseph Romaniuk, Sindy K Y Tang, and Ratmir Derda. Uniform amplification of phage display libraries in monodisperse emulsions. *Methods*, 58(1):18–27, 2012.

[130] Cheryl J. Dejournette, Joonyul Kim, Haley Medlen, Xiangpeng Li, Luke J. Vincent, and Christopher J. Easley. Creating biocompatible oil-water interfaces without synthesis: Direct interactions between primary amines and carboxylated perfluorocarbon surfactants. *Analytical Chemistry*, 85(21):10556–10564, 2013.

[131] Jan-Willi Willi Janiesch, Marian Weiss, Gerri Kannenberg, Jonathon Hannabuss, Thomas Surrey, Ilia Platzman, and Joachim P. Spatz. Key factors for stable retention of fluorophores and labeled biomolecules in droplet-based microfluidics. *Analytical Chemistry*, 87(4):2063–2067, 2015.

[132] Barbara Haller, Kerstin Göpfrich, Martin Schröter, Jan Willi Janiesch, Ilia Platzman, and Joachim P. Spatz. Charge-controlled microfluidic formation of lipid-based single- and multicompartment systems. *Lab on a Chip*, 18(17):2665–2674, 2018.

[133] Wynter J Duncanson, Tina Lin, Adam R Abate, Sebastian Seiffert, Rhutesh K Shah, and David A Weitz. Microfluidic synthesis of advanced microparticles for encapsulation and controlled release. *Lab on a chip*, 12(12):2135–2145, 2012.

[134] Benjamin J. Hindson, Kevin D. Ness, Donald A. Masquelier, Phillip Belgrader, Nicholas J. Heredia, Anthony J. Makarewicz, Isaac J. Bright, Michael Y. Lucero, Amy L. Hiddessen, Tina C. Legler, Tyler K. Kitano, Michael R. Hodel, Jonathan F. Petersen, Paul W. Wyatt, Erin R. Steenblock, Pallavi H. Shah, Luc J. Bousse, Camille B. Troup, Jeffrey C. Mellen, Dean K. Wittmann, Nicholas G. Erndt, Thomas H. Cauley, Ryan T. Koehler, Austin P. So, Simant Dube, Klint A. Rose, Luz Montesclaros, Shenglong Wang, David P. Stumbo, Shawn P. Hodges, Steven Romine, Fred P. Milanovich, Helen E. White, John F. Regan, George A. Karlin-Neumann, Christopher M. Hindson, Serge Saxonov, and Bill W. Colston. High-throughput droplet digital PCR system for absolute quantitation of DNA copy number. *Analytical Chemistry*, 83(22):8604–8610, 2011.

[135] Andrew D. Griffiths and Dan S. Tawfik. Miniaturising the laboratory in emulsion droplets. *Trends in Biotechnology*, 24(9):395–402, 2006.

[136] Assaf Rotem, Oren Ram, Noam Shoresh, Ralph A Sperling, Alon Goren, David A Weitz, and Bradley E Bernstein. Single-cell ChIP-seq reveals cell subpopulations defined by chromatin state. *Nature Biotechnology*, 33(11):1165–72, 2015.

[137] Assaf Rotem, Oren Ram, Noam Shoresh, Ralph A. Sperling, Michael Schnall-Levin, Huidan Zhang, Anindita Basu, Bradley E. Bernstein, and David A. Weitz. High-throughput single-cell labeling (Hi-SCL) for RNA-Seq using drop-based microfluidics. *PLoS ONE*, 10(5):1–14, 2015.

[138] Audrey E. Fischer, Susan K. Wu, Jody B.G. Proescher, Assaf Rotem, Connie B. Chang, Huidan Zhang, Ye Tao, Thomas S. Mehoke, Peter M. Thielen, Abimbola O. Kolawole, Thomas J. Smith, Christiane E. Wobus, David A. Weitz, Jeffrey S. Lin, Andrew B. Feldman, and Joshua T. Wolfe. A high-throughput drop microfluidic system for virus culture and analysis. *Journal of Virological Methods*, 213:111–117, 2015.

[139] Ye Tao, Assaf Rotem, Huidan Zhang, Connie B. Chang, Anindita Basu, Abimbola O. Kolawole, Stephan A. Koehler, Yukun Ren, Jeffrey S. Lin, James M. Pipas, Andrew B. Feldman, Christiane E. Wobus, and David A. Weitz. Rapid, targeted and culture-free viral infectivity assay in drop-based microfluidics. *Lab on a chip*, 15(19):3934–40, 2015.

[140] Ye Tao, Assaf Rotem, Huidan Zhang, Shelley K. Cockrell, Stephan A. Koehler, Connie B. Chang, Lloyd W. Ung, Paul G. Cantalupo, Yukun Ren, Jeffrey S. Lin, Andrew B. Feldman, Christiane E. Wobus, James M. Pipas, and David A. Weitz. Artifact-Free Quantification and Sequencing of Rare Recombinant Viruses by Using Drop-Based Microfluidics. *ChemBioChem*, 16(15):2167–2171, 2015.

[141] Huidan Zhang, Shelley K Cockrell, Abimbola O Kolawole, Assaf Rotem, Adrian W R Serohijos, Connie B Chang, Ye Tao, Thomas S Mehoke, Yulong Han, Jeffrey S Lin, Nicholas S Giacobbi, Andrew B Feldman, Eugene Shakhnovich, David A Weitz, Christiane E Wobus, and James M Pipas. Isolation and Analysis of Rare Norovirus Recombinants from Coinfected Mice Using Drop-Based Microfluidics. *Journal of Virology*, 89(15):7722–7734, 2015.

[142] Michael J Hey, Stephen M Ilett, and George Davidson. Temperature on Poly(ethylene oxide) Chains in Aqueous Solution. *J. Chem. Soc. Faraday Trans*, 91(21):3897–3900, 1995.

[143] Barbora Malisova, Samuele Tosatti, Marcus Textor, Karl Gademann, and Stefan Zürcher. Poly(ethylene glycol) adlayers immobilized to metal oxide substrates through catechol derivatives: Influence of assembly conditions on formation and stability. *Langmuir*, 26(6):4018–4026, 2010.

[144] Sebastian Seiffert and David A. Weitz. Controlled fabrication of polymer microgels by polymer-analogous gelation in droplet microfluidics. *Soft Matter*, 6(14):3184–3190, 2010.

[145] Jung-Uk Shim, Rohan T. Ranasinghe, Clive A. Smith, Shehu M. Ibrahim, Florian Hollfelder, Wilhelm T S Huck, David Klenerman, and Chris Abell. Ultrarapid generation of femtoliter microfluidic droplets for single-molecule-counting immunoassays. *ACS Nano*, 7(7):5955–5964, 2013.

[146] Manhee Lee, Jesse W Collins, Donald M Aubrecht, Ralph A Sperling, Laura Solomon, Jong-Wook Ha, Gi-Ra Yi, David A Weitz, and Vinothan N Manoharan. Synchronized reinjection and coalescence of droplets in microfluidics. *Lab on a chip*, 14(3):509–513, 2014.

[147] Paschalis Alexandridis and Josef F Holzwarth. Differential Scanning Calorimetry Investigation of the Effect of Salts on Aqueous Solution Properties of an Amphiphilic Block Copolymer (Poloxamer). *Langmuir*, 13(23):6074–6082, 1997.

[148] Maurice Bourrel, Alain Graciaa, Robert S. Schechter, and William H. Wade. The relation of emulsion stability to phase behavior and interfacial tension of surfactant systems. *Journal of Colloid And Interface Science*, 72(1):161–163, 1979.

[149] Hans-Jurgen Butt, Karlheinz Graf, and Michael Kappl. *Physics and Chemistry of Interfaces*. Wiley-VCH, 2003.

[150] R. A. Hann. Molecular Structure and Monolayer Properties. In *Langmuir-Blodgett Films*, pages 17–92. Springer, 1990.

[151] Junlong Song, Wendy E. Krause, and Orlando J. Rojas. Adsorption of polyalkyl glycol ethers and triblock nonionic polymers on PET. *Journal of Colloid and Interface Science*, 420:174–181, 2014.

[152] Susan J Sofia, V Premnath, and Edward W Merrill. Poly(ethylene oxide) Grafted to Silicon Surfaces: Grafting Density and Protein Adsorption. *Macromolecules*, 31(15):5059–70, 1998.

[153] Douglas B. Weibel and George M. Whitesides. Applications of microfluidics in chemical biology. *Current Opinion in Chemical Biology*, 10(6):584–591, 2006.

[154] H. F. Chan, S. Ma, J. Tian, and K. W. Leong. High-throughput screening of microchip-synthesized genes in programmable double-emulsion droplets. *Nanoscale*, 9(10):3485–3495, 2017.

[155] Jean-Christophe Baret, Oliver J. Miller, Valerie Taly, Michaël Ryckelynck, Abdeslam El-Harrak, Lucas Frenz, Christian Rick, Michael L. Samuels, J. Brian Hutchison, Jeremy J. Agresti, Darren R. Link, David A. Weitz, and Andrew D. Griffiths. Fluorescence-activated droplet sorting (FADS): efficient microfluidic cell sorting based on enzymatic activity. *Lab on a Chip*, 9(13):1850–1858, 2009.

[156] Staffan L. Sjostrom, Yunpeng Bai, Mingtao Huang, Zihe Liu, Jens Nielsen, Haakan N. Joensson, and Helene Andersson Svahn. High-throughput screening for industrial enzyme production hosts by droplet microfluidics. *Lab on a Chip*, 14(4):806–813, 2014.

[157] Deniz Pekin, Yousr Skhiri, Jean Christophe Baret, Delphine Le Corre, Linas Mazutis, Chaouki Ben Salem, Florian Millot, Abdeslam El Harrak, J. Brian Hutchison, Jonathan W. Larson, Darren R. Link, Pierre Laurent-Puig, Andrew D. Griffiths, and Valérie Taly. Quantitative and sensitive detection of rare mutations using droplet-based microfluidics. *Lab on a Chip*, 11(13):2156–2166, 2011.

[158] Valerie Taly, Deniz Pekin, Leonor Benhaim, Steve K. Kotsopoulos, Delphine Le Corre, Xinyu Li, Ivan Atochin, Darren R. Link, Andrew D. Griffiths, Karine Pallier, Hélène Blons, Olivier Bouché, Bruno Landi, J. Brian Hutchison, and Pierre Laurent-Puig. Multiplex picodroplet digital PCR to detect KRAS mutations in circulating DNA from the plasma of colorectal cancer patients. *Clinical Chemistry*, 59(12):1722–1731, 2013.

[159] Audrey Didelot, Steve K. Kotsopoulos, Audrey Lupo, Deniz Pekin, Xinyu Li, Ivan Atochin, Preethi Srinivasan, Qun Zhong, Jeff Olson, Darren R. Link, Pierre Laurent-Puig, Hélène Blons, J. Brian Hutchison, and Valerie Taly. Multiplex picoliter-droplet digital PCR for quantitative assessment of DNA integrity in clinical samples. *Clinical Chemistry*, 59(5):815–823, 2013.

[160] Yousr Skhiri, Philipp Gruner, Benoît Semin, Quentin Brosseau, Deniz Pekin, Linas Mazutis, Victoire Goust, Felix Kleinschmidt, Abdeslam El Harrak, J. Brian Hutchison, Estelle Mayot, Jean-François Bartolo, Andrew D. Griffiths, Valérie Taly, and Jean-Christophe Baret. Dynamics of molecular transport by surfactants in emulsions. *Soft Matter*, 8(41):10618–10627, 2012.

[161] Gabrielle Woronoff, Abdeslam El Harrak, Estelle Mayot, Olivier Schicke, Oliver J. Miller, Patrice Soumillion, Andrew D. Griffiths, and Michael Ryckelynck. New generation of amino coumarin methyl sulfonate-based fluorogenic substrates for amidase assays in droplet-based microfluidic applications. *Analytical Chemistry*, 83(8):2852–2857, 2011.

[162] Yunhan Chen, Adi Wijaya Gani, and Sindy K.Y. Tang. Characterization of sensitivity and specificity in leaky droplet-based assays. *Lab on a Chip*, 12(23):5093–5103, 2012.

[163] Fabienne Courtois, Luis F. Olguin, Graeme Whyte, Ashleigh B. Theberge, Wilhelm T S Huck, Florian Hollfelder, and Chris Abell. Controlling the retention of small molecules in emulsion microdroplets for use in cell-based assays. *Analytical Chemistry*, 81(8):3008–3016, 2009.

[164] James A. Stapleton and James R. Swartz. Development of an in vitro compartmentalization screen for high-throughput directed evolution of [FeFe] hydrogenases. *PLoS ONE*, 5(12), 2010.

[165] Patrick A. Sandoz, Aram J. Chung, Westbrook M. Weaver, and Dino Di Carlo. Sugar additives improve signal fidelity for implementing two-phase resorufin-based enzyme immunoassays. *Langmuir*, 30(23):6637–6643, 2014.

[166] Majdi Najah, Estelle Mayot, I. Putu Mahendra-Wijaya, Andrew D. Griffiths, Sylvain Ladame, and Antoine Drevelle. New glycosidase substrates for droplet-based microfluidic screening. *Analytical Chemistry*, 85(20):9807–9814, 2013.

[167] Ott Scheler, Tomasz S. Kaminski, Artur Ruszczak, and Piotr Garstecki. Dodecylresorufin (C12R) outperforms resorufin in microdroplet bacterial assays. *ACS Applied Materials and Interfaces*, 8(18):11318–11325, 2016.

[168] Jana Bahtz, Deniz Z. Gunes, Eric Hughes, Lea Pokorny, Francesca Riesch, Axel Syrbe, Peter Fischer, and Erich J. Windhab. Decoupling of mass transport mechanisms in the stagewise swelling of multiple emulsions. *Langmuir*, 31(19):5265–5273, 2015.

[169] A. Vian, B. Reuse, and E. Amstad. Scalable production of double emulsion drops with thin shells. *Lab on a Chip*, 18(13):1936–1942, 2018.

[170] L. R. Arriaga, E. Amstad, and D. A. Weitz. Scalable single-step microfluidic production of single-core double emulsions with ultra-thin shells. *Lab on a Chip*, 15(16):3335–3340, 2015.

[171] Paula Malo De Molina, Mengwen Zhang, Alexandra V. Bayles, and Matthew E. Helgeson. Oil-in-water-in-oil multinanoemulsions for templating complex nanoparticles. *Nano Letters*, 16(12):7325–7332, 2016.

[172] Mengwen Zhang, Patrick T. Corona, Nino Ruocco, David Alvarez, Paula Malo de Molina, Samir Mitragotri, and Matthew E. Helgeson. Controlling complex nanoemulsion morphology using asymmetric cosurfactants for the preparation of polymer nanocapsules. *Langmuir*, 34:978–990, 2018.

[173] C. S. Chern. Emulsion polymerization mechanisms and kinetics. *Progress in Polymer Science*, 31(5):443–486, 2006.

[174] William D. Harkins. A General Theory of the Mechanism of Emulsion Polymerization. *Journal of the American Chemical Society*, 69(6):1428–1444, 1947.

[175] Wendell Smith and Roswell Ewart. Kinetics of emulsion polymerization. *Journal of Chemical Physics*, 16(4):592–599, 1948.

[176] Aaron P. Esser-Kahn, Susan A. Odom, Nancy R. Sottos, Scott R. White, and Jeffrey S. Moore. Triggered release from polymer capsules. *Macromolecules*, 44(14):5539–5553, 2011.

[177] Bernard F. Gibbs, Selim Kermasha, Inteaz Alli, and Catherine N. Mulligan. Encapsulation in the food industry: A review. *International Journal of Food Sciences and Nutrition*, 50(3):213–224, 1999.

[178] Atmane Madene, Muriel Jacquot, Joël Scher, and Stéphane Desobry. Flavour encapsulation and controlled release - A review. *International Journal of Food Science and Technology*, 41(1):1–21, 2006.

[179] Anne Ammala. Biodegradable polymers as encapsulation materials for cosmetics and personal care markets. *International Journal of Cosmetic Science*, 35(2):113–124, 2013.

[180] Hyomin Lee, Chang Hyung Choi, Alireza Abbaspourrad, Chris Wesner, Marco Caggioni, Taotao Zhu, and David A. Weitz. Encapsulation and Enhanced Retention of Fragrance in Polymer Microcapsules. *ACS Applied Materials and Interfaces*, 8(6):4007–4013, 2016.

[181] Michael T. Cook, George Tzortzis, Dimitris Charalampopoulos, and Vitaliy V. Khutoryanskiy. Microencapsulation of probiotics for gastrointestinal delivery. *Journal of Controlled Release*, 162(1):56–67, 2012.

[182] Katsuhiko Sato, Kentaro Yoshida, Shigehiro Takahashi, and Jun-ichi Anzai. PH- and sugar-sensitive layer-by-layer films and microcapsules for drug delivery. *Advanced Drug Delivery Reviews*, 63(9):809–821, 2011.

[183] Esther Amstad. Capsules: Their past and opportunities for their future. *ACS Macro Letters*, 6(8):841–847, 2017.

[184] Angus P R Johnston, Christina Cortez, Alexandra S. Angelatos, and Frank Caruso. Layer-by-layer engineered capsules and their applications. *Current Opinion in Colloid and Interface Science*, 11(4):203–209, 2006.

[185] Alisa L. Becker, Angus P.R. Johnston, and Frank Caruso. Layer-by-layer-assembled capsules and films for therapeutic delivery. *Small*, 6(17):1836–1852, 2010.

[186] Gero Decher. Fuzzy nanoassemblies: Toward layered polymeric multicomposites. *Science*, 277(5330):1232–1237, 1997.

[187] Joseph J. Richardson, Jiwei Cui, Mattias Björnmalm, Julia A. Braunger, Hirotaka Ejima, and Frank Caruso. Innovation in Layer-by-Layer Assembly. *Chemical Reviews*, 116(23):14828–14867, 2016.

[188] Christopher J. Ochs, Tam Hong, Georgina K. Such, Jiwei Cui, Almar Postma, and Frank Caruso. Dopamine-mediated continuous assembly of biodegradable capsules. *Chemistry of Materials*, 23(13):3141–3143, 2011.

[189] Junling Guo, Yuan Ping, Hirotaka Ejima, Karen Alt, Mirko Meissner, Joseph J. Richardson, Yan Yan, Karlheinz Peter, Dominik Von Elverfeldt, Christoph E. Hagemeyer, and Frank Caruso. Engineering multifunctional capsules through the assembly of metal-phenolic networks. *Angewandte Chemie - International Edition*, 53(22):5546–5551, 2014.

[190] Hirotaka Ejima, Joseph J. Richardson, Kang Liang, James P. Best, Martin P. Van Koeverden, Georgina K. Such, Jiwei Cui, and Frank Caruso. One-step assembly of coordination complexes for versatile film and particle engineering. *Science*, 341(6142):154–157, 2013.

[191] Alireza Abbaspourrad, Sujit S. Datta, and David A. Weitz. Controlling release from pH-responsive microcapsules. *Langmuir*, 29(41):12697–12702, 2013.

[192] Alireza Abbaspourrad, Nick J. Carroll, Shin Hyun Kim, and David A. Weitz. Polymer microcapsules with programmable active release. *Journal of the American Chemical Society*, 135(20):7744–7750, 2013.

[193] Sebastian Berger, Haiping Zhang, and Andrij Pich. Microgel-based stimuli-responsive capsules. *Advanced Functional Materials*, 19(4):554–559, 2009.

[194] Kang Liang, Georgina K. Such, Zhiyuan Zhu, Yan Yan, Hannah Lomas, and Frank Caruso. Charge-shifting click capsules with dual-responsive cargo release mechanisms. *Advanced Materials*, 23(36):273–277, 2011.

[195] Christopher J. Ochs, Georgina K. Such, Yan Yan, Martin P. Van Koeverden, and Frank Caruso. Biodegradable click capsules with engineered drug-loaded multilayers. *ACS Nano*, 4(3):1653–1663, 2010.

[196] R. Georgieva, S. Moya, M. Hin, R. Mitlöhner, E. Donath, H. Kiesewetter, H. Möhwald, and H. Bäumler. Permeation of macromolecules into polyelectrolyte microcapsules. *Biomacromolecules*, 3(3):517–524, 2002.

[197] Antoine Vian and Esther Amstad. Mechano-responsive microcapsules with uniform, thin shells. *Soft Matter*, 2018.

[198] Ho-Cheol Kang, Byung Min Lee, Jungho Yoon, and Minjoong Yoon. Synthesis and Surface-Active Properties of New Photosensitive Surfactants Containing the Azobenzene Group. *Journal of Colloid and Interface Science*, 231(2):255–264, 2000.

[199] Muris Kobašlija and D. Tyler McQuade. Polyurea microcapsules from oil-in-oil emulsions via interfacial polymerization. *Macromolecules*, 39(19):6371–6375, 2006.

[200] Wei He, Xiaochen Gu, and Song Liu. Surfactant-free one-step synthesis of dual-functional polyurea microcapsules: Contact infection control and drug delivery. *Advanced Functional Materials*, 22(19):4023–4031, 2012.

[201] T. Y. Dora Tang, C. Rohaida Che Hak, Alexander J. Thompson, Marina K. Kuimova, D. S. Williams, Adam W. Perriman, and Stephen Mann. Fatty acid membrane assembly on coacervate microdroplets as a step towards a hybrid protocell model. *Nature Chemistry*, 6(6):527–533, 2014.

[202] Segolena Leclercq, Kristin R. Harlander, and Gary A. Reineccius. Formation and characterization of microcapsules by complex coacervation with liquid or solid aroma cores. *Flavour and Fragrance Journal*, 24(1):17–24, 2009.

[203] Elena M. Shchukina and Dmitry G. Shchukin. Layer-by-layer coated emulsion microparticles as storage and delivery tool. *Current Opinion in Colloid and Interface Science*, 17(5):281–289, 2012.

[204] Craig Priest, Anthony Quinn, Almar Postma, Alexander N. Zelikin, John Ralston, and Frank Caruso. Microfluidic polymer multilayer adsorption on liquid crystal droplets for microcapsule synthesis. *Lab on a Chip*, 8(12):2182–2187, 2008.

[205] Sheldon Okada, Susan Peng, Wayne Spevak, and Deborah Charych. Color and Chromism of Polydiacetylene Vesicles. *Accounts of Chemical Research*, 31(5):229–239, 1998.

[206] Jianzhong Du and Steven P. Armes. pH-responsive vesicles based on a hydrolytically self-cross-linkable copolymer. *Journal of the American Chemical Society*, 127(37):12800–12801, 2005.

[207] Bohdana M. Discher, Harry Bermudez, Daniel A. Hammer, Dennis E. Discher, You yeon Won, and Frank S. Bates. Cross-linked polymersome membranes: Vesicles with broadly adjustable properties. *Journal of Physical Chemistry B*, 106(11):2848–2854, 2002.

[208] Ann Christin Bijlard, Svenja Winzen, Kenji Itoh, Katharina Landfester, and Andreas Taden. Alternative pathway for the stabilization of reactive emulsions via cross-linkable surfactants. *ACS Macro Letters*, 3(11):1165–1168, 2014.

[209] Marcin Kaczorowski and Gabriel Rokicki. Reactive surfactants – chemistry and applications Part I. Polymerizable surfactants. *Polimery/Polymers*, 61(11-12):747–757, 2016.

[210] H. Lee, N. F. Scherer, and P. B. Messersmith. Single-molecule mechanics of mussel adhesion. *Proceedings of the National Academy of Sciences*, 103(35):12999–13003, 2006.

[211] N. Holten-Andersen, M. J. Harrington, H. Birkedal, B. P. Lee, P. B. Messersmith, K. Y. C. Lee, and J. H. Waite. pH-induced metal-ligand cross-links inspired by mussel yield self-healing polymer networks with near-covalent elastic moduli. *Proceedings of the National Academy of Sciences*, 108(7):2651–2655, 2011.

[212] Bruce P. Lee, P.B. Messersmith, J.N. Israelachvili, and J.H. Waite. Mussel-Inspired Adhesives and Coatings. *Annual Review of Materials Research*, 41(1):99–132, 2011.

[213] Seonki Hong, Kisuk Yang, Bobae Kang, Changhyun Lee, In Taek Song, Eunkyoung Byun, Kook In Park, Seung Woo Cho, and Haeshin Lee. Hyaluronic acid catechol: A biopolymer exhibiting a pH-dependent adhesive or cohesive property for human neural stem cell engineering. *Advanced Functional Materials*, 23(14):1774–1780, 2013.

[214] Mary J Sever and Jonathan J Wilker. Visible absorption spectra of metal – catecholate and metal – tironate complexes. *The Royal Society of Chemistry*, pages 1061–1072, 2004.

[215] Niels Holten-Andersen, Aditya Jaishankar, Matthew J. Harrington, Dominic E. Fullenkamp, Genevieve Dimarco, Lihong He, Gareth H. McKinley, Phillip B. Messersmith, and Ka Yee C. Lee. Metal-coordination: Using one of nature's tricks to control soft material mechanics. *Journal of Materials Chemistry B*, 2(17):2467–2472, 2014.

[216] Devin G. Barrett, Dominic E. Fullenkamp, Lihong He, Niels Holten-Andersen, Ka Yee C. Lee, and Phillip B. Messersmith. PH-based regulation of hydrogel mechanical properties through mussel-inspired chemistry and processing. *Advanced Functional Materials*, 23(9):1111–1119, 2013.

[217] H. Lee, Shara M. Dellatore, William M. Miller, and Phillip B. Messersmith. Mussel-Inspired Surface Chemistry for Multifunctional Coatings. *Science*, 318:426–431, 2007.

GIANLUCA ETIENNE

gianluca.etienne@epfl.ch

Rue des Echelettes 11 ⋄ 1004 Lausanne, Vaud, Switzerland

EPFL-STI-IMX-SMAL, MXC 232, Station 12 ⋄ 1015 Lausanne, Vaud, Switzerland

EDUCATION

École Polytechnique Fédéreale de Lausanne (EPFL), Lausanne   *2014 - 2019*
Ph.D. in Materials Science & Engineering
Soft Materials Laboratory, Thesis Advisor: Prof. Esther Amstad
Title: Fluorinated surfactants in droplet-based microfluidics: Influence of their composition on the properties of emulsion drops

Eidgenössische Technische Hochschule Zürich (ETH), Zurich   *2014*
M.Sc. in Materials Science

Master's thesis at Experimental Soft Condensed Matter Group, Prof. David Weitz
Harvard University, Cambridge, *September 2013 - May 2014*

IARU summer school on nanoscience (Santander Scholar)
University of Tokyo, Tokyo, *July 2013*

Eidgenössische Technische Hochschule Zürich (ETH), Zurich   *2012*
B.Sc. in Materials Science

Research assistant at State Key Laboratory of Ceramic and Fine Processing, Prof. Jinlong Yang
Tsinghua University, Beijing, *August 2011 - June 2012*

PEER-REVIEWED PUBLICATIONS

Etienne, G., Amstad, E. Bio-inspired self-healing capsules: Delivery vehicles and beyond (submitted).

Zdrali, E., **Etienne, G.**, Smolentsev, N., Amstad, E., Roke, S. Correlating stability of micrometer- and nanometer-sized droplets with interfacial surfactant structure. (submitted).

Etienne, G., Vian, A. Biočanin, M., Deplancke, B & Amstad, E. Cross-talk between emulsion drops: How are hydrophilic reagents transported across oil phases? Lab Chip (2018).

Etienne, G., Kessler, M. Amstad, E. Influence of fluorinated surfactant composition on the stability of emulsion drops. Macromol. Chem. Phys. (2017).

Håti, A. G., Arnfinnsdottir, N. B., Østevold, C., Sletmoen, M., **Etienne, G.**, Amstad, E., Stokke, B. T., Microarrays for the study of compartmentalized microorganisms in alginate microbeads and (W/O/W) double emulsions. RSC Adv. (2016).

CONFERENCE PRESENTATIONS

Etienne, G. Stop cross-talking: How surfactants influence leakiness from emulsions. Presentation at Soft Matter Interfaces: From Biology to Engineering Applications, Ascona, Switzerland, November, 2017.

Etienne, G. Stop cross-talking: How surfactants influence leakiness from emulsions. Presentation at the Swiss Soft Days No.21, Lausanne, Switzerland, September, 2017.

Etienne, G., Kessler, M. Amstad, E. Influence of fluorinated surfactant composition on the stability of emulsion drops. Poster presentation at Swiss Soft Days No.20, Geneva, Switzerland, February, 2017.

Etienne, G., Kessler, M. Amstad, E. Influence of fluorinated surfactant composition on the stability of emulsion drops. Invited flash talk and poster presentation at Microfluidics 2016, EMBL, Heidelberg, Germany, July, 2016.

PATENTS

Etienne, G., Amstad, E. April 2018, Self-healing Cross-linkable Shells, EU Patent Application EP18170186

TEACHING/ADVISING EXPERIENCE

École Polytechnique Fédéreale de Lausanne (EPFL), Lausanne 2014 - 2017
Bachelor's and master's students *Lausanne, Switzerland*

Institute of Materials - Soft Materials Laboratory
Master Students: Vance Nguyen, Kamyar Mehrabi, Elaheh Zare, Ludovic Bescher, Julie Perroton, Michael Kessler, Lucien Berret, Xavier Deville, Alan Böhlen, Bruno Charlety
Bachelors Student: Theo Lachat

École Polytechnique Fédéreale de Lausanne (EPFL), Lausanne 2015 - 2017
Teaching Assistant *Lausanne, Switzerland*

Institute of Materials
MSE-425 Soft Matter graduate course

Eidgenössische Technische Hochschule Zürich (ETH Zurich) Spring 2010 & 2011
Teaching Assistant *Zurich, Switzerland*

Department of Materials (Dr. Martin Willeke)
327-0211-00L Practical laboratory course II
327-0311-00L Practical laboratory course III

OTHER RESEARCH EXPERIENCE

· **Eidgenössische Technische Hochschule Zürich (ETH Zurich)** March 2013 - July 2013
Research Assistant *Zurich, Switzerland*

deMello Group, (Prof. Andrew deMello) working on controlled PbS nanoparticle synthesis in droplet-based microfluidics.

Eidgenössische Technische Hochschule Zürich (ETH Zurich) August 2012 - October 2012
Research Assistant *Zurich, Switzerland*

Complex Materials Group (Prof. André Studart) working on grafting of multiresponsive polymers on colloidosomes with silica nanoparticle shells.

EXTRACURRICULAR

Co-founder of Swingtime Lausanne, Swing Dance School in Lausanne, Switzerland, 2015 - present

Rotaract Club of Lucerne, Switzerland District 1980, 2006 - present

Rotary Youth Leadership Award, March 2016

Languages: German (fluent), English (fluent), French (conversational)